QEX

May/June 2007

$5

A Forum for Communications Experimenters

Issue No. 242

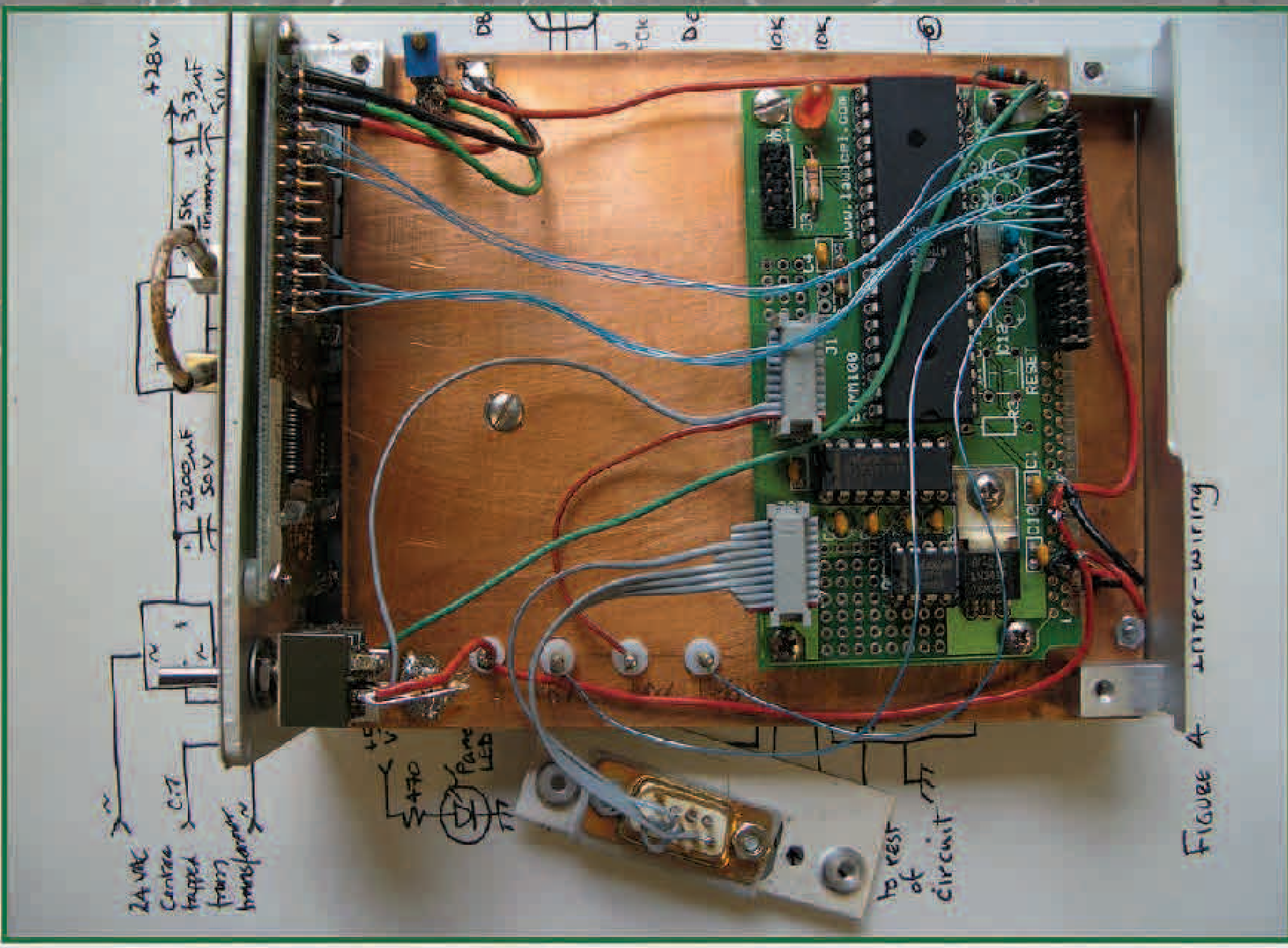

VE5FP gives us his design for "An Automatic Noise-Figure Meter." Use this project to measure NF of your preamplifier projects from 3 MHz to over 400 MHz.

ARRL *The national association for* ***AMATEUR RADIO***
225 Main Street
Newington, CT USA 06111-1494

Complies with New FCC Rules.

Available Now with 12m and 10m Built-in!

TOKYO HY-POWER

HL-1.5KFX

HF/50MHz Linear Power Amplifier

This compact and lightweight 1kW desktop HF/50MHz linear power amplifier has a maximum input power of 1.75kW. Our solid-state broadband power amp technology makes it **the smallest and lightest self-contained amplifier in the industry**.

Typical output power is 1kW PEP/SSB on HF and 650W on 6m band with the drive power of 85-90W. Bands set automatically with the **built-in band decoder**. You can forget about the band setting when the amplifier is connected to your modern radio through **supplied band data cables for ICOM CI-V, DC voltage (ICOM, Yaesu), and RS-232C (Kenwood)**. Manual band setting selectable as well.

NEW! All these data cables are included with the amplifier.

Debuting Dayton 2007

HL-1.2KFX
HF amp 750W out*

HL-2.5KFX
HF amp 1500w out*

HC-1.5KAT
HF 1.5KW Auto Tuner*

* These devices have not been authorized as required by the rules of the FCC. These devices are not, and may not be, offered for sale or lease, or sold or leased until authorization is obtained."

See these and more at **Dayton Hamvention™ Booths 511 & 512**

Features

- Lightest and most compact 1kW HF amplifier in the industry.
- The amplifier's decoder changes bands automatically with most ICOM, Kenwood, Yaesu.
- The amp utilizes an advanced 16 bit MPU (microprocessor) to run the various high speed protection circuits such as overdrive, high antenna SWR, DC overvoltage, band miss-set etc.
- Built in power supply.
- AC (200/220/235/240V) and (100/110/115/120V) selectable.
- Equipped with a control cable connection socket, for the HC-1.5KAT, auto antenna tuner by Tokyo Hy-Power Labs.
- Two antenna ports selectable from front panel.
- Great for desktop or DXpedition!

Specifications

Frequency:
1.8 ~ 28MHz all amateur bands including WARC bands and 50MHz

Mode:
SSB, CW, RTTY

RF Drive:
85W typ. (100W max.)

Output Power:
HF 1kW PEP max.
50MHz 650W PEP max.

Matching Transceivers for Auto Band Decoder:
Most modern ICOM, Yaesu, Kenwood

Drain Voltage:
53V (when no RF drive)

Drain Current:
40A max.

Input Impedance:
50 OHM (unbalanced)

Output Impedance:
50 OHM (unbalanced)

Final Transistor:
SD2933 x 4 (MOS FET by ST micro)

Circuit:
Class AB parallel push-pull

Cooling Method:
Forced Air Cooling

MPU:
PIC 18F452 x 2

Multi-Meter:
Output Power – Pf 1Kw
Drain Voltage – Vd 60V
Drain Current – Id 50A

Input/Output Connectors:
UHF SO-239

AC Power:
AC 240V default (200/220/235) – 10 A max.
AC 120V (100/110/115) – 20 A max.

AC Consumption:
1.9kVA max. when TX

Dimension:
10.7 x 5.6 x 14.3 inches (WxHxD)/272 x 142 x 363 mm

Weight:
Approx. 20kgs. or 45.5lbs.

Accessories Included:
AC Power Cord
Band Decoder Cables included for Kenwood, ICOM and Yaesu
Spare Fuses and Plugs
User Manual

Optional Items:
Auto Antenna Tuner (HC-1.5KAT)
External Cooling Fan (HXT-1.5KF for high duty cycle RTTY)

TOKYO HY-POWER

TOKYO HY-POWER LABS., INC. – USA
487 East Main Street, Suite 163
Mount Kisco, NY 10549
Phone: 914-602-1400
e-mail: thpusa@optonline.net

TOKYO HY-POWER LABS., INC. – JAPAN
1-1 Hatanaka 3chome, Niiza Saitama 352-0012
Phone: +81 (48) 481-1211 FAX: +81 (48) 479-6949
e-mail: info@thp.co.jp
Web: http://www.thp.co.jp

HAM RADIO OUTLET WORLDWIDE DISTRIBUTION

Exclusively from Ham Radio Outlet!

www.hamradio.com

Western US/Canada
1-800-854-6046

Mid-Atlantic
1-800-444-4799

Mountain/Central
1-800-444-9476

Northeast
1-800-644-4476

Southeast
1-800-444-7927

New England/Eastern Canada
1-800-444-0047

QEX

QEX (ISSN: 0886-8093) is published bimonthly in January, March, May, July, September, and November by the American Radio Relay League, 225 Main Street, Newington, CT 06111-1494. Periodicals postage paid at Hartford, CT and at additional mailing offices.

POSTMASTER: Send address changes to: QEX, 225 Main St, Newington, CT 06111-1494
Issue No 242

Harold Kramer, WJ1B
Publisher

Doug Smith, KF6DX
Editor

Larry Wolfgang, WR1B
Managing Editor

Lori Weinberg, KB1EIB
Assistant Editor

L. B. Cebik, W4RNL
Zack Lau, W1VT
Ray Mack, W5IFS
Contributing Editors

Production Department

Steve Ford, WB8IMY
Publications Manager

Michelle Bloom, WB1ENT
Production Supervisor

Sue Fagan
Graphic Design Supervisor

Devon Neal, KB1NSR
Technical Illustrator

Joe Shea
Production Assistant

Advertising Information Contact:

Janet L. Rocco, W1JLR
Business Services
860-594-0203 direct
800-243-7768 ARRL
860-594-4285 fax

Circulation Department

Cathy Stepina, *QEX Circulation*

Offices

225 Main St, Newington, CT 06111-1494 USA
Telephone: 860-594-0200
Fax: 860-594-0259 (24 hour direct line)
e-mail: **qex@arrl.org**

Subscription rate for 6 issues:

In the US: ARRL Member $24, nonmember $36;

US by First Class Mail: ARRL member $37, nonmember $49;

Elsewhere by Surface Mail (4-8 week delivery): ARRL member $31, nonmember $43;

Canada by Airmail: ARRL member $40, nonmember $52;

Elsewhere by Airmail: ARRL member $59, nonmember $71.

Members are asked to include their membership control number or a label from their *QST* when applying.

In order to ensure prompt delivery, we ask that you periodically check the address information on your mailing label. If you find any inaccuracies, please contact the Circulation Department immediately. Thank you for your assistance.

About the Cover

Jim Koehler, VE5FP, built "An Automatic Noise-Figure Meter." In this article, Jim explains how to build the noise-figure meter and measure the NF of your preamplifier projects from 3 MHz to over 400 MHz.

Features

Columns

May/June 2007 *QEX* Advertising Index

THE AMERICAN RADIO RELAY LEAGUE

The American Radio Relay League, Inc, is a noncommercial association of radio amateurs, organized for the promotion of interest in Amateur Radio communication and experimentation, for the establishment of networks to provide communications in the event of disasters or other emergencies, for the advancement of the radio art and of the public welfare, for the representation of the radio amateur in legislative matters, and for the maintenance of fraternalism and a high standard of conduct.

ARRL is an incorporated association without capital stock chartered under the laws of the state of Connecticut, and is an exempt organization under Section 501(c)(3) of the Internal Revenue Code of 1986. Its affairs are governed by a Board of Directors, whose voting members are elected every three years by the general membership. The officers are elected or appointed by the Directors. The League is noncommercial, and no one who could gain financially from the shaping of its affairs is eligible for membership on its Board.

"Of, by, and for the radio amateur," ARRL numbers within its ranks the vast majority of active amateurs in the nation and has a proud history of achievement as the standard-bearer in amateur affairs.

A *bona fide* interest in Amateur Radio is the only essential qualification of membership; an Amateur Radio license is not a prerequisite, although full voting membership is granted only to licensed amateurs in the US.

Membership inquiries and general correspondence should be addressed to the administrative headquarters:

ARRL, 225 Main Street, Newington, CT 06111 USA.

Telephone: 860-594-0200

FAX: 860-594-0259 (24-hour direct line)

Officers

President: JOEL HARRISON, W5ZN
528 Miller Rd, Judsonia, AR 72081
Chief Executive Officer: DAVID SUMNER, K1ZZ

The purpose of *QEX* is to:

1) provide a medium for the exchange of ideas and information among Amateur Radio experimenters,
2) document advanced technical work in the Amateur Radio field, and
3) support efforts to advance the state of the Amateur Radio art.

All correspondence concerning *QEX* should be addressed to the American Radio Relay League, 225 Main Street, Newington, CT 06111 USA. Envelopes containing manuscripts and letters for publication in *QEX* should be marked Editor*, QEX*.

Both theoretical and practical technical articles are welcomed. Manuscripts should be submitted in word-processor format, if possible. We can redraw any figures as long as their content is clear. Photos should be glossy, color or black-and-white prints of at least the size they are to appear in *QEX* or high-resolution digital images (300 dots per inch or higher at the printed size). Further information for authors can be found on the Web at **www.arrl.org/qex/** or by e-mail to **qex@arrl.org**.

Any opinions expressed in *QEX* are those of the authors, not necessarily those of the Editor or the League. While we strive to ensure all material is technically correct, authors are expected to defend their own assertions. Products mentioned are included for your information only; no endorsement is implied. Readers are cautioned to verify the availability of products before sending money to vendors.

Empirical Outlook

Doug Smith, KF6DX
kf6dx@arrl.org

Amateur Radio: At the State of the Art

For what must seem like eons, many have bemoaned the decline of experimentation and homebrewing in Amateur Radio. Look at the numbers participating in that sort of activity and you might indeed find a significant downward trend. If you were to examine instead the level of technical accomplishment of the new and remaining participants, we think you'd find quite a different situation. We try to support the latter view — and combat the former — on a regular basis here on these pages.

As delineated in rules and regulations, the Amateur Radio Service charter addresses content and means equally: what we communicate and how we communicate it. In actual fact, our roles in emergencies and disasters tend to outshine our technical prowess, at least in the mainstream press. Regular folks are concerned chiefly with what the technology does for them and not with how it's done. That attitude carries over to ham radio and to most other facets of our lives, really. No matter how elegant is some solution, its prime value lies in how well it fills a need.

It's hard to do innovative design in this era, but experience has shown that the best inventions are relatively simple in concept. Furthermore, they create capabilities that the end user didn't know he needed but which make life better somehow. VCRs, cellular telephones, e-mail and cable television are among our favorite examples. Remember: All that stuff came along only in the last 30 years or so!

Now in Amateur Radio we have digital signal processing, high-speed data, digital voice and image, and a host of other tools at our disposal. The doors are open to experimentation on all fronts. Just look at what Flex Radio Systems have done (see the advertisement in this issue and in May *QST*). You could elect to write some software for the SDR-5000 to make it do new things, or you could choose to use its considerable capabilities to set up an emergency communications network, a cross-band repeater, Internet gateway, or other useful systems — the sky's the limit.

Some of the inspiration for Flex Radio came out of the ARRL Software Radio Working Group, now headed by Bob McGwier, N4HY, who works with Flex. The technology is so far advanced that interest extends far beyond ham radio.

The same is true of what the ARRL High-Speed Multimedia Working Group are achieving. Now we're seeing radios with Internet remote controls and other networking features. The D-STAR system has been well documented here, for example. Opportunities exist for command, control and communications that were undreamed of just five years ago. The use of inexpensive spread-spectrum equipment by hams on our shared microwave bands helps establish and maintain our presence there so we don't lose them.

The initial round of work by the ARRL Digital Voice Working Group is largely finished. Witness the AOR AR-9800 as developed by Yoshi Nishimura, JA6UHL, and similar, compatible units developed by Dennis Silage, K3DS, and his students at Temple University. It all started with the work of Charles Brain, G4GUO, several years ago.

Amateurs have also done extensive work on adaptive, so-called "smart" antennas; deconvolution for "moonbounce" (EME) and other dispersive channels; and MF and LF narrowband modes, among other areas.

The point is: Amateur Radio *is* on the leading edge of technology, perhaps more so than ever before. It doesn't matter whether you concern yourself with what or how you communicate. You have the ability, resources and assistance to make a difference in the future of our Service. Write us a letter and let us know what interests you most. We want this forum to reflect your likes. It's a medium for the exchange of ideas and information, putting people together for a common goal.

Slow-scan fans in Southern and Central Florida take note: Joshua Heath, KI4NNQ, has started a slow-scan net on the 146.625 MHz machine (W4JUP/R) out of Jupiter (TX = 146.025 MHz, CTCSS = 114.8 Hz). It's called the Jupiter/Tequesta Repeater Group Slow-Scan and Ragchew Net. It meets at 7:30 PM every Wednesday night. Check-ins are welcome whether you have slow-scan capability or not. The group is also interested in digital slow-scan via the G4GUO/AOR/K3DS digital voice/image/data format. Many in the group are now reading *QEX*.

A Direct-Conversion, Phasing-Type SSB Rig — Revisited

If carefully built and adjusted, a phasing-type SSB rig can sound better than a superhet. Here's an improved version of a previously-published transceiver for ragchewing on 75 and 40 meters.

Rod Brink, KQ6F

A few years ago I was inspired by Rick Campbell, KK7B, and his work with direct-conversion phasing-type rigs.[1] I began playing around with these types of circuits and built a two-band transceiver that performed well enough to merit a *QEX* article.[2] The tinkering continued, and improvements have been made. This article discusses those improvements and presents an updated design.

Diode Mixers Are Okay, but A Tayloe Detector is Better

The original design employed two conventional diode mixers for developing the in-phase (I) and quadrature (Q) channels. While ubiquitous and easy-to-use, diode mixers suffer from a 7 dB mixing loss. For proper termination, I used 6 dB resistive pads at the IF outputs and this increased the total loss to 13 dB. Additional downstream amplification was required in the receiver to compensate for the loss, and this added to the overall noise. There had to be a better way.

Enter the Quadrature-Sampling Detector, known in some literature as the Tayloe detector. Its beauty is found both in its simple elegance and its exceptional performance. Figure 1 illustrates a single-balanced version. It can be visualized as a four-position rotary switch revolving at a rate equal to the carrier frequency. The 50 Ω antenna impedance is connected to the rotor and each of the four switch positions is connected to a *sampling capacitor*. Since the switch rotor is turning at exactly the rate of the RF carrier, each capacitor will track the carrier's amplitude for one-quarter of the cycle and will hold its value for the remainder of the cycle. The rotating switch will therefore sample the signal at 0°, 90°, 180° and 270°, respectively. Stated another way, the rotating switch performs a downward conversion to audio baseband and the sampling capacitors each store ¼ of the RF cycle. If we connect the sampling capacitors to differential-input op amps as shown in Figure 1, we obtain the I and Q channels necessary for sideband selection.

This circuit may also be thought of as a *digital commutating filter*. This means that it operates as a high-Q *tracking* filter, where Equation 1 determines the 3-dB bandwidth,

[1]Notes appear on page 12.

25950 Paseo De los Robles
Corral de Tierra, CA 93908
kq6f@arrl.net

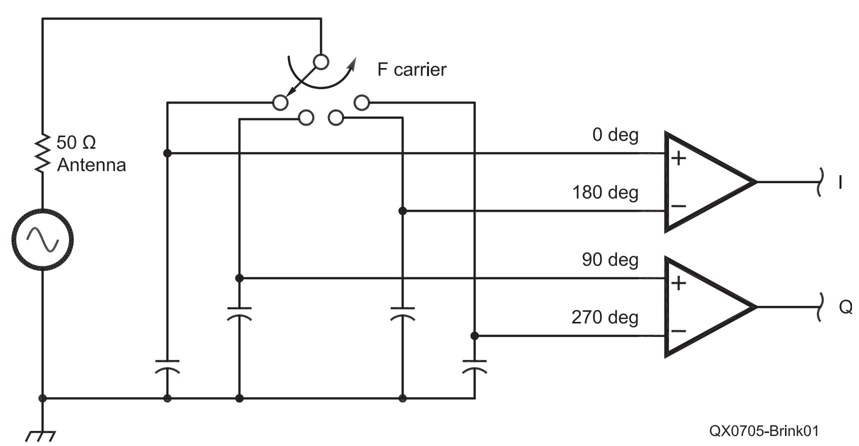

Figure 1 — Quadrature Sampling Detector — The switch rotates at the carrier frequency, so that each capacitor samples the signal once per revolution. The 0° and 180° capacitors differentially sum to provide the in-phase (I) signal and the 90° and 270° capacitors differentially sum to provide the quadrature (Q) signal.

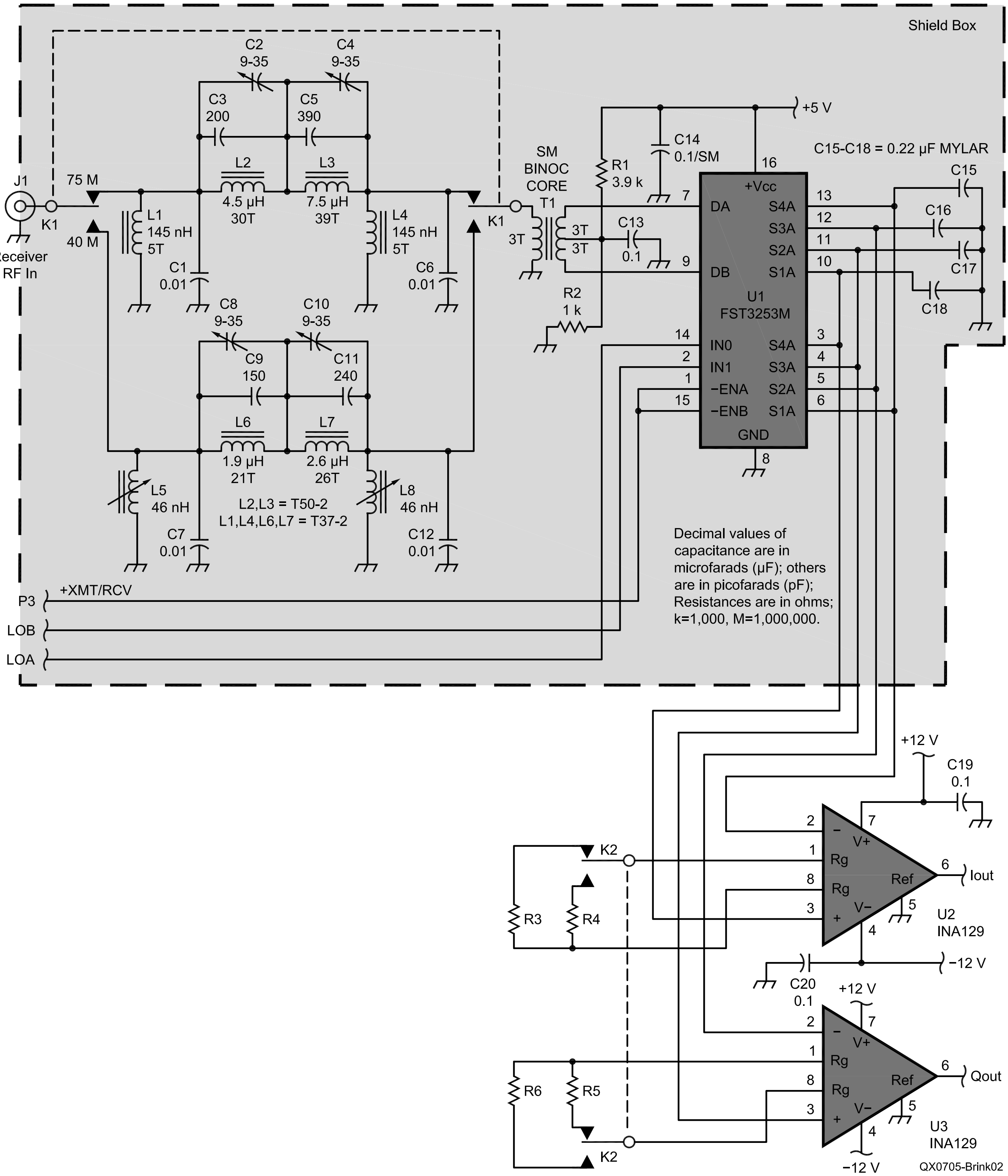

Figure 2 — Receiver Front End — Preselection filters are Cauer-configuration. Note the preculiar component values.

n is the number of sampling capacitors, R_{ANT} is the antenna impedance and C_S is the value of a single sampling capacitor.

$$BW \text{ of the detector} = \frac{1}{\pi\ n\ R_{ANT}\ C_S} \qquad \text{[Eq. 1]}$$

It gets its high Q factor from the fact that the four capacitors are being charged via the common impedance R_{ANT}. At or near resonance, the caps are being charged and discharged a very small amount at a time and thus are drawing extremely small currents. Well away from resonance, however, the capacitors are randomly charged and discharged, and the input impedance becomes low.

Conversion Loss

The real payoff with the Quadrature Sampling Detector (QSD) is its performance. It has about 1 dB of conversion loss. Compare that with the total 13 dB loss in the diode mixer and its termination pad, and you begin to gain an appreciation. The small loss occurs because the sampling capacitors are drawing such small currents at or near resonance, and thus the loss in the commutating switch is correspondingly small. I purposely chose 4:1 multiplex bus switches with only 4 Ω of ON resistance.

Receiver Front End

Figure 2 shows the preselector filters, QSD and first-stage amplifiers. The preselector filters are Cauer bandpass configuration and have some peculiar component values. The end-capacitor values (0.01µF) seem high, and the inductors connected in parallel with those capacitors seem inordinately small. In fact, adjustment of these filters requires a spectrum analyzer and tracking generator, and is a bit touchy. Just spreading the turns on the small end inductors produces significant changes in the passband characteristics. In light of this, you might question the wisdom of using these types of bandpass filters. I chose them because they present a smoother passband response than the triple-tuned circuit used in the original design, and have fewer parts (10 versus 13). For shielding purposes, I wanted all front end components to fit within a small cast-aluminum can that I had. The triple-tuned filters would have been too large.

The Cauer filters were designed using a clever software program called *Elsie* from my friend Jim Tonne, WB6BLD.[3] The responses of the two filter types are compared in Figure 3.

The single-balanced QSD configuration shown in Figure 1 is very simple, but I chose to use the double-balanced version in Figure 2 for its superior common-mode and even-harmonic rejection.[4]

The first-stage amplifiers U2 and U3 are low-noise, low-distortion instrumentation amplifiers. Relay K2 permits switching the gain between 40 dB and 27 dB.

Audio Phasing Network Improvements

In the original design I copied the audio phasing network directly from Rick Campbell's chapter in *Experimental Methods in RF Design*. Had everything else in the receiver been perfect in terms of phase and amplitude variations, this network would have provided nearly 60 dB of opposite sideband suppression over a range of 270 to 3600 Hz. I was never able to achieve that, however, since the other critical receiver circuits were, of course, less than perfect. About the best suppression I could achieve was 40 dB.

This time around I wanted to achieve 60 dB of opposite sideband suppression, and additionally to widen out the audio range over which this suppression occurs. To obtain that, I turned to another of Jim Tonne's programs called *Quad.* To obtain a suppression range of 50 to 5000 Hz requires five op-amps in each of the I and Q channels. In Figure 4, relay K3 switches the inputs of these phasing networks between the U2 and U3 outputs for receive and the U4 output for transmit. Amplifier U4 functions simply as a unity-gain buffer for the incoming transmit audio.

Phase Tweak Improvements

My original design employed *quadrature hybrid transformers* for developing the local oscillator I and Q signals. These are frequency sensitive and therefore one was required for each band. Furthermore, achieving near-perfect 90° phase shifts between I and Q oscillator signals required *tweak* capacitors at the hybrid outputs. The tweak procedure was a bit clumsy.

In the new design, the phase tweaks are made at the output of the audio phasing networks, instead of in the LO circuitry. The adjustment is made with one potentiometer for receive (R62) and another for transmit (R64). This is accomplished by driving one side of the phasing potentiometers with the Q-channel output, and driving the other side with the same signal inverted. A small sample of the signal at the potentiometer wiper is then mixed with the I-channel signal. This adjustment procedure is not only easier to perform, but gives better performance. With the old way there was just one adjustment for both receive and transmit, and because phase variations between the two were unequal, the final setting became a compromise. Amplitude imbalances are nulled out for receive (R55) and transmit (R51).

Local Oscillator Improvements

The AD9835 DDS chip is used in both the old and new designs. In the old design, spur suppression was more or less "winked" at with the use of low-pass filters connected between the DDS output and the quadrature hybrid transformers. Performance wasn't bad, but a few birdies could be heard within both the 75 and 40-meter bands.

This time I decided on a more rigorous approach and added a low-distortion VFO and a phase locked loop to generate the LO. See Figure 5. The DDS now becomes the reference input to the PLL, and the VFO (Q1) runs at four times the DDS input. Relay K4 selects taps on the VFO tank transformer, T2, for 75 or 40-meter operation. With this arrangement the PLL loop filter functions as a *tracking filter* and spurs are limited to those that can squeeze through its narrow bandwidth. A Johnson counter, U16, divides the 4× VFO signal back down for phase comparison with the DDS in U14. The counter also generates the necessary quadrature clocking signals for the 4:1 multiplexers.

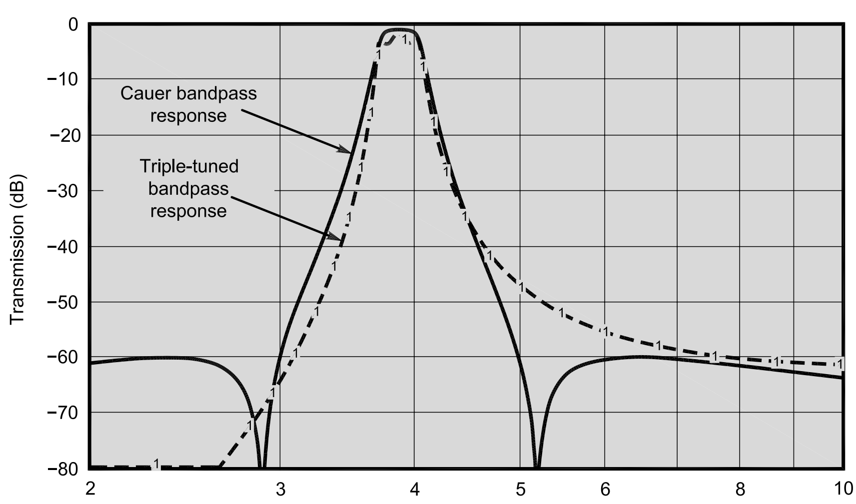

Figure 3 — Comparison of preselector filter bandpass curves, simulated using *Elsie*.

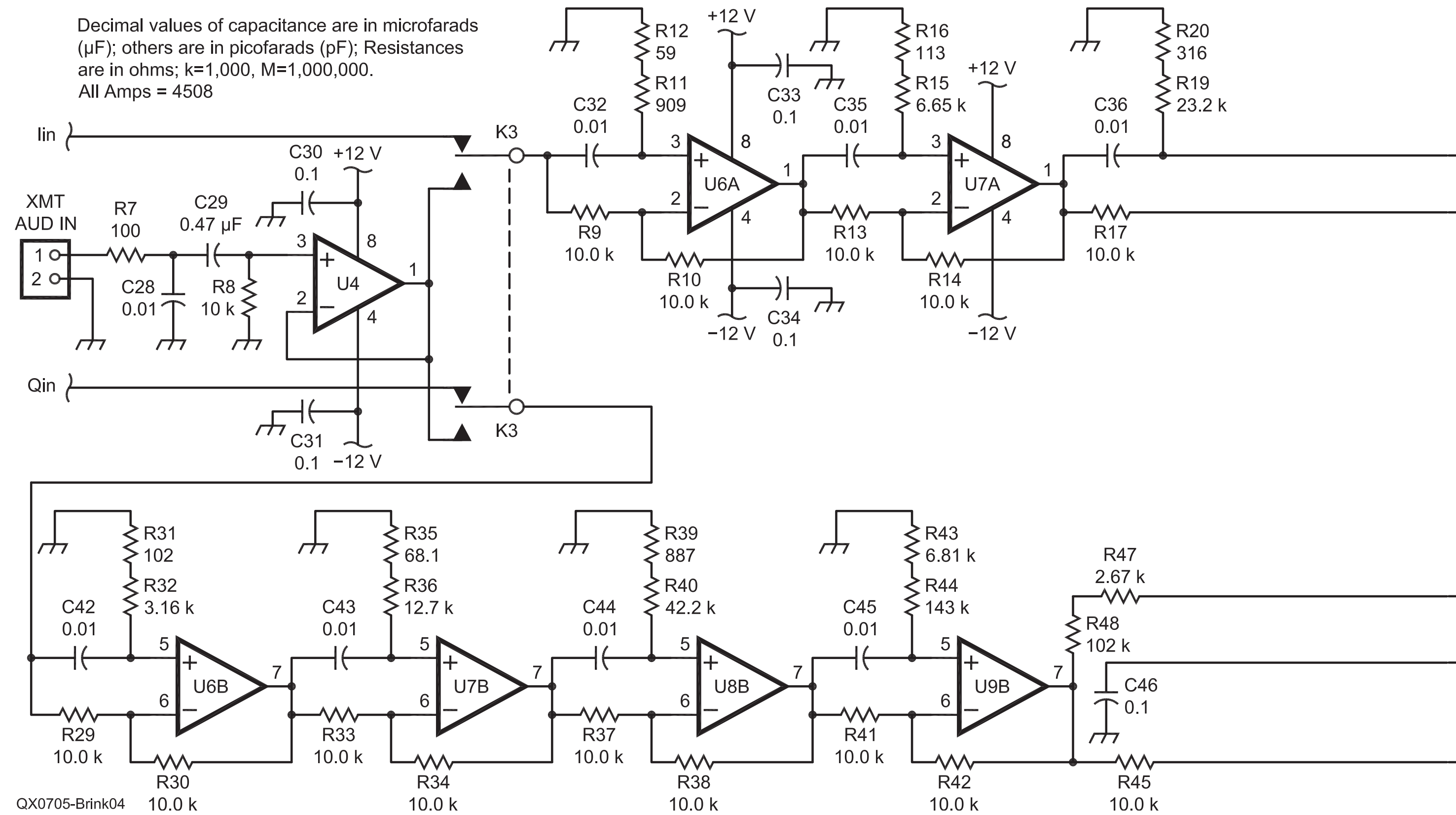

Figure 4 — Hilbert transformer for 60 dB opposite sideband suppression over a 50 to 5000 Hz range. Relay K3 is the transmit/receive switch. There are separate phase and amplitude tweaking adjustments for receive and transmit.

Sideband Selection

The old design was set up for lower sideband only. This seemed like a reasonable choice at the time since 99% of the phone operation in the 75 and 40-meter bands occurs on LSB. This time I decided that an extra relay was well worth the step-up in flexibility. Relay K5 reverses the phase of the Johnson counter outputs to both the receiver and transmit multiplexers (U1 and U19, respectively).

With phasing rigs, there are other ways of switching sidebands, but they are more complicated. For example, reversing the I and Q *outputs* to the modulator drivers changes sidebands in transmit and reversing the *inputs* to the I and Q channels works for receive. But reversing the LO signals accomplishes both and requires only one relay.

Transmit Generator

In Figure 5 the QSD is turned around for up-converting audio to RF and thus becomes a *Quadrature Sampling Exciter* (QSE). The I and Q-channel transmit audio signals feed audio drivers U17 and U18, which provides complementary outputs to the QSE, U19. The push-pull RF signals that appear at U19 pins 7 and 9 are transformer coupled by T3 to band-selection relay, K6, and thence to the low-pass filters. The filters remove undesirable upper harmonics that appear at the QSE output. The filters are designed for 220 Ω termination instead of the usual 50 Ω, in order to reduce the loading on the QSE, and thereby improve its up-conversion efficiency.

The filtered RF drives the pre-driver U20 in Figure 6. Q2 is a shunt switch at the input, which suppresses an undesirable RF surge that occurs when switching from receive to transmit. The surge results from the charging of coupling capacitors C63 to C66 by unequal dc voltages that appear across them when U19 is enabled by the +XMT signal. The Stamp microcontroller (see Figure 9) generates the +XMT INH signal for 30 ms when switching to transmit to squelch the surge.

With Q3 turned off, the pre-driver gain is set by R81 and R80. In this half-power mode the RF at the pre-driver output is about 0 dBm. The following RF driver and PA stages boost this up to about 50 W, which is sufficient to drive my Alpha 89 to legal-limit. For operating "bare-foot," Q3 is turned on by the +FULL PWR signal from the microcontroller, which increases the pre-driver output to +4 dBm and then gets amplified to 125 W peak output.

Transmitter IMD

The SSB signal that appears on J6 in Figure 6 is essentially free of IMD. Why? Unlike a superheterodyne radio with its multiple mixers and phase-erratic filters, the transmit path consists primarily of low-distortion op-amps. The up-conversion to RF is done in one step with a *sampler*, not a mixer.

From J6, the signal passes to the RF driver (Figure 7) and PA where it is amplified by 47 dB, and this is where some inevitable IMD is introduced.

Two-tone audio testing (results shown later) indicated that most of the IMD was being introduced in the RF driver stage. To improve its performance, the following changes were made:

- The turns ratio on T2 was changed to improve impedance matching between the two amplifier stages and to increase the overall gain by +6 dB.
- The extra gain permitted more intra-stage feedback. R4 was decreased from 220 to 150 Ω. A feedback loop was added to the second stage, consisting of R12 and a 1-turn winding on T3.
- Q4 and Q5 were changed from NTE236 transistors to the more robust MRF475 devices.

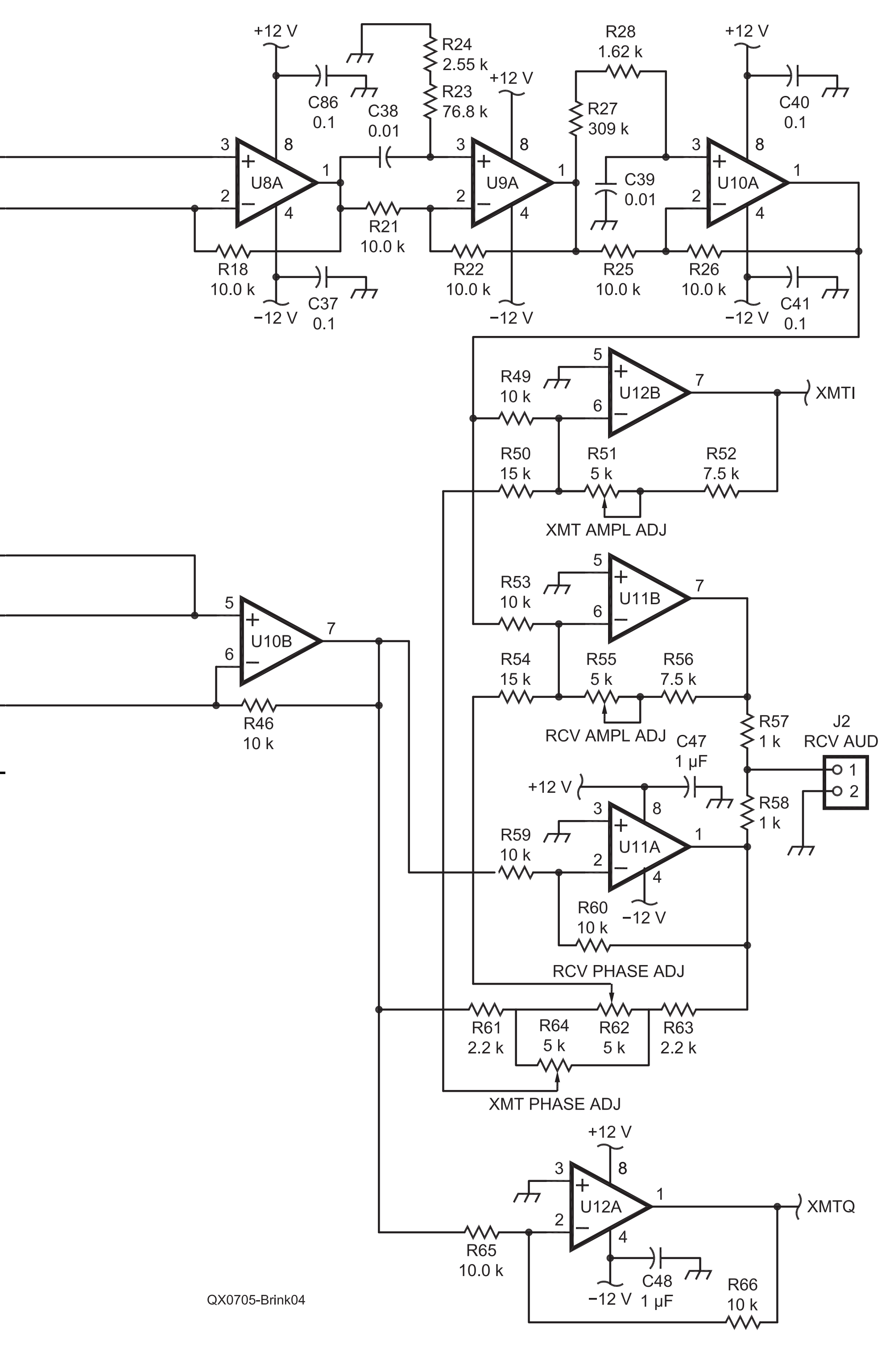

Emitter degeneration in both stages (R5, R6, R10, R11) also helps reduce IMD, although their main purpose is to stabilize and ensure nearly equal bias currents in both transistors of each stage.

The PA stage in Figure 8 is relatively clean. It's the popular Helge Granberg design with the output transistors changed from MRF454 type to the less-expensive 2SC2879. Granberg did a good job and I've never been able to improve his circuit.[5]

Microcontroller and DDS

The Stamp II microcontroller connects to the host PC via a 9600-baud serial link and runs firmware stored in its EEPROM. It provides control signals to the DDS and to the various other circuits in both the receiver and transmitter sections. See Figure 9.

R1 and R3 are chosen to produce about 1.5 V p-p into the U13 inverter load in Figure 5.

ADC and XMT Relay

U3 is an 8-bit 4-channel ADC that measures and digitizes analog voltages from the receiver AGC, forward and reflected voltages from the directional coupler on the RF low-pass filter board, and voltage from a temperature sensor mounted to the PA heat sink. See Figure 10. The forward and reflected voltages are peak detected by U4 and associated components, and represent *peak* power values at the transceiver output.

The XMT relay, K1, is keyed when switching to transmit, and supplies +12 V dc to the PA driver and to the T/R relay on the low-pass filter board.

Receive Audio Processing

Figure 11 shows the receive audio processing section. The audio signal that appears on J2 in Figure 4 is that of the selected sideband, but is extremely wide; its bandwidth is limited only by the combined selectivities of the preselector filter and the QSD. (Essentially *no* audio rolloff occurs in the phasing networks — only a 90° phase shift between the I and Q channels). Therefore, more processing is required to improve receiver selectivity.

The signal from J2 enters the processing board at J7 and passes through a 5-element Chebyshev low-pass filter with rolloff beginning at 6 kHz. It then is amplified by as much as 40 dB by U7, a variable gain amplifier (VGA). The VGA gain is controlled by the full-wave AGC amplifier, U8. The band limiting action of the Chebyshev low-pass filter keeps off-channel audio from falsely driving the AGC.

The gain-controlled audio at U7 pin 7 is passed to an 8th order, low-pass switched capacitor filter to obtain further selectivity and for audio passband selection.

Audio Passband Selection

The audio bandwidth in the old design was rolled off at about 3500 Hz for both transmit and receive. This was higher than most commercial rigs and, along with its low end response extending down to 25 Hz, made for high quality transmit audio. I received a lot of compliments on my transmit audio.

Recently there has developed a growing group of hams who like to play around with enhanced sideband audio (ESSB). So in keeping with the trend, I decided to extend the Receive passband range and to make it variable. This is accomplished with the switched capacitor filter, U6.

The U6 cutoff frequency is determined by the rate at which it is clocked — the clock-to-corner frequency ratio is 50:1. The clock requirement is a square wave, which is provided by U5, a divide-by-2 flip-flop. I chose corner frequencies of 6.7, 5, 4, and 3.3 kHz. U9 is a presettable counter clocked by a 2 MHz crystal oscillator. Its output pulses are 100 times the corner frequencies, or 666, 500, 400, and 333 kHz, respectively, depending upon the preset inputs from the microcontroller.

A Little Bass Boost to Sweeten the Receive Audio

U6 contains an uncommitted op-amp that normally is configured as a low-pass filter at

Okay, How Did It Turn Out?

The original design was done casually. I wasn't trying to set the world on fire by breaking any performance barriers or coming up with any new techniques. I just wanted to learn about direct-conversion and play around with new-to-me circuits. But, above all, it had to sound good.

This time casual gave way to a little rigor. Sounding good was still paramount, but I also wanted to soup up performance, especially in the areas of receiver intercepts and audio fidelity.

Receiver Noise Floor/MDS

Minimum Discernible Signal is defined as the input signal level that produces a 3 dB increase in the receiver audio output power above that with no input signal. I've always had a problem with that definition.

For one thing, how do you accurately measure the output power with no signal applied? After all, it's noise! It will vary with time, will be heavily influenced by the audio bandwidth setting, and will be very difficult to nail down. So instead, I use my own definition: the minimum signal I can discern, or hear. On that basis, the pseudo-MDS is –120 dBm.

This is not as spectacular as some receivers, but hey, do we really want a super-sensitive receiver on the low bands? In general, the more sensitive a receiver, the more apt it will be to overload on strong signals. And most signals on 75 and 40 meters are strong! So –120 dBm seems about right to me.

Receiver S/N

The receiver is a lot quieter than either of my two commercial rigs (at least to my ears). I made measurements to confirm this, and while the measurements bear it out, they don't tell the whole story. The real difference shows up in comparative listening tests.

The measurements were made on three transceivers: Kenwood TS-870, ICOM 756 Pro, and my phasing rig. A signal generator with RF output set to –72 dBm was connected to each of the receiver inputs and the receiver tuned off the carrier to produce a 1 kHz tone in its speaker. Audio bandwidths were all set equal. A scope was connected to the speaker output and peak-to-peak measurements made of the 1 kHz audio output and the noise output with the signal generator disconnected. The S/N ratio was then converted to dB. Table 1 shows the results.

The phasing rig sounded much quieter than the figures indicate. The reason is that the phasing rig noise is much higher in frequency, essentially inaudible, whereas that of the others is lower in pitch.

Receiver 3rd-Order Intercept

To make this measurement, I used Dr Ulrich (KA2WEU) Rhode's setup and procedure as described on page 11-20 of *The ARRL Handbook*, 2007 Edition. I adjusted the two signal generators to equal amplitude into my homebrewed hybrid combiner and set them 20 kHz apart to 3.85 and 3.87 MHz, respectively.

The signal levels out of the hybrid into the attenuator was –3 dBm. The IMD product, 2f1 – f2 = 3.83 MHz. With just one signal applied and the receiver tuned to that signal, I adjusted the attenuator to obtain 1 Vp-p audio output. Then, with both signals and the receiver tuned to 3.83 MHz, I again adjusted the attenuator to obtain an identical 1 Vp-p output, noting the difference in attenuator settings. I now had all the necessary values to plug into the formula:

$$IP3 = \frac{3(-3)-(-3-60)}{3-1} = +27 \text{ dBm}$$

Receiver Audio Bandpass

The curves in Figure 14 show the various effects of the receive audio processing. With no bass boost and with 6.7 kHz bandwidth selected for the switched-capacitor filter, the response is flat out to 6 kHz. At that point the Chebyshev passive filter begins to roll off. The bandwidth can be reduced by changing the switched-capacitor filter to 5 kHz bandwidth (as shown), or 4 kHz, or 3.3 kHz. These are selected by depressing virtual buttons on the GUI. The bass boost is always in effect and peaks at about 100 Hz as shown.

Transmitter Two-Tone IMD Tests

I built a two-tone audio generator based on the schematic in *The ARRL Handbook*, 1994 Edition. Ultra-low distortion tones at 700 and 1900 Hz were injected into the line input of the transmitter and the level adjusted to produce 100 W into a dummy load. An RF sampler was connected in series and the sampler output run into a spectrum analyzer. Figure 15 shows the results.

Note that the 3rd and 5th-order IMD products are referenced down from 0 dBm, a level 6 dB above the two tone peaks. This is the correct method of measurement. The reason is that we are measuring PEP values, and if only one tone was injected, its amplitude would be 6 dB higher than that of two tones. With two tones the power is divided evenly between them and so each is 6 dB lower. The one-tone level is the correct reference.

Table 1
Output Signal to Noise Ratio Comparisons

Rig	*1 kHz Audio Output (V)*	*Noise Output (V)*	*S/N (dB)*
Kenwood TS-870	4.844	0.906	14.6
ICOM IC-756 Pro	1.556	0.112	22.2
Phasing rig	1.766	0.092	25.7

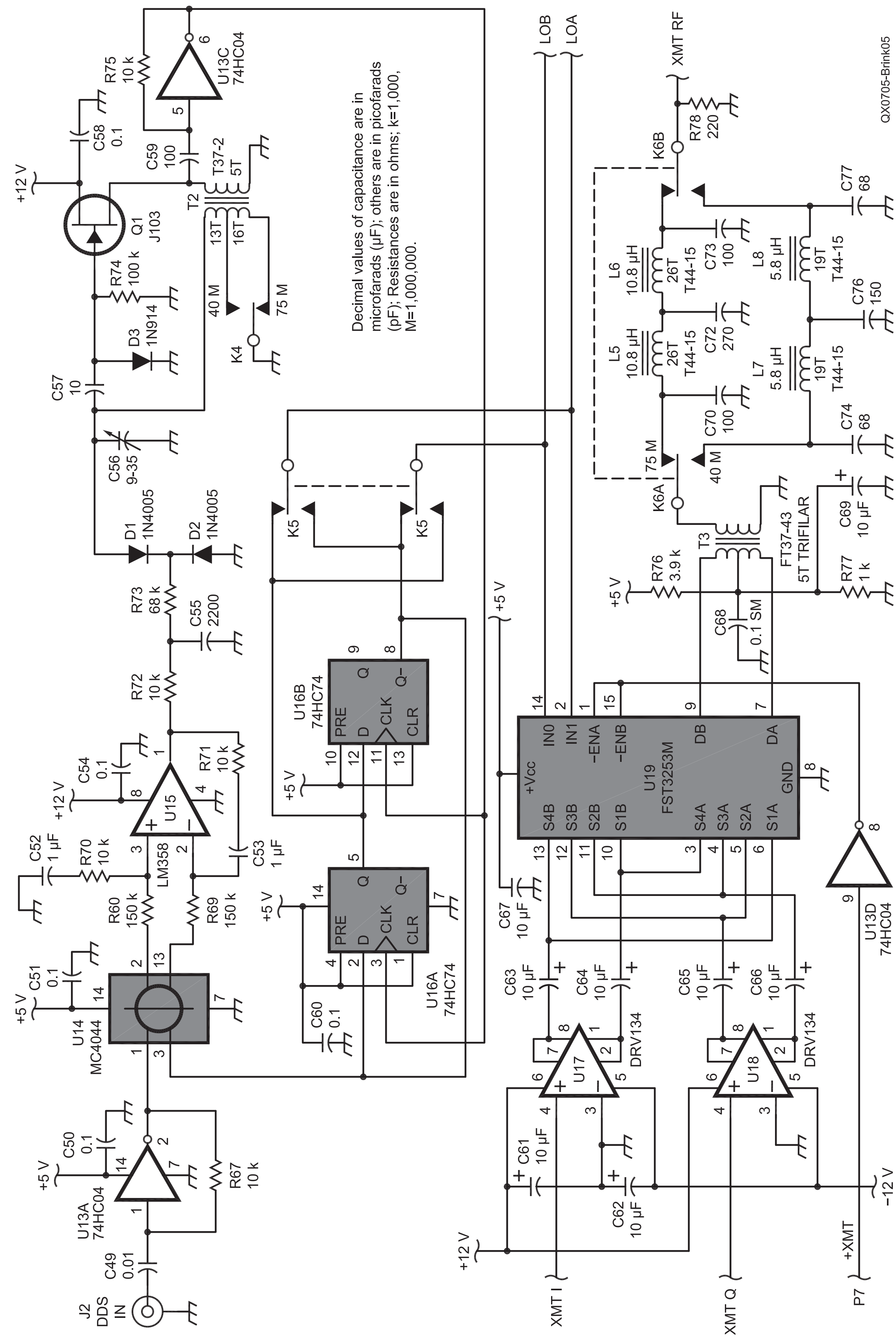

Figure 5 — Phase-locked-loop VFO for LO generation and quadrature sampling exciter (QSE) for transmit.

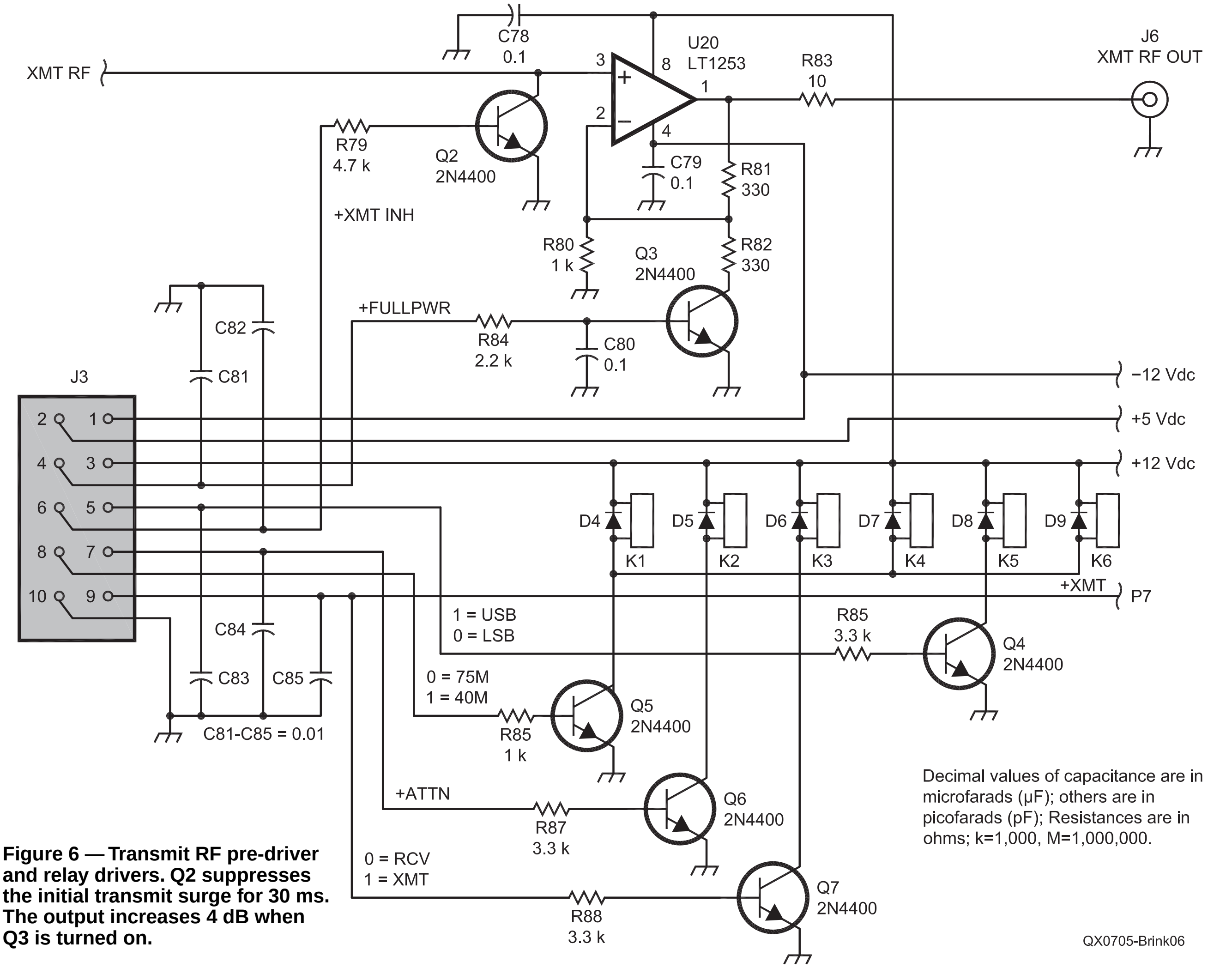

Figure 6 — Transmit RF pre-driver and relay drivers. Q2 suppresses the initial transmit surge for 30 ms. The output increases 4 dB when Q3 is turned on.

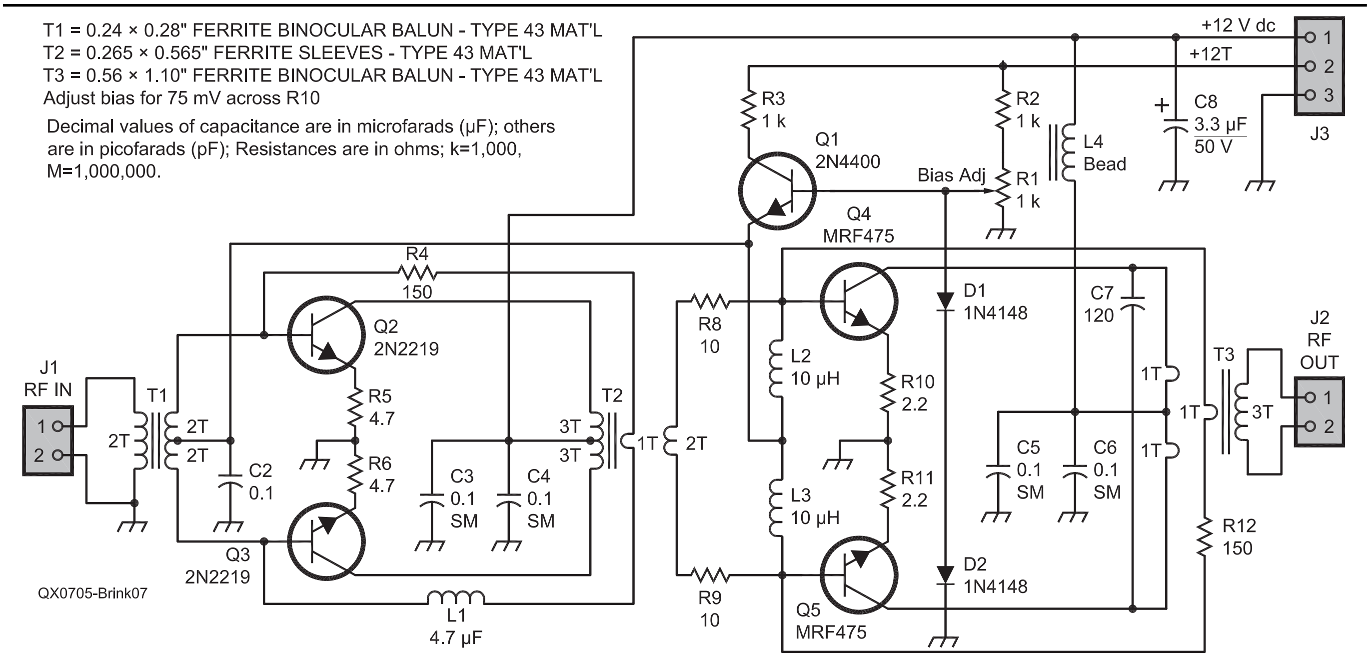

Figure 7 — RF Driver — To reduce IMD, the first stage feedback was increased and a feedback loop added to the second stage. The turns ratio for T2 was changed for more overall gain, to support the extra feedback.

the output of the switched capacitor filter, to reduce clocking noise. Since the noise is inaudible in this design, I decided instead to use the op-amp in a medium-Q circuit that boosts the bass about 8 dB at 100 Hz. I found that this improves the receive audio, and is particularly effective when listening to stations running enhanced audio.

Volume Control and Audio Output Amp

U10 is a digital pot designed for use in audio circuits. It receives serial data commands and clock signals from the microcontroller. In addition to setting the volume level, it also mutes the audio during transitions from transmit to receive, to prevent loud transient pops in the speaker.

The HA13118 amplifier board came as a small inexpensive kit, and uses a proprietary audio amp IC that drives the speaker in a bridge configuration. It can supply up to 6 W into a 4 Ω speaker when operated from +12 V dc.

A Power Supply (Actually Two)

The astute reader may notice that both positive and negative supply voltages appear in the schematics. Normally a transceiver operates entirely from a single 13.8 V dc supply and op-amps and other circuits that require dual supplies are biased at a single supply midpoint. Of course I could have followed suit. But some op-amps operate better from +12 and –12 V supplies, and so I opted to provide the dual voltages to accommodate these parts and to avoid the extra complications of midpoint biasing.

I actually use *two* supplies. The first is the traditional 13.8 V dc, 20 A supply that operates the PA. The second is a small switcher left over from an auxiliary hard disk unit, capable of supplying +5 V dc, +12 V dc, and –12 V dc, all at currents well exceeding the transceiver requirements. At first I was apprehensive about supplying the receiver circuits with power from an inexpensive switcher designed solely for computer use, but I have been pleased with the results. I placed it in a separate shielded enclosure and have experienced *no* discernible birdies or hash from it.

Firmware/Software

The firmware that runs in the Stamp II employs a BASIC-type instruction set and was developed using the PC-based editor supplied by Parallax, the Stamp manufacturer.

The PC software was developed using Microsoft *Visual Basic*. The Graphic User Interface (GUI) is a very simple virtual transceiver control panel. Figure 12 is a screen shot from that software.

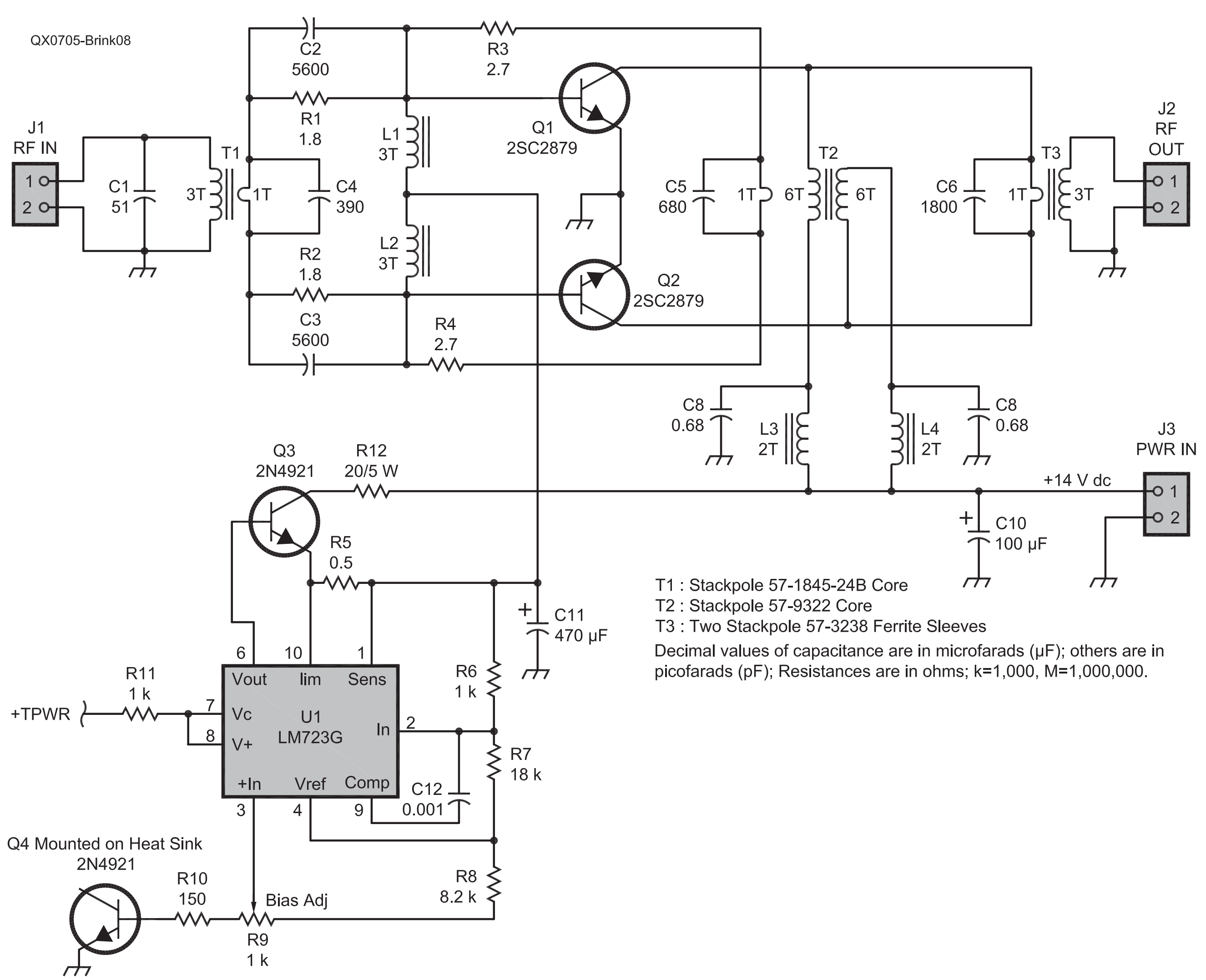

Figure 8 — PA Schematic — The circuit is nearly identical to Helge Granberg's well-known design, which has been around for decades.

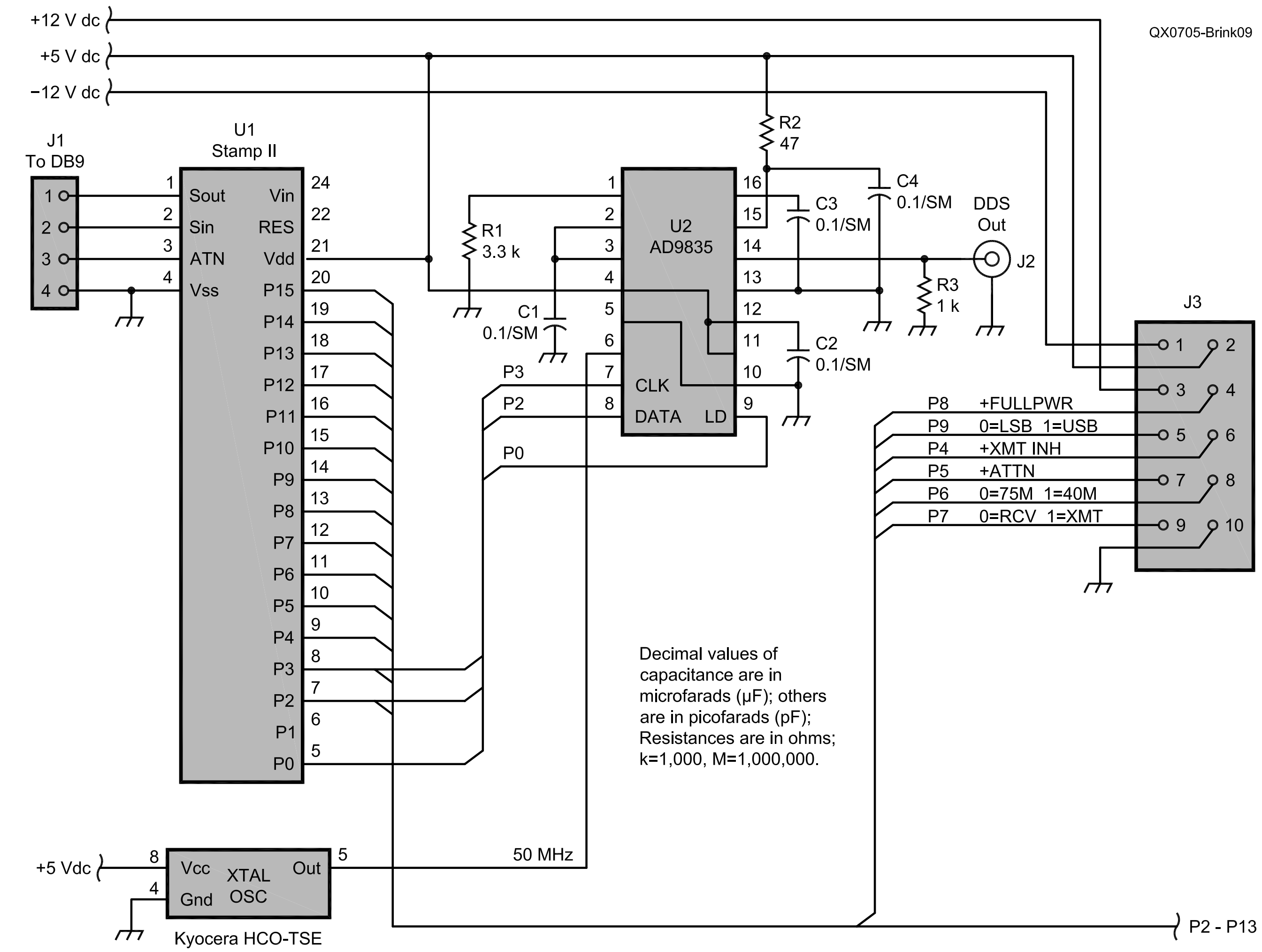

Figure 9 — Microcontroller and DDS — R1 and R3 were chosen to generate about 1.5 Vp-p at J2.

Packaging

A chassis that once saw life as an external hard disk enclosure was used to house the transceiver. PC boards were laid out on a functional basis — one for RF, one for control and a third for the transmit output filters and directional coupler — all sized to fit comfortably inside. Figure 13 shows the finished unit with cover removed.

It's worth pointing out something important about the RF board. *It is imperative that the board be laid out with an extensive ground plane*. This is especially important for the circuits shown in Figure 3. I worked hard to get most of the traces onto the back (solder) side of the board in order to provide as much uninterrupted ground plane on the front side. But if I had it to do over, I'd probably split the traces about 50/50 between front and back, use flooded ground planes on *both* sides with plenty of vias to interconnect the two. Either way, it's extremely important to make the ground system as close to zero impedance as possible.

For more information about this transceiver and additional photos, you can visit my Web page: **www.redshift.com/~kq6f/KQ6F/indexx.html**

Rod Brink first became interested in ham radio during his high school days, back in the 1950s, but later got busy with college and work, and forgot all about it. After retiring in 1995, he became licensed as KE6RSF, then AD6TV and now KQ6F. He holds BSEE and MSEE degrees, and worked 37 years for various Silicon Valley companies, serving as VP of Engineering for the last 20 years of his work life. He now spends much of his leisure time designing and building computer-controlled radios.

Notes

[1]W. Hayward, W7ZOI, R. Campbell, KK7B and B. Larkin, W7PUA, *Experimental Methods in RF Design,* ARRL, Newington, CT, 2003, Chapter 9. *Experimental Methods in RF Design* is available from your local ARRL dealer, or from the ARRL Bookstore, ARRL order no. 8799. Telephone toll-free in the US 888-277-5289, or call 860-594-0355, fax 860-594-0303; **www.arrl.org/shop**; **pubsales@arrl.org**.

[2]Rod Brink, KQ6F, *A Direct-Conversion Phasing-type SSB Rig, QEX* Nov/Dec 2005, pp 3-18.

[3]Available from **www.tonnesoftware.com**. Student version is free. The student version of *Elsie* is also included as one of the utility programs on the CD included with *The ARRL Handbook*, 2007 Edition. *The ARRL Handbook* is available from your local ARRL dealer, or from the ARRL Bookstore, ARRL order no. 9760. Telephone toll-free in the US 888-277-5289, or call 860-594-0355, fax 860-594-0303; **www.arrl.org/shop**; **pubsales@arrl.org**.

[4]C. Ping, BA1HAM, *An Improved Switched Capacitor Filter,* QEX, Sept/Oct 2000, pp 41-45.

[5]Helge Granberg, K7ES, was a well-known Motorola engineer, now SK. His circuit originally appeared in the 1986 *Motorola RF Data Manual*, Vol 2.

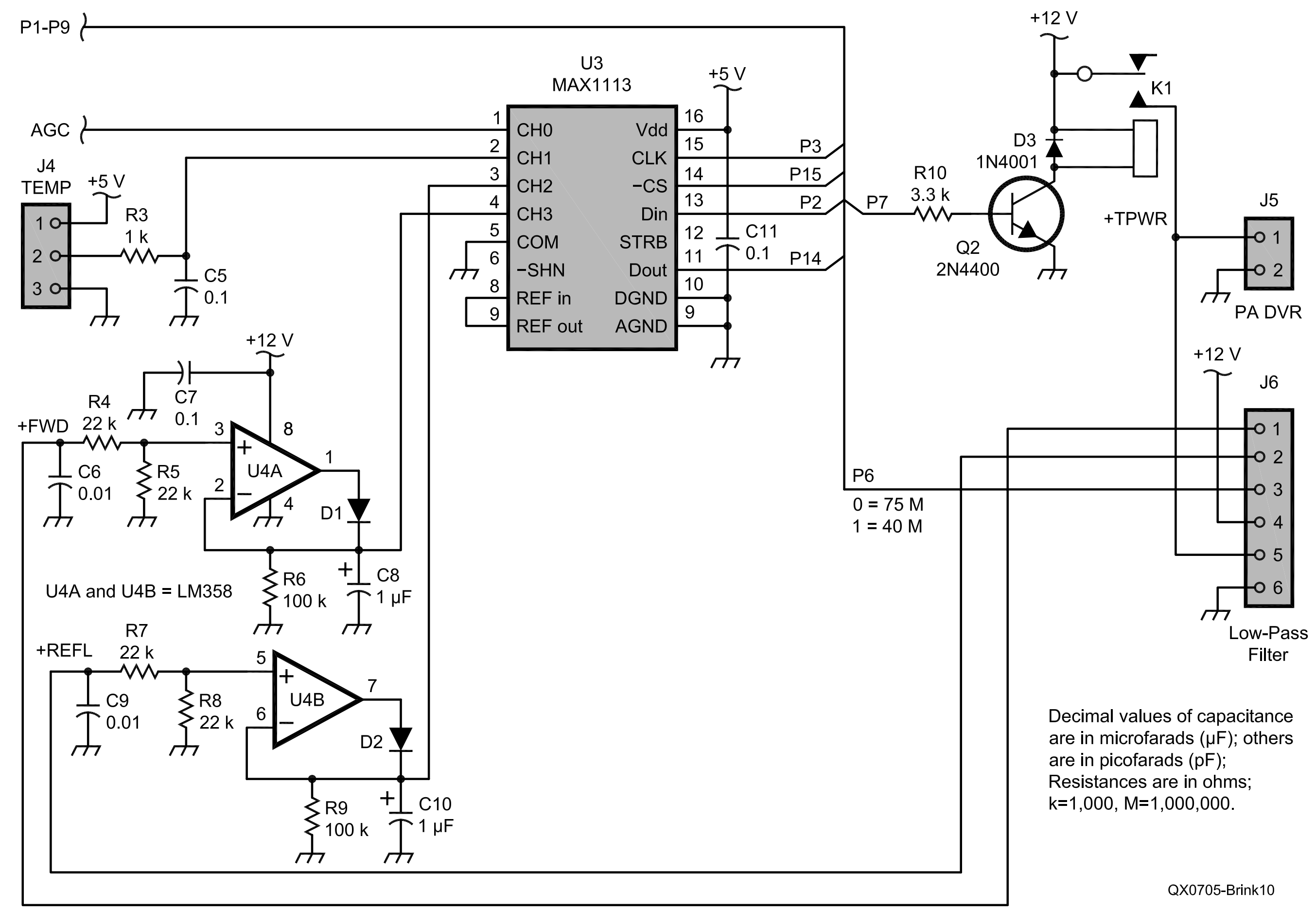

Figure 10 — ADC and Transmit Relay — ADC measures AGC voltage, heatsink temperature, forward and reflected transmit power.

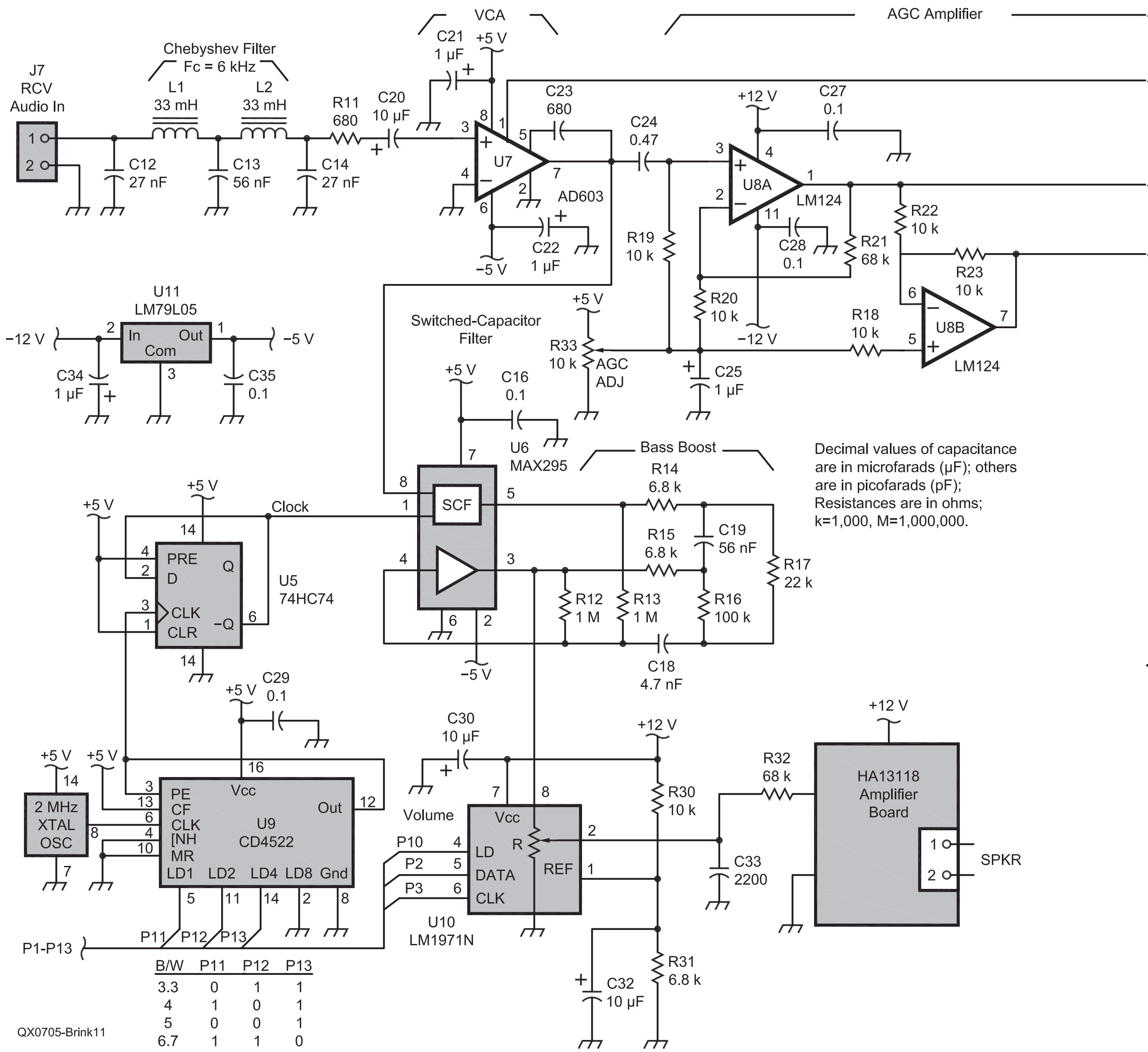

Figure 11 — Receiver Audio Processing — Switched capacitor filter, U6, is an eighth order, low-pass Butterworth type. The cutoff frequency is determined by the input clock frequency from U9, a presettable counter.

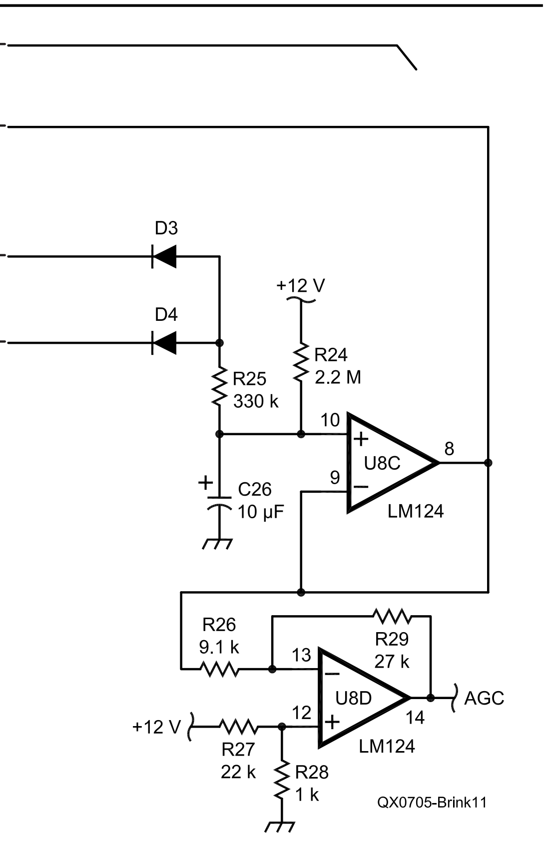

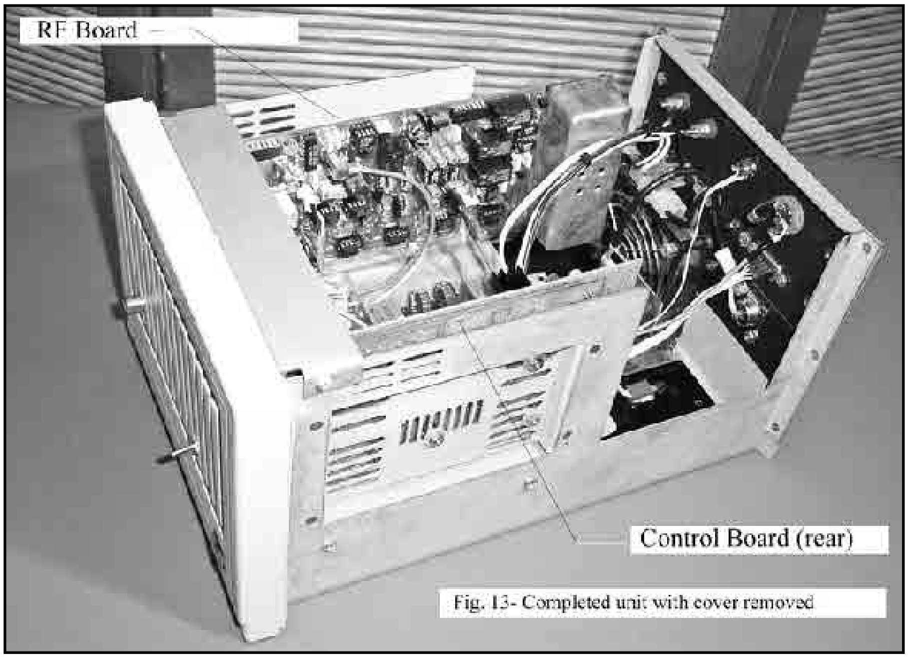

Figure 13 — This photo shows the completed unit, with the top cover removed.

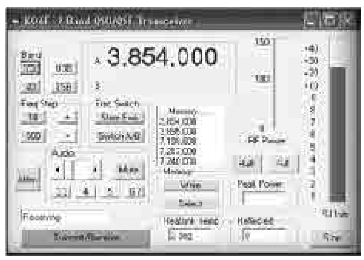

Figure 12 — This screen shot shows the graphic user interface (GUI). The PC software was written in *Virtual Basic*.

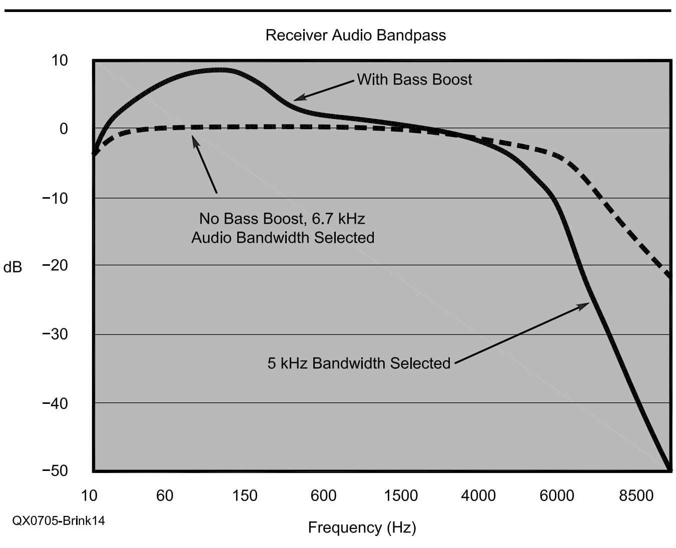

Figure 14 — With 6.7 kHz bandwidth selected, the response is rolled off above 6 kHz by the Chebyshev filter.

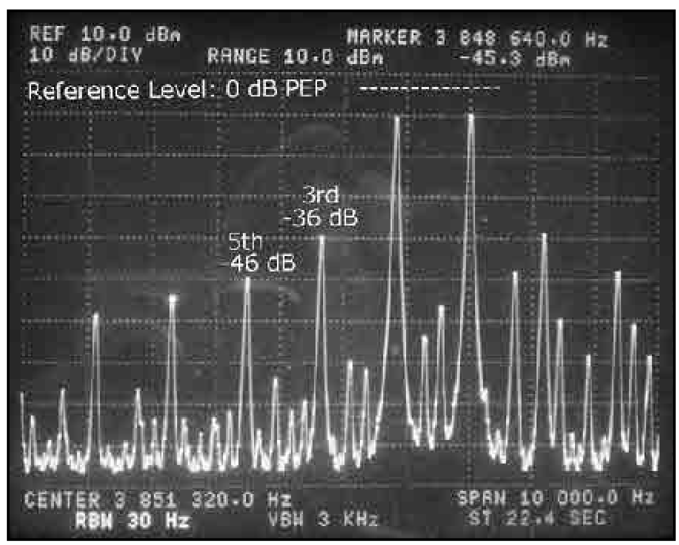

Figure 15 — Transmitter IMD — The reference level is 6 dB above the two input tones. See the text for an explanation.

Designing the Z90's Gaussian Crystal Filter

This article presents a detailed design review of the Gaussian crystal filters in the Z90 panadapter.

Jack Smith, K8ZOA

A critical part of the Z90 panadapter described in the March/April 2007 issue of *QEX* are the two crystal filters. Because a panadapter's filter has different requirements than a receiver filter for CW or SSB, and because filter design is often — but incorrectly — viewed as "black magic" we'll look at the filter in more detail. Although centered around a Gaussian filter, the procedure is identical for other filter types.

Before settling on the design discussed in this article, I built more than a dozen experimental crystal filters, with center frequencies from 3.58 MHz to 13.5 MHz. Based on that work, my design employs inexpensive microprocessor crystals manufactured by ECS, Inc International (**www.ecsxtal.com**). I used part number ECS-80-S-1X 8.0, with a nominal 8 MHz center frequency.[1] We start the design by selecting the target bandwidth, filter response type and number of sections:

Bandwidth

The target bandwidth is a judgment call. Our design permits two filters, "narrow" and "wide." Commercial analog spectrum analyzers provide automatic bandwidth selection between about 0.3% and 2% of the total frequency span. To analyze an SSB signal — a common use of a panadapter —a total span of about 10 kHz is appropriate. This suggests a bandwidth of perhaps 30 Hz to 200 Hz for the narrow filter. Experience with inexpensive microprocessor crystals shows that at 8 MHz bandwidths below 200 Hz become increasingly difficult due to crystal *Q* limitations, so we set the target narrow bandwidth at 200 Hz. Further, the narrower the filter, the slower the sweep speed must be to avoid amplitude and frequency errors.[2]

Also entering into the bandwidth choice is the Z90's maximum horizontal sample size of 240 data points. To reduce amplitude-measuring errors, the filter should have a 3 dB bandwidth significantly greater than the data point spacing. With a 20 kHz span, the data points are spaced 83.3 Hz apart. With a 200 kHz span, representing viewing ±100 kHz from the tuned frequency, data points are spaced every 833 Hz. A 1-kHz-bandwidth "wide" filter is a reasonable choice, albeit a bit on the narrow side. Perhaps more importantly, experience shows that as the filter bandwidth increases much beyond 1 kHz for these 8 MHz crystals, our simple circuit topology fails to provide acceptable symmetry. Hence, we select 1 kHz as a reasonable "wide" bandwidth.

Filter Response Type

By juggling passband flatness against how fast the passband rolls off and other parameters, designers have developed many filter types, such as Butterworth, Chebyshev, Bessel and Gaussian. Gaussian or near Gaussian filters are traditionally in a spectrum analyzer or panadapter.[3, 4] A Gaussian filter provides an optimum amplitude response as it is swept through continuous or pulsed waveforms. (A true Gaussian filter requires an infinite number of elements; our four-section filter is, however, "close enough" to Gaussian response to be more than acceptable.)

Number of Sections

Increasing the number of filter sections improves the flank selectivity, or rejection of signals far outside the passband. Increasing the number of filter sections, however, makes the filter more demanding in terms of component quality and tolerance. As a judgment call, the Z90 uses a four-section filter. The standard reference on filter design is Zverev's *Handbook of Filter Synthesis*.[5] That book shows that a four-section Gaussian filter has a –60 dB bandwidth that is 10 times the –3 dB bandwidth, so our filter will have a 3 dB: 60 dB shape factor of 10:1. (Spectrum analyzers traditionally use a 3 dB: 60 dB shape factor, instead of the 6 dB:60 dB shape often found in Amateur Radio specifications.) Even if we use a 10-section Gaussian filter, the shape factor only improves to 4.8:1.

Characterize the Crystal Resonators to be Used

It is impossible to approach filter design in a systematic fashion without a decent knowledge of the motional parameters of the crystals to be used. As James Clerk Maxwell, of Maxwell equation fame, observed some 130 years ago:

"The most important aspect of any phenomenon from a mathematical point of view is that of a measurable quantity."[6]

Lord Kelvin expressed similar views:

"When you can measure what you are speaking about, and express it in numbers, you know something about it; but when you cannot measure it, when you cannot express it in numbers, your knowledge is of a meager and unsatisfactory kind: it may be the beginning of knowledge, but you have scarcely, in your thoughts, advanced to the state of science."[7]

Figure 1 shows the simplest useful

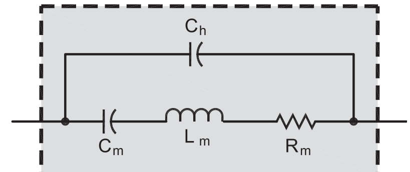

Figure 1 — Simple but useful model of a quartz crystal.

[1]Notes appear on page 26.

7236 Clifton Road
Clifton, VA 20124
Jack.Smith@cliftonlaboratories.com

electrical model of a crystal.[8, 9, 10] It has four elements:

C_h — the capacitance of the holder, including the plated electrodes on either side of the quartz blank

C_m — the *motional* capacitance

L_m — the *motional* inductance

R_m — the *motional* resistance

The parameters C_m, L_m and R_m are called "motional" elements because they are electrical analogs of the physical vibrations of the quartz element; in other words, they result from motion of the quartz plate, with L_m corresponding to the plate's mass, C_m corresponding to its elasticity and R_m to frictional loss. (In the professional literature, C_h is identified as C_0, and the motional parameters as C_1, L_1 and R_1.) Nonetheless, C_m, L_m and R_m may be measured and are as real to us as any physical capacitor, inductor or resistor. Removing the protective case from a crystal, of course, does not reveal three tiny circuit components. Rather, you will find a thin circular quartz blank with electrodes deposited onto both sides.

The parameters shown in Figure 1 may be measured through a variety of methods. We will compare three:

1. Derive the parameters by measuring the holder capacitance and the series and parallel resonant frequencies of the crystal;
2. Use the oscillator-frequency-shift method developed by G3UUR;
3. Compare these two measurements with data from an HP87510A gain-phase analyzer's automatic crystal resonator characterization.

Holder Capacitance

Before measuring the motional parameters, we first measure the holder capacitance. Although we won't use C_h in our narrow band filter design equations, it is an important parameter in more sophisticated designs, particularly for wider bandwidth filters, as described in Dishal's classic paper.[11, 12] We'll also see C_h used in some methodologies to calculate motional parameters. Hence, it is important to measure C_h as accurately as we can. To disentangle it from the motional parameters, C_h should be measured at a frequency far below the crystal's resonant frequency. Table 1 summarizes my holder capacitance measurements. Disregarding the one 4.13 pF value as an outlier, the holder capacitance can be taken as the average of the remaining five measurements, 3.83 pF.

Series and Parallel Resonance Method

If we place the crystal to be measured in series between a signal generator and a signal level detector, as we tune the generator near the frequency marked on the crystal can, we see two points of resonance. The first produces a transmission maximum and corresponds to the series resonant frequency, or the frequency at which C_m and L_m resonate. If we tune the signal generator a bit higher in frequency, however, we see a transmission minimum, corresponding to parallel resonance of C_h with the series combination of C_m and L_m. If our equipment permits, we observe a phase shift as well — at both the series and parallel resonant frequen-

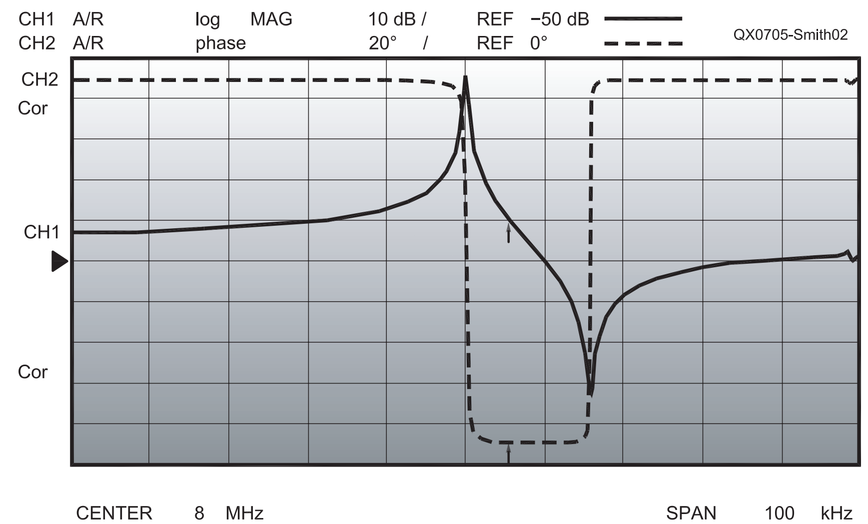

Figure 2 — Impedance and phase of a crystal at both series and parallel resonance.

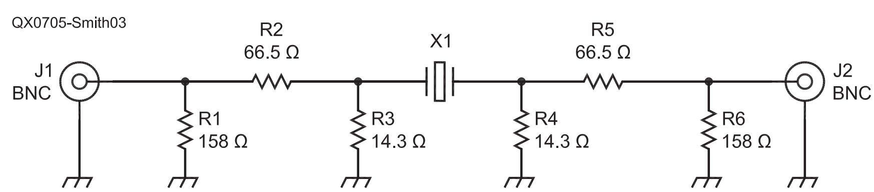

Figure 3 — Resistive pi fixture for measuring crystal parameters.

Table 1
Crystal Holder Capacitance Measurements

Method	*Value*	*Comments*
Digital capacitance meter	3.7 pF	BP Model DCM-601 meter.
Resolution	0.1 pF	
Gain-Phase Analyzer		
HP87510A	4.13 pF	@ 100 kHz
	3.89 pF	@ 300 kHz
	3.83 pF	@ 1 MHz
	3.90 pF	@ 2 MHz
HP4342A Q-meter with Boonton 103A-32 2.5 mH working coil via resonance shift method	3.85 pF	@ 145 kHz
Mean	3.83 pF	Exclude 4.13 pF data point

cies the phase shift is zero.[13] Figure 2 shows a transmission amplitude and phase plot for the 8 MHz crystals used in our filter design.

The measurements in this article are taken with an HP87510A gain-phase meter, a 100 kHz to 300 MHz vector network analyzer, optimized for component measurement, including a feature to automatically compute and display the equivalent parameters of a crystal resonator. The HP87510A combines the function of signal generator and signal strength (and phase) detector. The principles we use, however, are applicable to a variety of measurement equipment. See, Hayward[14] and Pivnichny[15] for test methods not requiring sophisticated equipment.

As convenient as using a network analyzer is, it's not as simple as plugging a crystal into a port on the 87510A. Rather, the crystal must be installed in a test fixture so that it is presented with the correct impedance and drive level, and, for some measurements but not for our purposes, the correct shunt capacitance. Although I do not have the recommended HP41900A crystal holder, it is possible to make a substitute capable of the accuracy we need for filter design. (We consider stray shunting capacitance in the substitute fixture only to the extent it increases C_h, an omission that limits the achievable accuracy.)

The IEC standard for crystal measurement requires the crystal be driven from a 12.5 Ω source and terminated in a 12.5 Ω load.[16] This is traditionally accomplished through back-to-back resistive pi attenuators, providing impedance matching to 50 Ω test equipment, resulting in a net 29.6 dB loss. See Salt[17] or Pivnichny.[18] My version of the attenuator, using standard 1% resistors, is shown at Figure 3 and pictured at Figure 4. Figure 5 shows how the test fixture is connected to the 87510A. 10 dB attenuators (Mini-Circuits Laboratories model CAT-10) at the input and output ports of the fixture further improve the 12.5 Ω impedance match. (Some of my data was taken with an earlier design — a transformer-based 50:12.5 Ω matching test fixture. It exhibited greater error than the resistive fixture.)

It's also important to drive the crystal under test with a signal level representative of the circuit in which it will be used, since motional parameters vary with drive level, a phenomenon known in the industry as "drive level dependency" or DLD. (It's also possible to shatter a crystal with grossly excessive drive.) All test data presented is taken with a signal level of –20 dBm presented to the input of the test fixture. Figures 6 and 7, for example, show R_m varies significantly as the drive level varies from –50 dBm to 0 dBm. (The 10 dB pads were removed for these tests.) Both crystals exhibit abrupt jumps in R_m and show a general trend toward lower R_m with increasing drive. To test whether the jumps were an instrument or calibration artifact, I substituted a 9.1 Ω, ¼ W carbon film resistor for the crystal swept

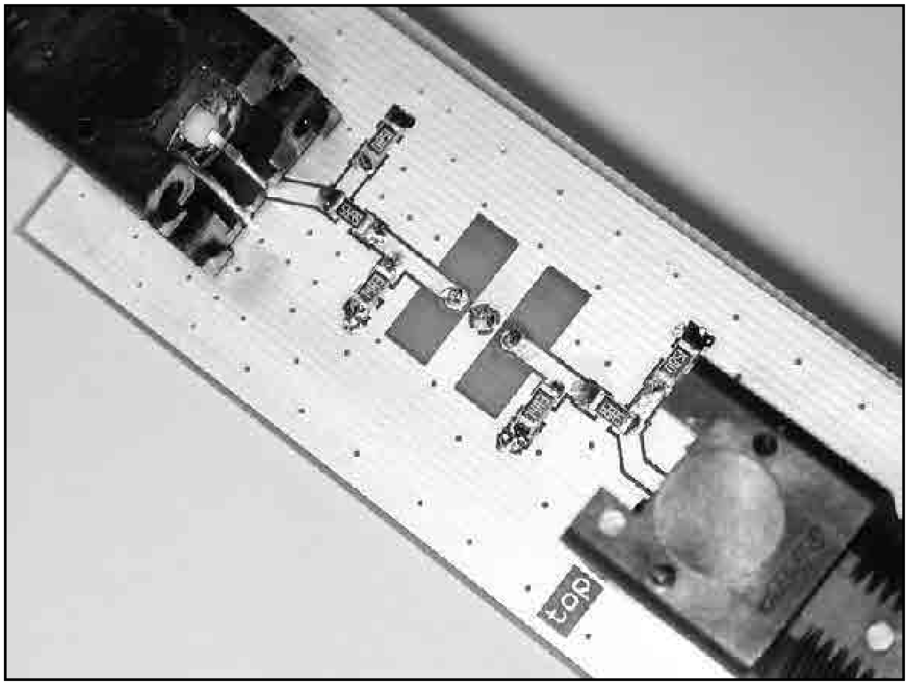

Figure 4 — Resistive pi fixture printed circuit board.

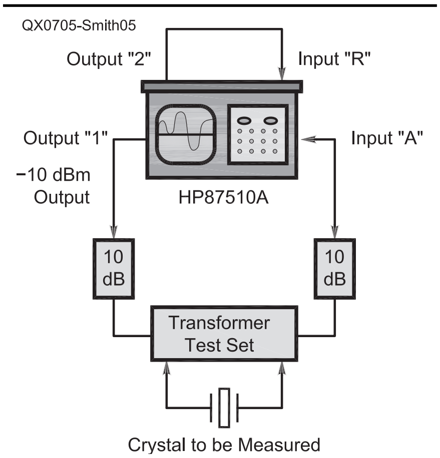

Figure 5 — Setup for measuring crystal parameters using HP87510A VNA.

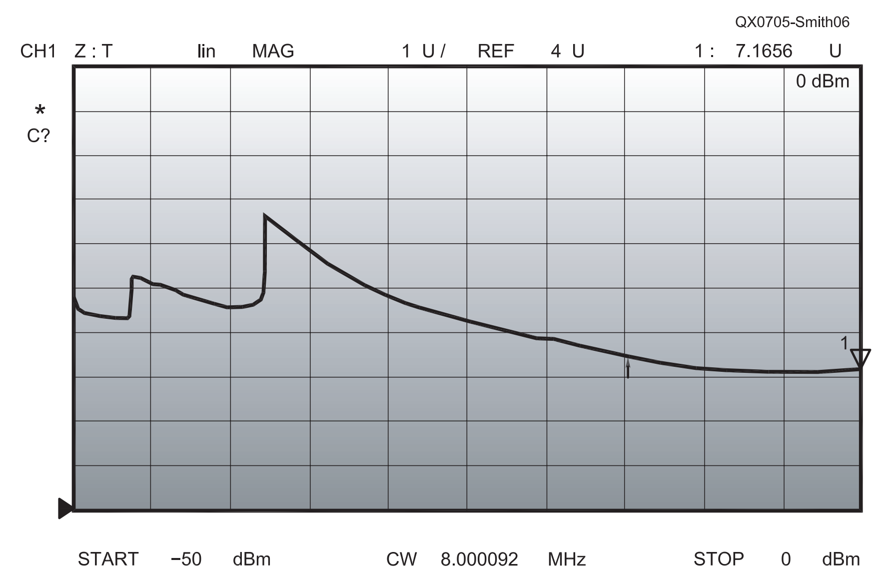

Figure 6 — Variation in crystal series resistance versus drive level. Note the abrupt jumps in resistance as drive is varied.

in Figure 6. As Figure 8 shows, its resistance is essentially unchanged over the –50 to 0 dBm level. Salt describes R_m jumps, similar to those seen in Figures 6 and 7, as resulting from coupling among multiple resonance modes, as the dominant resonance shifts from one mode to another with slight changes in operating conditions.[19] Fortunately for us, these resonance modes differ only slightly in frequency. C_m and L_m also change their values slightly with varying drive levels. (Changes in motional values with applied signal level are why a crystal filter can be a source of intermodulation.)

With the crystal installed in an impedance matching test fixture, we measure four parameters, and, if your setup permits, a fifth parameter:

- Series resonant frequency — f_s
- Parallel resonant frequency — f_p
- Series resonant 3 dB bandwidth — Δf
- Parasitic capacitance of the test fixture — C_p
- (Optional) Series resonant attenuation (dB) — α

Figures 9 and 10 show the swept frequency data for a typical ECS-80-S-1X 8.0 crystal, from which we obtain the parameters summarized in Table 2. The value for C_p was measured separately.

The following motional parameter analysis is based upon Omicron Lab's Application Note.[20] From standard circuit theory, we first state the series and parallel resonant frequencies and the resonator Q in terms of the crystal parameters:

$$f_s = \frac{1}{2\pi\sqrt{L_m C_m}} \qquad \text{[Eq 1]}$$

$$f_p = f_s\sqrt{1+\frac{C_m}{C_h}} \approx f_s\left(1+\frac{C_m}{2C_h}\right) \qquad \text{[Eq 2]}$$

$$Q = \frac{2\pi\ f_s L_m}{R_m} = \frac{1}{2\pi\ f_s C_m R_m} \qquad \text{[Eq 3]}$$

Since these parameters are measured with the crystal installed in the test fixture, we must add the fixture capacitance to the true holder capacitance to find the adjusted holder capacitance, $C_{h\,adj}$:

$$C_{h\,adj} = C_h + C_p = 3.83\text{ pF} + 0.67\text{ pF} = 4.50\text{ pF} \qquad \text{[Eq 4]}$$

We recast these equations to solve for the motional parameters in terms of our known parameters f_s, f_p, C_h and Q_L:

$$C_m = 2C_{h\ adj}\left(\frac{f_p}{f_s}-1\right) \qquad \text{[Eq 5]}$$

$$C_m = \left(\frac{8.016250\text{ MHz}}{8.0000625\text{ MHz}}-1\right)\times 2\times 4.50\text{pF}$$

$$C_m = 0.01821\text{ pF}$$

$$L_m = \frac{1}{4\pi^2 f_s^2 C_m} \qquad \text{[Eq 6]}$$

$$L_m = \frac{1}{4\pi^2\,(8.0000625\times10^6\ \text{Hz})^2\times 18.21\times10^{-15}\ \text{F}}$$

$$L_m = 21.728\text{ mH}$$

We next calculate Q_L, the loaded Q of the crystal:

$$Q_L = \frac{f_s}{\Delta f} \qquad \text{[Eq 7]}$$

$$Q_L = \frac{8.000\times10^6\text{ Hz}}{256.2\text{Hz}} = 31{,}226$$

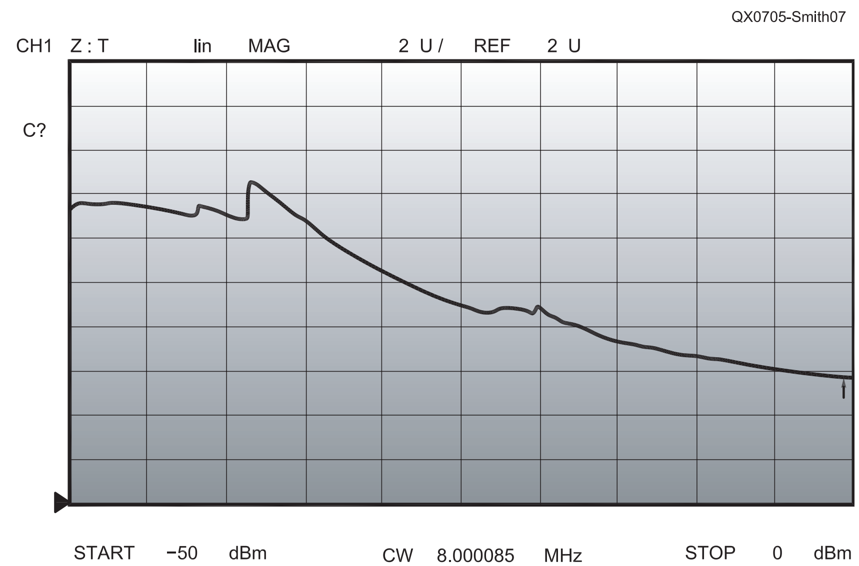

Figure 7 — Second sample crystal shows similar drive level dependency.

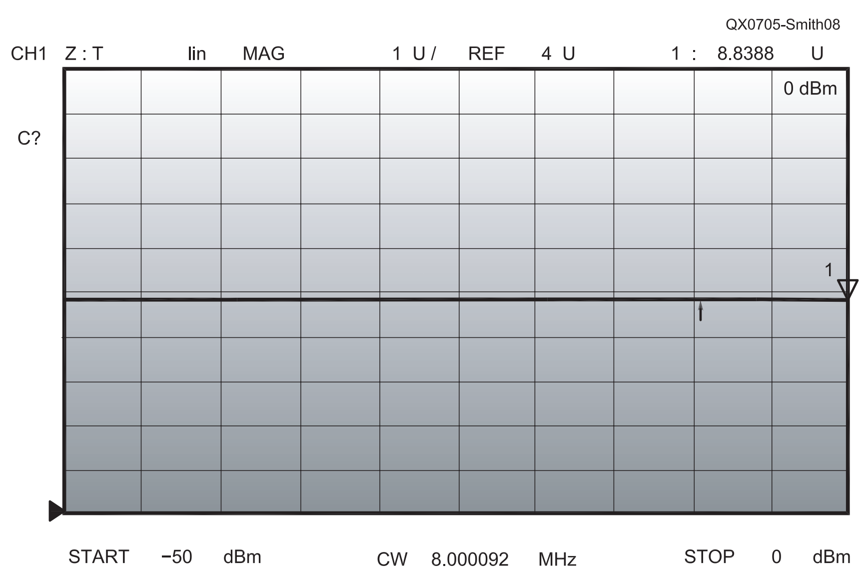

Figure 8 — A resistor shows no indication of drive level dependency.

Table 2
Measured ECS-80-S-1X 8.0 Crystal Parameters

Parameter	*Value*
f_s	8.0000625 MHz
f_p	8.0162500 MHz
Δf	256.2 Hz
C_p	0.67 pF
α	3.1 dB

From the definition of Q, we calculate the series resistance, R_{Total}, seen by the crystal, consisting of R_m plus the source and load resistance. See Figure 11.

$$R_{Total} = \frac{2\pi \ f_s L_m}{Q_L}$$

Solving for R_{Total}:

$$R_{Total} = \frac{2\pi \ f_s L_m}{Q_L}$$

$$R_{Total} = \frac{2 \times \pi \times 8.000 \times 10^6 \ \text{Hz} \times 21.728 \times 10^{-3} \ \text{H}}{31226}$$

$$R_{Total} = 34.98 \ \Omega$$

The source and load resistances presented to the crystal are both 12.5 Ω, which we subtract from R_{Total} to obtain R_m:

$$R_m = R_{Total} - R_{Termination} \qquad \text{[Eq 8]}$$

$$R_m = 34.98 \ \Omega - 12.5 \ \Omega - 12.5 \ \Omega = 9.98 \ \Omega$$

Is it possible to determine the motional values without knowledge of the holder and test fixture capacitance? The answer is yes.

Figure 10 shows the measured attenuation $\alpha = 3.0397$ dB. Assuming this value is correct — and we should certainly not accept attenuation stated to four decimal places as accurate to all four places[21] — we can compute the loaded Q, deriving L_m from it and the source and load impedance:

The relationship between series resistance and attenuation is:[22]

$$R_s = 2 R_0 \left(10^{\frac{\alpha}{20}} - 1 \right) \qquad \text{[Eq 9]}$$

Where:

R_s is the series resistance

R_0 is the impedance of the source and load, assumed equal

α is the attenuation, in decibels

Applying this to our measured data, we determine the motional resistance:

$$R_m = 2 \times 12.5 \ \Omega \times \left(10^{\frac{3.0397}{20}} - 1 \right) = 10.475 \ \Omega$$

The total resistance seen by L_m is thus 10.475 Ω plus the 12.5 Ω source and terminating impedance, or 35.475 Ω total.

We now find L_m:

$$L_m = \frac{Q \times R_{Total}}{2\pi \ f_s}$$

$$L_m = \frac{31226 \times 35.475 \ \Omega}{2 \times \pi \times 8.0000625 \times 10^6 \ \text{Hz}}$$

$L_m = 22.03$ mH

C_m can be determined from the series resonant frequency:

$$C_m = \frac{1}{4\pi^2 \ f_s^2 L_m}$$

$$C_m = \frac{1}{4 \times \pi \times \left(8.000 \times 10^6 \ \text{Hz}\right)^2 \times 22.03 \times 10^{-3} \ \text{H}}$$

$$C_m = 0.01797 \ \text{pF}$$

In truth, these calculations trade lack of knowledge about the holder capacitance for lack of knowledge of the exact attenuation and the source and load terminations. We should, however, — at least in principle — be able to measure attenuation and the source and load terminations at least as accurately as the holder and fixture capacitance.

G3UUR Method

David Gordon-Smith, G3UUR, has developed a simple method of measuring crystal parameters, popularized by Wes Hayward.[23] G3UUR's method involves measuring the shift in frequency of a series-tuned Colpitts oscillator when a small capacitor is added in series with the crystal. L_m and C_m are then calculated from the following equations:[24]

$$C_m \approx \frac{2\Delta f}{f}\left(C_h + C_s\right) \qquad \text{[Eq 10]}$$

Where:

C_s is the series capacitor

Δf is the shift in frequency when C_s is inserted.

L_m is determined from the resonant frequency, using Equation 6:

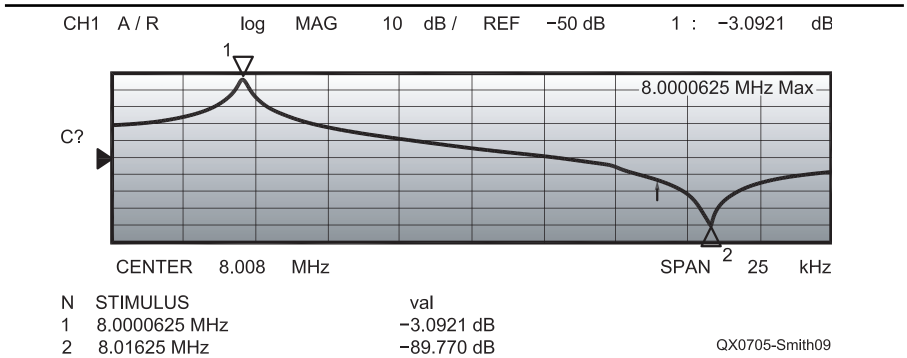

Figure 9 — Swept frequency data for a typical 8 MHz crystal, showing both series and parallel resonant points.

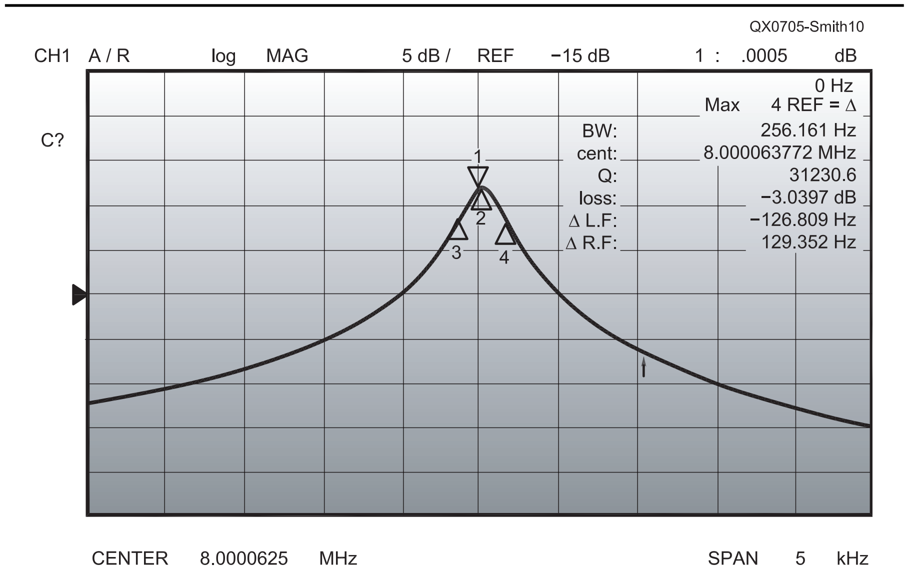

Figure 10 — Expanded view of series resonance in the 8 MHz crystal.

Table 3
ECS-80-S-1X 8.0 Crystal Frequencies Measured With G3URR Method

Condition	*Value*
Switch closed, no extra series C	8.000613 MHz
Extra series C	8.002418 MHz
Shift in frequency	1805 Hz

Table 4
Comparison of Crystal Motional Parameters Found by Four Different Methods

Method	C_m	L_m	R_m
Series & Parallel resonance frequency measurement	18.215 fF	21.728 mH	9.98 Ω
Series resonance only, with Q from attenuation	17.97 fF	22.03 mH	10.48 Ω
G3UUR	17.06 fF	23.2 mH	Not determinable by G3UUR method
HP87510A auto characterization	18.776 fF	21.079 mH	11.682 Ω

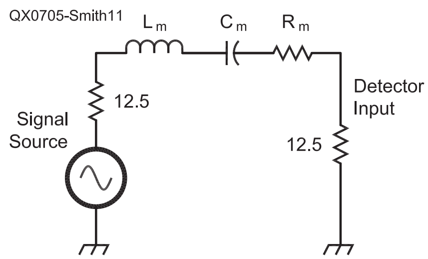

Figure 11 — Equivalent circuit of crystal installed in the resistive pi fixture.

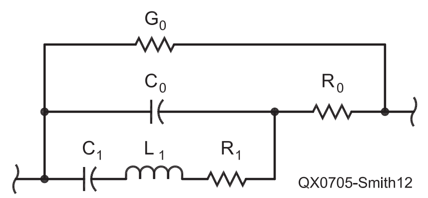

Figure 12 — Six element crystal model as used in the 87510A's automatic parameter characterization function.

$$L_m = \frac{1}{4\pi^2 f^2 C_m}$$

I constructed a G3UUR circuit with C_s measured at 34.1 pF, including stray capacitance. Plugging the same ECS-80-S-1X 8.0 crystal into the G3UUR circuit gave the results shown in Table 3.

Plugging these measured values into the two equations shows the motional parameters as C_m = 0.01706 pF and L_m = 22.2 mH.

This data is approximately 5.5% below the values measured by the network analyzer.

Automated Measurement Results — 87510A

The 87510A operates in transmission mode for crystal characterization. The *Operation Manual* describes the methodology used to calculate the six parameter values in the model illustrated at Figure 12:[25]

1) Obtains the admittance characteristic circle diagram
2) Obtains the maximum conductance (G_{max})
3) Obtains frequencies f_1 and f_2 ($f_1 < f_2$) of two points where conductance is half the maximum conductance.
4) Calculate f_s by

$$f_s = \sqrt{f_1 \times f_2}$$

5) Obtains susceptance B_{fs} at f_s
6) Calculate ω_s by $\omega_s = 2\pi f_s$
7) Assumes that the frequency at which the phase difference becomes 0° near the parallel resonance frequency is f_a and obtains its conductance G_a.
8) Calculate ω_a by $\omega_a = 2\pi f_a$
9) Assumes that the frequency at which the phase difference becomes 0° near the series resonance frequency is f_r.
10) Calculates the constants using the above values and the following equations:

$$Q_s = \frac{f_s}{f_2 - f_1} \quad \text{[Eq 11]}$$

$$L_1 = \frac{Q_s}{\omega_s G_{\max}} \quad \text{[Eq 12]}$$

$$C_1 = \frac{G_{\max}}{\omega_s Q_s} \quad \text{[Eq 13]}$$

$$C_0 = \frac{B_{f_s}}{\omega_s} \quad \text{[Eq 14]}$$

$$C_0' = \frac{B_1 + B_2}{2\omega_s} \quad \text{[Eq 15]}$$

$$R_1 = \frac{C_0'}{C_0 G_{\max}} \quad \text{[Eq 16]}$$

$$R_0 = \frac{1}{G_{\max}} - R_1 \quad \text{[Eq 17]}$$

$$R_0 = \frac{1}{G_{\max}} - R_1 \quad \text{[Eq 18]}$$

Table 5
Mean and Standard Deviation for 65 Crystals Using the HP87510A Auto Characterization

	C_m (fF)	*L_m (mH)*	*R_m (Ω)*	*F_0 (Hz)*	*Q*
Mean	18.59	21.30	14.0	8000071	76380
Standard Deviation	0.90	1.03	2.2		17500

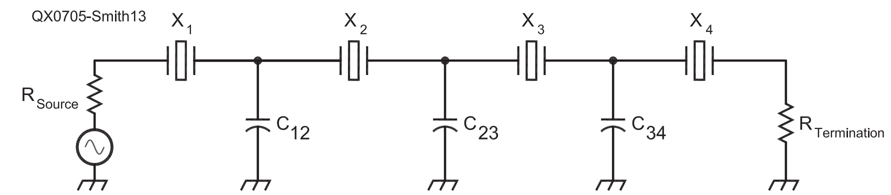

Figure 13 — Standard crystal ladder filter configuration.

Applying these equations by pressing the 87510A's appropriate soft key produced the following motional parameters:

C_m = 18.776 fF

[Yes, that is 18.776 femtofarads, or 18.776 × 10^{-15} F — *Ed.*]

L_m = 21.079 mH

R_m = 11.682 Ω

Table 4 compares our measurements made using the four methods.

I believe the most accurate measurements are the first two, as the auto-characterization shows some sensitivity to selected span width.[26] The automatic characterization is a major time saver, however, and permits efficiently collecting crystal statistics. I measured 65 ECS-80-S-1X 8.0 crystals using the HP87510A's auto characterization mode and determined the mean value and standard deviation of their motional parameters. See Table 5.

Our design work will use these mean values. The filters, however, will be built from selected crystals, matched in frequency within ±20 Hz and with a measured Q > 75,000.

Designing and Tuning the Filter

Knowing the motional and holder parameters of our crystals, we now design the panadapter's 200-Hz-bandwidth Gaussian filter.[27] Our filter will have the standard ladder topology shown at Figure 13.

We first start by computing the fractional bandwidth, Q_f, of the filter:

Table 6
Predistorted *k* and *q* Values for Four-Section Gaussian Filter

N=4	q_o	I_L	q_1	q_n	k_{12}	k_{23}	k_{34}
	infinity	0	0.2747	0.4083	2.2792	0.7553	0.9896
	7.053	2.454	0.2913	0.4213	2.1131	0.7226	0.9268
	3.526	5.036	0.3102	0.4349	1.9513	0.6933	0.865
	2.351	7.755	0.3318	0.4493	1.7951	0.6687	0.8040
	1.763	10.617	0.3565	0.4650	1.6462	0.6503	0.7436

Table 7
Interpolated *k* and *q* Values for a Four-Section Gaussian Filter

N=4	q_o	I_L	q_1	q_n	k_{12}	k_{23}	k_{34}
	2.351	7.755	0.3318	0.4493	1.7951	0.6687	0.8040
Interpolated	1.910	9.902	0.3503	0.4611	1.6833	0.6549	0.7587
	1.763	10.617	0.3565	0.4650	1.6462	0.6503	0.7436

Table 8
De-normalized Coupling Coefficients

	k_{12}	k_{23}	k_{34}
Normalized	1.6833	0.6549	0.7587
De-normalized	4.2082E-05	1.6372E-05	1.8966E-05

Table 9
Effective Series Capacitance of the Filter Circuit

Mesh	*Net Capacitance*
1	C1 = 442 pF
2	C1 and C2 in series = 318 pF
3	C2 and C3 in series = 526 pF
4	C3 = 980 pF

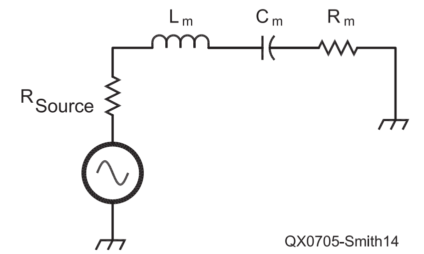

Figure 14 — Equivalent circuit at End 1 of the crystal filter.

$$Q_f = \frac{f_{Center}}{f_{3\ dB\ Bandwidth}} \qquad \text{[Eq 19]}$$

$$Q_f = \frac{8 \times 10^6 \text{ Hz}}{200 \text{ Hz}} = 4.0 \times 10^4$$

Where:

f_{Center} is the center frequency of the filter, technically the geometric mean of the upper and lower 3 dB points. For narrowband filters we will use the quartz resonator frequency instead, without appreciable loss of accuracy.

$f_{3\ dB\ Bandwidth}$ is the 3 dB bandwidth of our filter, 200 Hz in this case.

We now compute the *normalized Q*, q_0, defined as:

$$q_0 = \frac{Q_u}{Q_f} \qquad \text{[Eq 20]}$$

$$q_0 = \frac{7.638 \times 10^4}{4.0 \times 10^4} = 1.910$$

Q_u is the unloaded crystal resonator *Q*, which we have measured as a mean value of 76380.

From Zverev[28] Chapter 6, Table 6.10-26, we find the predistorted *k* and *q* values for a four-section Gaussian filter. These values are given in Table 6.

Since our q_0 of 1.910 is not matched in the table, we find the corresponding *q* and *k* values by interpolation between the two nearest values. Table 7 gives the interpolated values.

Source and Termination Resistance

We start by calculating the source and termination resistance. (It's arbitrary whether the source is at end 1 or end n; we'll use end 1 as the source and end n as the termination.) Again following Zverev, we note that q_1 and q_n are the normalized *Q* values of the end inductors. These values are de-normalized by multiplying by Q_f:

$$Q_1 = q_1 Q_f \qquad \text{[Eq 21]}$$
$$Q_1 = 0.3503 \times 4 \times 10^4 = 1.401 \times 10^4$$

where Q_1 is the required real (de-normalized) *Q* of the circuit at end 1 of the filter. We assume that all filter element loss is contained within the crystal, and that is accounted for by the series motional resistance, R_m.

As illustrated in Figure 14, our equivalent circuit at end 1 of the filter has two loss elements, R_m and R_{Source}, with a total series resistance of $R_m + R_{Source}$. Knowing Q_1, R_m and L_m, we now can calculate R_{Source}. We start with the definition of Q for the series resistance model:

$$Q_1 = \frac{2\pi\ f\ L_m}{R_m + R_{Source}} \qquad \text{[Eq 22]}$$

where *f* is the filter center frequency in Hz.

Solving for R_{Source}, we find:

$$R_{Source} = \frac{2\pi\ f\ L_m - Q_1 R_m}{Q_1} \qquad \text{[Eq 23]}$$

$$R_{Source} = \frac{2 \times \pi \times 8 \times 10^6 \times 21.3 \times 10^{-3} - 1.401 \times 10^4}{1.401 \times 10^4}$$

$$R_{Source} = 62.4\ \Omega$$

Likewise, using the values for q_n, we find $R_{Termination}$ is 44.0 Ω.

Nodal Capacitance

Next, we calculate the nodal capacitors, $C_1 \ldots C_3$.

We start by de-normalizing the coupling coefficients k_{12}, k_{23} and k_{34}:

$$K_{jk} = \frac{k_{jk}}{Q_f} \qquad \text{[Eq 24]}$$

where K_{jk} is the de-normalized coupling coefficient for normalized coefficient k_{jk}.

Q_f is the fractional bandwidth, 4.00×10^4, as computed earlier.

Table 8 provides the de-normalized coupling coefficients.

The value of coupling capacitor C_{jk}, where C_{jk} is the capacitor connected to the node between crystals X_j and X_k, is given by:

$$C_{jk} = \frac{C_m}{K_{jk}} \qquad \text{[Eq 25]}$$

Computing C_{12}:

$$C_{12} = \frac{C_m}{K_{12}} = \frac{1.8590 \times 10^{-14} \text{ F}}{4.2082 \times 10^{-5}}$$

$$C_{12} = 4.418 \times 10^{-10} \text{ F} = 441.8 \text{pF}$$

Computing the value of the remaining coupling capacitors in a similar fashion provides

C_{12} = 442 pF, C_{23} = 1,135 pF and C_{34} = 980 pF

Rather than maintain the C_{jk} notation, we will renumber them consistent with usual schematic practices as C1, C2 and C3. Figure 15 shows the results of our design efforts so far.

Tuning and Matching the Filter

Figure 15 is annotated to show the four meshes or loops that comprise the filter, with each mesh annotated with the effective series capacitance of the mesh, ignoring C_m, since it is common to all meshes. This follows the method used by Hayward in *Experimental Methods in RF Design*.[29] See Table 9.

We now must "tune" the filter so that each mesh has the same net series capacitance — otherwise, the differences in series capacitance will slightly shift the resonant frequency of each mesh, obviating our fundamental design assumption that all meshes resonate at identical frequencies. Failure to resonate all meshes at the same frequency yields a "lumpy" passband, with multiple peaks instead of the single smooth Gaussian response of our design target.

We tune the filter by adding series capacitors C_x, C_y and C_z as shown at Figure 16. Since adding series capacitance can only decrease the net capacitance, our objective is to select C_x, C_y and C_z so that all meshes have a series capacitance equal to that of the mesh with the smallest initial net capacitance, Mesh 2 at 318 pF.

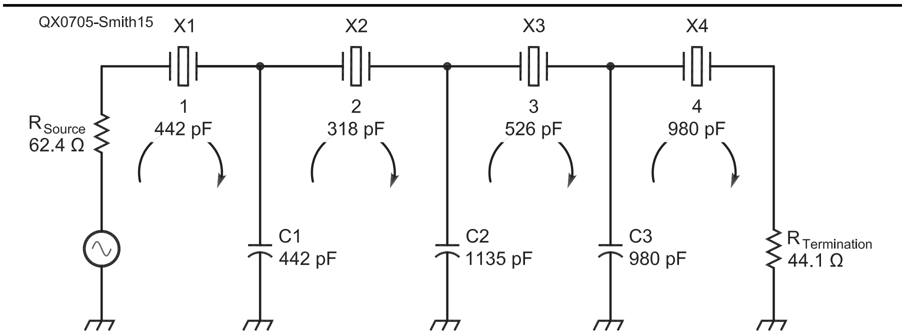

Figure 15 — Effective series capacitance of each filter mesh before tuning.

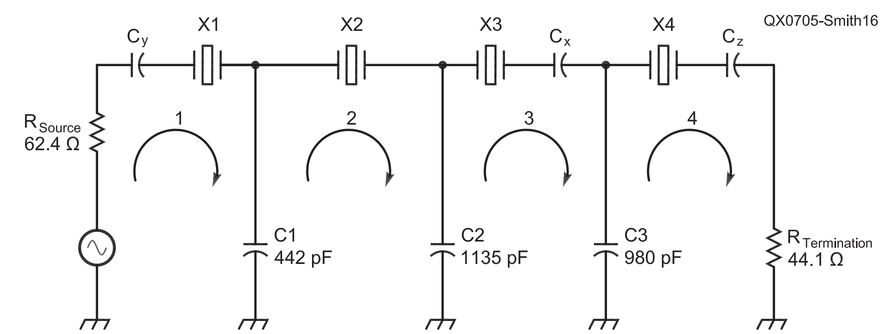

Figure 16 — Adding series capacitors C_x, C_y and C_z to tune each mesh for identical effective series capacitance.

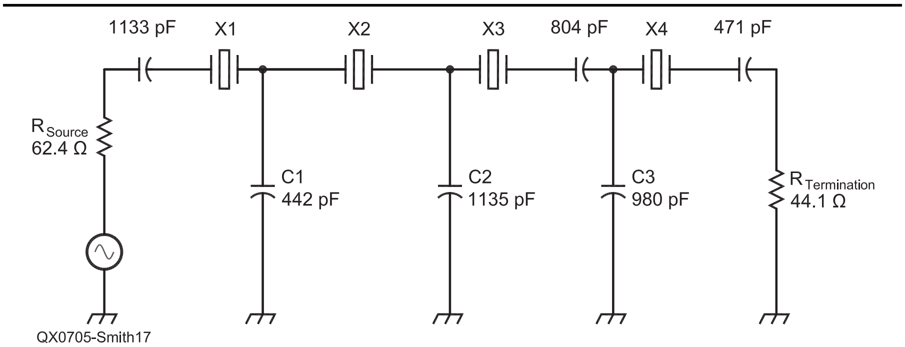

Figure 17 — Series capacitance required to tune all meshes to the same frequency.

This is easily done using the standard formula for series capacitance:

$$C_{Total} = \frac{1}{\frac{1}{C_a} + \frac{1}{C_b}} \qquad \text{[Eq 26]}$$

Where C_{Total} is the effective capacitance of the series combination of two capacitors C_a and C_b. Solving for C_b, we find:

$$C_b = \frac{1}{\frac{1}{C_{Total}} - \frac{1}{C_a}} \qquad \text{[Eq 27]}$$

Applying the formula this to mesh tuning, we know C_{Total} must equal 318 pF and C_a is the net capacitance from Table 9. As an example, C_x is:

$$C_x = \frac{1}{\frac{1}{318\,\text{pF}} - \frac{1}{526\,\text{pF}}} = 804\,\text{pF}$$

Using the same approach, we calculate the additional series capacitance for all four meshes, as shown in Table 10.

Figure 17 illustrates our nearly finished design. Our remaining task is to match the source and terminating impedances to 50 Ω, as our panadapter design uses 50 Ω for internal module interfaces. Before designing the matching section, however, we will first transform the series RC combination at the source and termination to a parallel RC configuration. The reason for the transformation is that our matching networks employ parallel capacitors that can be "absorbed" into the transformed parallel capacitance, simplifying our design.

The series to parallel transform is defined by two equations:

$$R_p = \frac{R_s^2 + X_s^2}{R_s} \qquad \text{[Eq 28]}$$

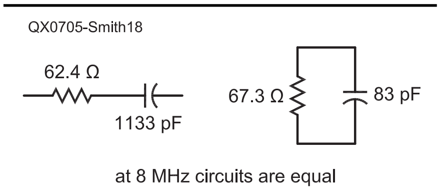

Figure 18 — Series to parallel conversion.

Table 10
Additional Series Capacitance Values for the Filter Design

Mesh	*Tuning Capacitor*	*Value*
1	C_y	1133 pF
2	None	None
3	C_x	804 pF
4	C_z	471 pF

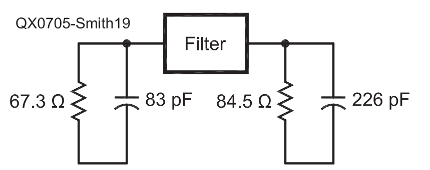

Figure 19 — The filter's input and output impedances. These are to be matched to 50 Ω.

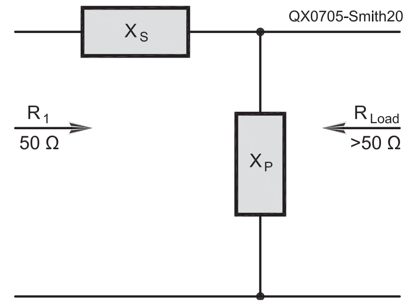

Figure 20 — L network for matching.

Table 11
Parallel Equivalent Values at Source and Termination of Filter

End	*Parallel R*	*Parallel C*
Source	67.3 Ω	83 pF
Termination	84.5 Ω	226 pF

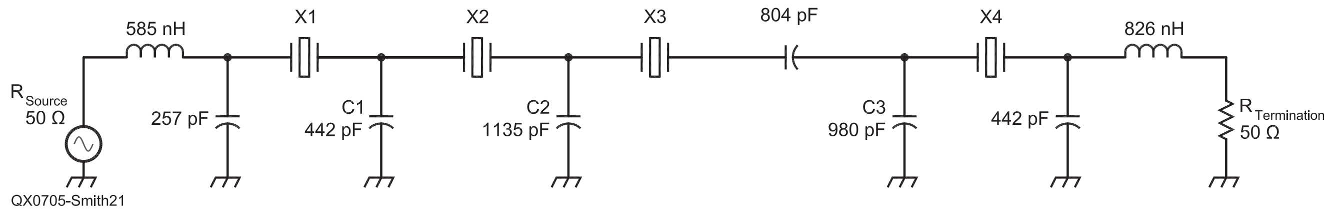

Figure 21 — Final filter design, with input and output impedance matched to 50 Ω.

$$X_p = \frac{R_s^2 + X_s^2}{X_s} \qquad \text{[Eq 29]}$$

Where R_s and X_s are the series resistance and reactance, respectively and R_p and X_p are the parallel resistance and reactance respectively. Of course, this transformation is valid only at the frequency for which the reactances are calculated.

Let's work through the transformation at the source end. In this case, the series element represented by X_s is the reactance of C_y, 1133 pF, at 8 MHz:

$$X_C = -\frac{1}{2\pi f \; C_y}$$

$$X_C = -\frac{1}{2 \times \pi \times 8 \times 10^6 \ \text{Hz} \times 1133 \times 10^{-12} \ \text{F}}$$

$$X_C = -17.6 \ \Omega$$

R_s is, of course, 62.4 Ω.

We now calculate R_p and X_p:

$$R_p = \frac{-17.6^2 + 62.4^2}{62.4} = 67.3 \ \Omega$$

$$C_p = \frac{1}{2\pi \ f \ X_C} = 8.33 \times 10^{-11} \ \text{F} = 83.3 \, \text{pF}$$

The minus sign is because the reactance is capacitive. The capacitance corresponding to –238.8 Ω reactance at 8 MHz is:

$$C_p = \frac{1}{2\pi \ f \ X_C} = 8.33 \times 10^{-11} \ \text{F} = 83.3 \, \text{pF}$$

Figure 18 shows the series and parallel equivalents. Performing the same conversion for the termination provides the values shown in Figure 19 and in Table 11.

We now design matching networks to transform 67.3 Ω to 50 Ω and 84.5 Ω to 50 Ω, following Kuhn.[30] Since both the input and output impedances are greater than 50 Ω, we will use the L-network of Figure 20. The series element X_s will be an inductor and the shunt element X_p will be a capacitor to provide a low pass configuration, which also permits combining the shunt capacitor with the input shunt capacitor required for mesh tuning.

We start by computing the impedance transformation ratio, q, which, for the filter's input side, is:

$$q = \sqrt{\frac{R_{Load}}{R_1} - 1}$$

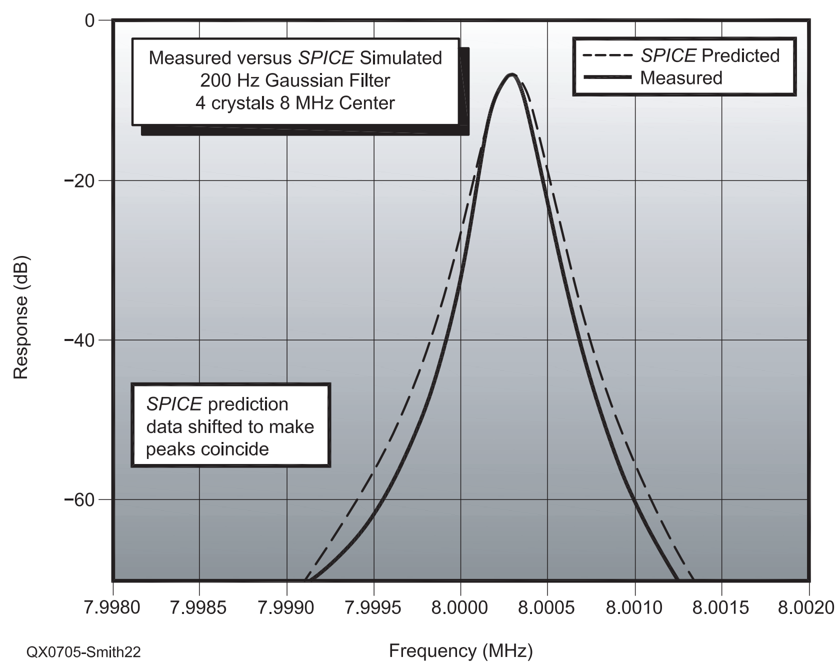

Figure 22 — Measured filter performance versus *Spice* simulation.

Table 12
Comparison of Design Goal and Measured Filter Shape Factor

	3 dB Bandwidth	*60 dB Bandwidth*	*3 dB:60 dB Shape Factor*
Design	200 Hz	2000 Hz	10.0:1
Measured	171 Hz	1893 Hz	11.0:1

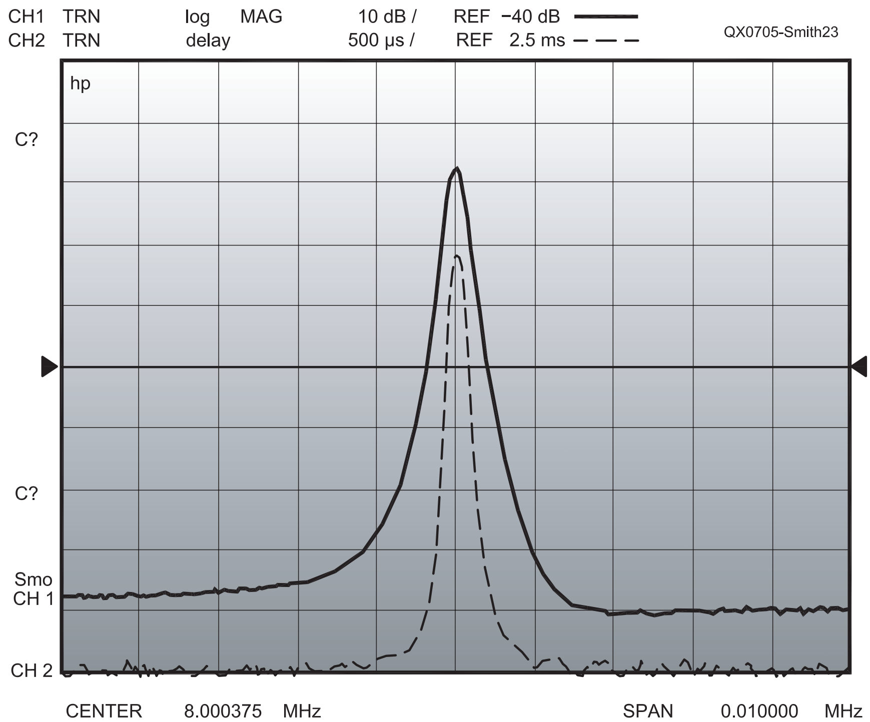

Figure 23 — Measured amplitude and group delay response for 1 kHz bandwidth filter.

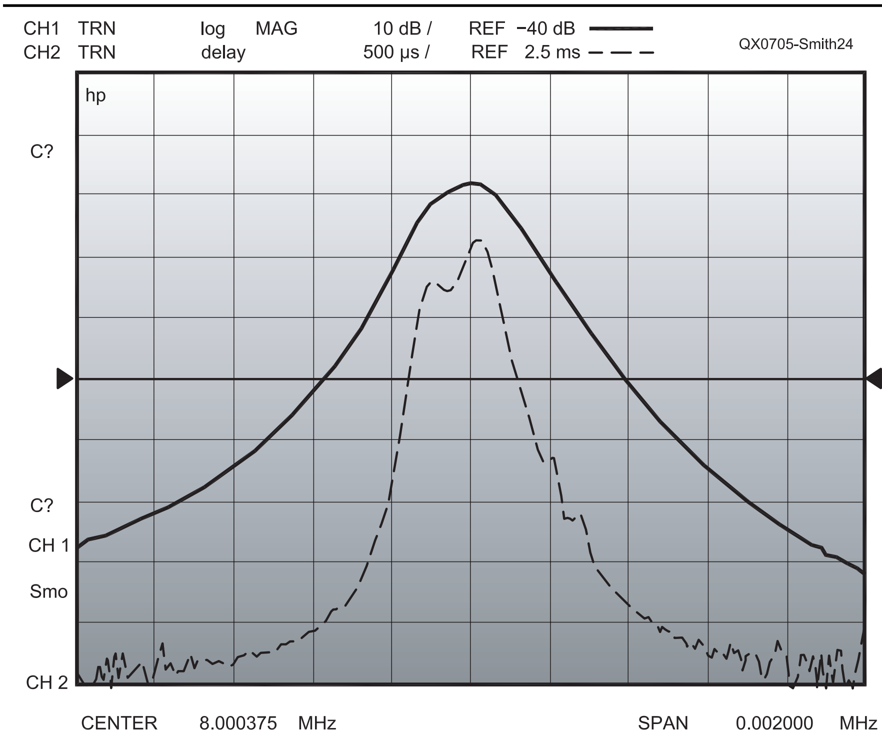

Figure 24 — Measured amplitude and group delay response for 200 Hz filter.

$$q = \sqrt{\frac{67.3\ \Omega}{50\ \Omega} - 1} = 0.588$$

Next, we compute the required series reactance, X_s:

$$X_s = \pm qR_1$$
$$X_s = 0.588 \times 50\ \Omega = 29.4\ \Omega$$

Since we use a series inductance, the sign of X_s is positive. We calculate the corresponding L_s:

$$L_s = \frac{X_s}{2\pi f}$$

$$L_s = \frac{29.4\ \Omega}{2 \times \pi \times 8 \times 10^6\ \text{Hz}} = 5.85 \times 10^{-7}\ \text{H}$$

$$L_s = 585\ \text{nH}$$

The required parallel reactance, X_p is:

$$X_p = \mp \frac{R_{Load}}{q}$$

$$X_p = \frac{67.3\ \Omega}{0.588} = 114\ \Omega$$

Note the sign inversion; if X_s is inductive, X_p must be capacitive and vice versa.

Now, compute the required capacitance C_p:

$$C_p = \frac{1}{2\pi f\ X_p}$$

$$C_p = \frac{1}{2 \times \pi \times 8 \times 10^6\ \text{Hz} \times 114\ \Omega}$$

$$C_p = 1.74 x 10^{-10}\ \text{F} = 174\ \text{pF}$$

We can combine C_p with the 83 pF shunt capacitance computed above, into a single shunt capacitance of 257 pF.

Performing the same computations for the termination results in a required series inductance of 826 nH and parallel capacitance of 196 pF, which we combine with the 226 pF shunt capacitance into a single 422 pF capacitor.

We are now finished with the design, illustrated at Figure 21. The remaining task is to select standard component values to match our design parameters, and build and test the completed design. We will add one step to this; to simulate the design with a *Spice* simulator, *LTspice/SwitcherCAD*.[31] Figure 22 shows excellent agreement between the simulated response and measured responses of an earlier version of this design. The *Spice* prediction in Figure 22 is shifted to align its peak with the measured peak, an adjustment necessitated because the simulation is based on measured motional parameters that are accurate only to within 2% or so. Figures 23 and 24 show the measured amplitude and group delay response of the earlier design. This filter's bandwidth is a bit narrower than the 200 Hz design target, measuring 171 Hz with an insertion loss of 7.8 dB. The last check on our earlier design is to compare the predicted and measured 3 dB:60 dB shape factor. Table 12 summarizes those results.

This design exercise should convince you that time spent characterizing the crystals and computing component values yields a filter that works — first time — as designed, without cut and try adjustments. Perhaps Lord Kelvin knew about which he spoke.

Notes

[1]Mouser Electronics part number 520-HCA800-SX; DigiKey part number X991-ND.

[2]For the relationship between sweep time, frequency span, resolution bandwidth and video bandwidth see, for example, Anritsu, "Technical Note: The Basis of Spectrum Analyzers" (2006), Slide 18 at **www.eu.anritsu.com/files/SpectrumAnalyzer_EE1200.pdf**.

[3]Hewlett Packard Co, Application Note 150, Spectrum Analysis Basics (1974); updated version available from Agilent at **www.home.agilent.com/upload/cmc_upload/All/5952-0292EN.pdf**.

[4]H.W. Batten, et al, *The Response of a Panoramic Receiver to CW and Pulse Signals*, Technical Report No. 3, (1952) Electronic Defense Group, Department of Electrical Engineering, University of Michigan, at **hdl.handle.net/2027.42/3473**.

[5]Anatol I. Zverev, *Handbook of Filter Synthesis*, John Wiley and Sons, Inc, (New York: 1967).

[6]James Clerk Maxwell, *A Treatise on Electricity and Magnetism*, Vol 1, Oxford Press, (1873), p vi.

[7]William Thompson (Lord Kelvin), *Popular Lectures and Addresses* [1891-1894], cited in *Bartlett's Familiar Quotations*, Fourteenth Edition, 1968. This was paraphrased in more memorable language by my Transmission Line professor in electrical engineering school, many years ago, as "if you can't measure it, it's not worth a damn."

[8]Zverev, see note 5, Ch 8.

[9]David Salt, *Hy-Q Handbook of Quartz Crystal Devices*, Van Nostrand Reinhold Co Ltd (UK: 1987).

[10]Wes Hayward, et al, *Experimental Methods in RF Design*, American Radio Relay League, (Newington, CT: 2003), ISBN 0-87259-879-9. *Experimental Methods in RF Design* is available from your local ARRL dealer, or from the ARRL Bookstore, ARRL order no. 8799. Telephone toll-free in the US 888-277-5289, 860-594-0355, or fax 860-594-0303; **www.arrl.org/shop/**; **pubsales@arrl.org**.

[11]M. Dishal, "Modern Network Theory Design of Single-Sideband Crystal Ladder Filters," *Proceedings of the IEEE*, December 1963.

[12]John Pivnichny, N2DCH, *Ladder Crystal Filters*, MFJ Enterprises, Inc (Starkville, MS: 1999).

[13]For imperfect elements, such *as* those with loss, the phase shift is not exactly zero at the point of maximum impedance, but the crystal Q is high enough that the difference between zero phase and maximum impedance is small. See F. E. Terman, *Radio Engineers' Handbook* (McGraw-Hill Book Co, Inc: 1943), Section 3, Paragraph 2 for all three definitions of parallel resonance.

[14]See note 10.

[15]See note 12.

[16]International Electrotechnical Commission, Standard IEC 60444 is an eight-part work defining how piezoelectric crystal parameters are to be measured. It replaces the former IEC 444 standard.

[17]See note 9.

[18]See note 12.

[19]See note 9.

[20]Omicron Lab, Application Note "Measurement of the equivalent circuit of a quartz crystal" available at **www.omicron-lab.com/customer_examples/pdf/Measuring_Equivalent_circuit_of_Quartz_crystal_II.pdf**.

[21]Figure 9 shows 3.0921 dB attenuation, while Figure 10 shows 3.0397 dB attenuation. Both figures were taken in sequence, with identical setup and calibration, separated by less than 15 minutes in time. Small changes in connection resistance as the crystal is held in a socket, for example, can easily cause 0.05 dB changes in series attenuation.

[22]Measurement of the equivalent circuit of a quartz crystal, see note 21.

[23]See note 10.

[24]See Hayward, *Experimental Methods in RF Design*, page 3.19. It states the relationship as

$$C_m \approx 2C_s \frac{\Delta f}{f}.$$

This equation omits the holder capacitance, which is paralleled with C_s via the voltage dividing capacitors C_p in Figure 3.35. In a private communication on 20 May 2006, Wes Hayward confirmed the corrected equation presented in the text of this article.

[25]Hewlett Packard, *87510A Gain-Phase Analyzer Operation Manual*, (1991), Manual Update for Software Release 2.10 (June 1994), pp 4-2 through 4-3.

[26]Subsequent to the work described in this article, the author acquired a Saunders & Associates model 7000022 Crystal Measurement Reference Crystal, which is a 20 MHz AT-cut crystal with a data sheet certifying the particular crystal's static and motional parameters, as measured with an S&A 250B automated crystal parameter test set. Measurements of the reference crystal's motional parameters show my G3UUR oscillator data to be about 2.5% low and the 87510A data to be about 2.5% high. The author's web site, **www.cliftonlaboratories.com**, has more discussion comparing reference crystal parameters measured with a variety of methodologies and test fixtures.

[27]The author is aware of only one free crystal filter design computer program, *AADE Filter Design*, available for download at **www.aade.com/filter32/download.htm**. However, *AADE Filter Design* bases its coupled resonator filter design on infinite q_0, as the help file crystal filter section states "Q and R_s values are not used in the design of the filter." The author of *AADE Filter Design* confirmed this understanding of the software in a private *e*-mail message to the author. The infinite q_0 assumption can result in significant error in many designs. Nonetheless, *AADE Filter Design* remains an excellent program for general filter design and the author encourages any reader interested in filter design to download it. In addition, the *Xlad* ladder crystal filter design assistance program is provided with *Experimental Methods in RF Design,* but is not as complete as *AADE Filter Design*.

[28]See note 5.

[29]See note 10.

[30]William B. Kuhn, "Matching Network Design," at **www.eece.ksu.edu/~wkuhn/useful_stuff/RFmatchingNetworks.PDF**.

[31]Randy Evans, KJ6PO, "PSpice for the Masses," Jan/Feb 2006 *QEX*, *LTSpice/SwitcherCAD* is available for free download via **www.linear.com/company/software.jsp**.

Jack Smith, K8ZOA, has been licensed since 1961, first as KN8ZOA, and has held an Amateur Extra Class license since 1963. He received a BSEE degree from Wayne State University in Detroit in 1968 and a JD degree magna cum laude from Wayne State University School of Law in 1976. Presently retired, he has enjoyed a career involving both engineering and telecommunications law. He is a co-founder of the telecommunications consulting firm TeleworX and is the author of Programming the PIC Microcontroller with MBasic *(Newnes Publishing, 2005), as well as many articles published in* 73 Amateur Radio *magazine. His Web site is* **www.cliftonlaboratories.com**. QEX

The Integration of Amateur Radio and 802.11

Amateur Radio and 802.11 wireless networking — a good fit for emergency message delivery.

Roderick D. Mitchell, KL1Y

Integrating two distinct and otherwise autonomous systems can provide rewarding results. There has been a lot of discussion about the use of commercial wireless protocols in the Amateur Radio community. These protocols, defined in the Institute of Electrical and Electronics Engineers (IEEE) 802.11 standards, specify several wireless bands and modulation schemes for local and wide area networks. There are many possibilities with great potential for using available low-cost high-speed devices. Recently I had an opportunity to integrate Amateur Radio and 802.11. The goal was to choose a project that was viable, worth while and feasible in regards to time constraints. I chose the *Winlink 2000* Paclink network. Paclink is a component of the *Winlink 2000* messaging system. The Paclink network allowed me to integrate a wireless local area network (WLAN) using 802.11b/g, a Paclink e-mail server and an Amateur Radio system into a single network. Each of the integrated devices contains protocols and/or technologies that allow it to interconnect with other systems and devices in the network. Protocols are rules that define how communications devices communicate in a network.

PO Box 35053
Fort Wainwright, AK 99703
kl1y@arrl.net

The integration of various systems to form a single diverse system is critical today. Budget cuts that result in equipment and personnel shortages plague many organizations. The ability to integrate non-profit organizations and leverage their experience is critical. Amateur Radio Operators provide non-profit services to the community. Now Amateur Radio's ability to support government and non-governmental efforts during a disaster has expanded. This added capability is due to the integration of current automation and networking technologies with Amateur Radios. Several Amateur Radio Operators (Vic Poor, W5SMM, and Rick Muething, KN6KB) have worked very hard to develop the Paclink messaging software that allow Amateur Radio to integrate seamlessly with modern networking equipment and e-mail clients such as Microsoft *Outlook*, *Netscape* and *Outlook Express*.

Table 1
Application Level Protocol Port Assignments

Protocol	*Port*
http	80
SMTP	25
POP3	110
TCP	8000

The following sections describe the technical details of the system that integrates Amateur Radio and 802.11. This project supports the implementation goals of high speed multimedia (HSMM) through the use of 802.11. This integrated network easily integrates with the Amateur Radio Internet (Hinternet).

Integrated Technologies Explained

The core technologies that form the nucleus of this Hinternet project are radio frequency (RF), IEEE standards, communications protocols and communications applications and software.

Each of the core technologies has a place in the Open Systems Interconnection (OSI) model. OSI is a model for understanding and developing computer-to-computer communications.[1] The OSI model consists of seven layers: physical, data link, network, transport, session, presentation and application. See Table 1. The following section describes the integrated technologies of this project, their protocols and their place in the OSI model.

OSI Model View of Integrated Technologies

The physical layer of the OSI model converts the ones and zeros to electrical signals

[1]Notes appear on page 32.

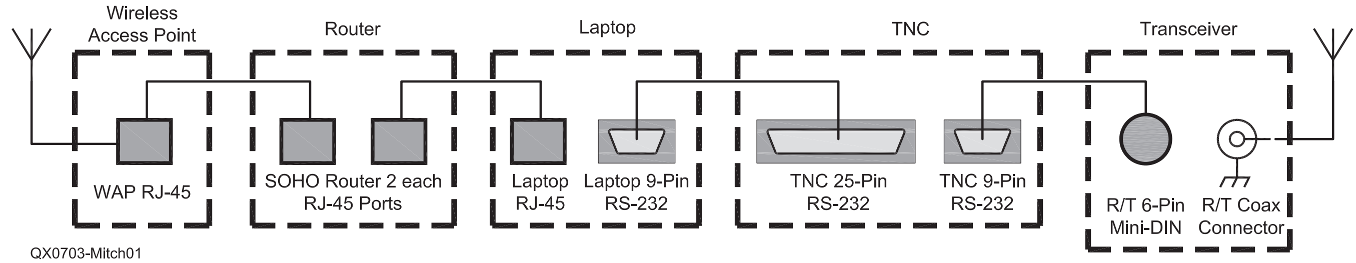

Figure 1 — Wiring diagram of integrated Amateur Radio and 802.11 network.

for transmission between devices.[2] The data link layer provides an error detection function. The network layer provides logical addressing and routing of information on the network. On the transport layer, error correcting techniques are employed.[3] The session layer allows provisions for data exchange between applications as explained by Tuma and Fajfar. Tuma and Fajfar explained the presentation layer as the layer that ensures that applications can communicate with each other when the applications use different formats. The application layer is where application protocols reside in the OSI model.

The following sections describe functions of the specific protocols and technologies used in this project. The descriptions are based on the protocol or technologies function in the OSI model. Table 1 provides a quick view of the communications technologies used and their place in the OSI model. Figures 3 through 6 show the elements of the system.

Physical Layer

IEEE 802.11 at the Physical Layer

An 802.11b/g wireless access point (WAP) provides LAN connectivity to wireless clients equipped with 802.11b/g wireless network interface cards (NICs). A high gain omnidirectional antenna is used for transmission and reception of signals. 802.11 is a member of the IEEE 802 family, a series of specifications for local area network (LAN) technologies. Figure 1 is a wire diagram. The diagram shows the physical connectivity of the integrated circuit. Figure 2 depicts interconnections from a three dimensional perspective.

IEEE 802.3u at the Physical Layer

IEEE 802.3u is the standard also known as Fast Ethernet. This project uses an SMC small office/home office (SOHO) router. The router provides connectivity at the physical layer between the computer and WAP via IEEE 802.3u interfaces.

Amateur Radio at the Physical Layer

The backbone (wide area network connectivity) of the network is dependent upon Amateur Radio at the physical Layer. Amateur Radio is used to move the data from the local area network (LAN) to the Internet or other areas outside the LAN. Amateur Radio technologies and protocols used at this layer include: radio frequency (RF), frequency modulation (FM), TNCs and the AX.25 packet protocol.

AX.25 at the Physical Layer

The Amateur Radio packet protocol AX.25 operates at the physical layer for connectivity between two terminals. AX.25 assumes that both ends of the link are of the same class.[4] This class distinction is in regards to data terminal equipment (DTE) and the data communications equipment (DCE). With AX.25 there is no DTE and DCE. Connectivity between the computer and TNC is over serial cable using an RS-232 serial cable.

RS-232 at the Physical Layer

This network uses RS-232 connectivity between the computer and TNC and between the TNC and radio. RS-232 is a set of standards that specify three types of interfaces: electrical, functional and mechanical.[5] The computer to TNC connection is a 9-pin D shape connector on the computer side and 25-pin D shape connector on the TNC side. The radio to TNC pin out for the 9-pin RS-232 connection and the 25-pin pin out are available at the Kantronics Web site: **www.kantronics.com/documents/kpc3ppinout.pdf**.

Coaxial Cable at the Physical Layer

Coaxial cable is used between the transceiver and the antenna. RG-8/U is used for this application. Some versions of RG-8/U have relatively low loss. We selected one that had a loss of approximately 1.8 dB per

Table 2
OSI Reference Model with Technologies Used in the Integrated Amateur Radio and 802.11 Networks

OSI Layer	*Protocol or Technology*
Application Layer (7)	SMTP, POP3, DHCP
Presentation Layer (6)	B2F
Session Layer (5)	TCP/IP (Sockets)
Transport Layer (4)	TCP, SMTP (Port 25), POP3 (Port 110), HTTP (Port 80)
Network Layer (3)	IP and Router
Data-Link Layer (2)	802.11, 802.3u, AX.25, KISS, Switch
Physical Layer (1)	AX.25, RF, RS-232, IEEE 802.3u, IEEE 802.11, Coaxial Cable (RG-8/U), UTP Cable

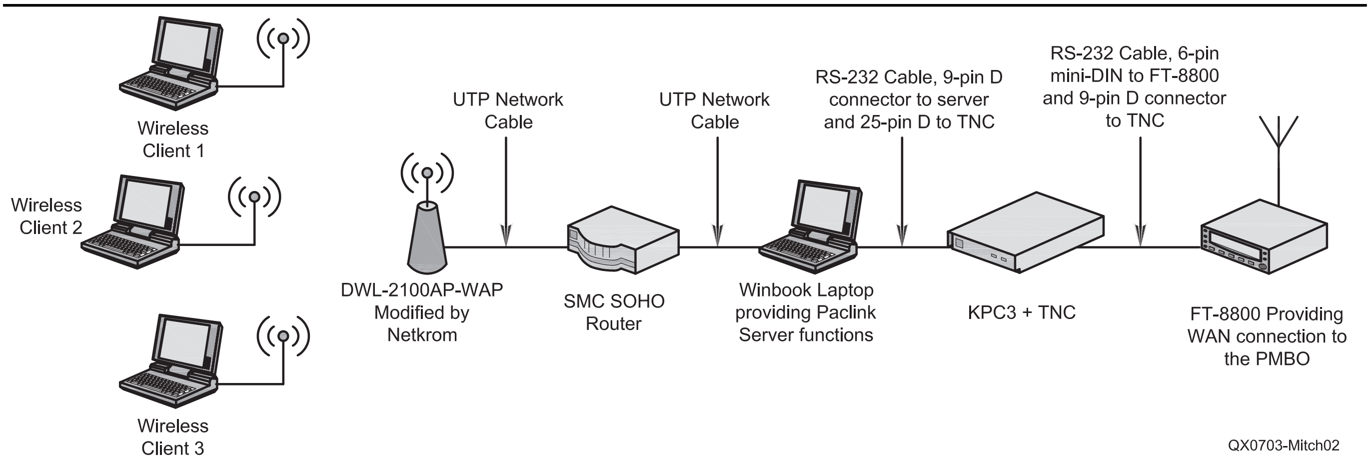

Figure 2 — Interconnections of integrated network.

100 feet over 144 to 148 MHz. With our 50 feet, power loss is about 0.7 dB.[6]

UTP Cable at the Physical Layer

Unshielded twisted pair (UTP) cabling is used to interconnect the router, WAP and server. UTP is less expensive than its shielded (STP) counterpart. STP provides the best immunity to stray RF interference. The short lengths of UTP have proved reliable in this project. The UTP cable consists of four insulated pairs of wire. Wires 1, 2, 3 and 6 are used for transmission and reception of signals.

Data Link Layer

Network Switch at the Data Link Layer

Switches are connectivity devices that make efficient use of bandwidth. Switches allow devices to establish a direct connection to another port on the switch. This is in contrast to hubs that broadcast data to all ports. The switch in this network implementation provides connectivity for the WAP and server. Other LAN computers or, a printer, may be attached to the switch as the need arises. The switch interprets media access control (MAC) address information to determine where to forward packets it receives.[7] The MAC address is a special address that is burned on the NIC during the manufacturing process. Each MAC address is unique. The switch, dynamic host control protocol (DHCP) server and router are all integrated in the SMC router housing.

IEEE 802.11 at the Data Link Layer

The definition of 802.11 functions at the MAC sublayer of layer 2 of the OSI model stated that "802.11 allows for mobile network access; in accomplishing this goal a number of additional features were incorporated into the MAC."[8] As a result the 802.11 MAC may seem baroquely complex compared to other 802 MAC specifications".

IEEE 802.11 is not a far departure from other 802 standards. 802.11 adopted Ethernet-style networking to radio links. In a similar way that Ethernet operates, 802.11 uses a carrier sense multiple access (CSMA) scheme to control access to the transmission medium.

IEEE 802.11 uses carrier sense multiple access collision avoidance (CSMA/CA) rather than the carrier sense multiple access collision detection (CSMA/CD) scheme used by 802.3 (Ethernet). CSMA/CA attempts to avoid collisions. CSMA/CD detects collisions, stops transmitting and then retransmits the data.

IEEE 802.2 at the Data Link Layer

IEEE 802.11 uses the IEEE 802.2 encapsulation. The logical link control (LLC) sublayer protocol allows the 802.3 and 802.11 protocols to carry multiple, logical sub-network traffic of each protocol over the

LARRY LEDLOW JR, N1TX

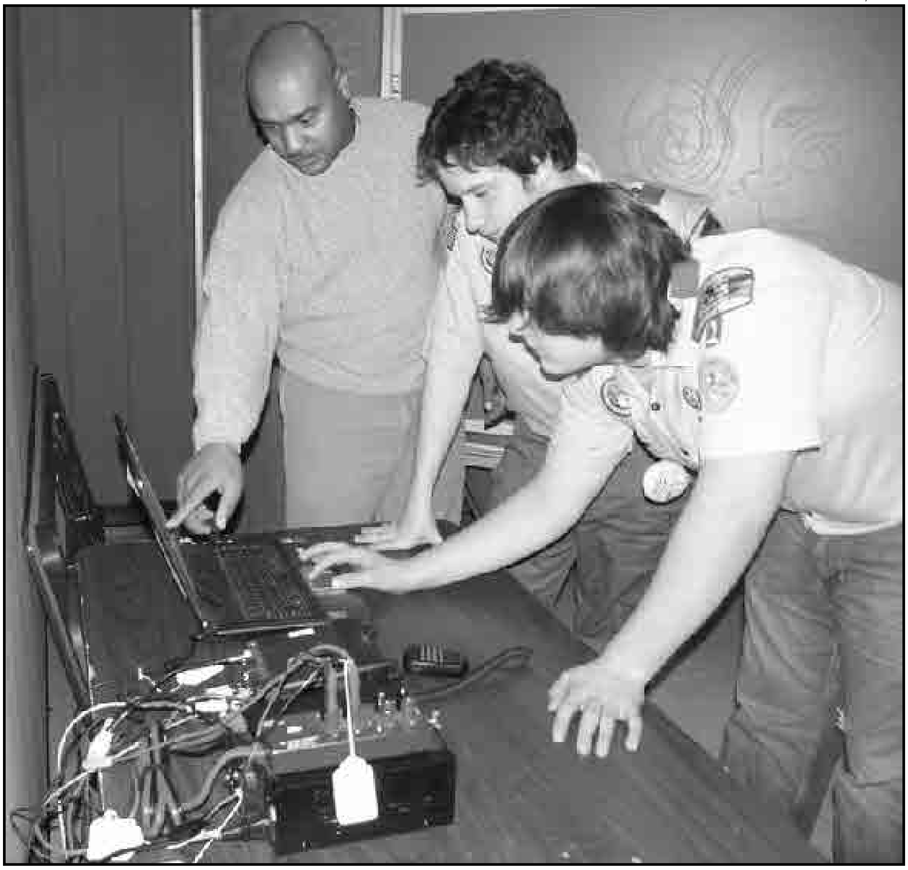

Fig 3 — Rod, KL1Y, explaining the possiblities that exist when using 802.11 with Amateur Radio. The two Boy Scouts are Michael Walsh (closest to Rod) and Jackson Drew.

Figure 4 — Denise Mitchell, KL1OP (Rod's wife), sits at the operating position and monitors activities on the Paclink server.

Figure 5 — Breannah Jayde Mitchell (Rod's daughter) prepares a message for transmission from a wireless enabled computer on the integrated network.

same physical medium such as the LAN.[9]

The LLC sublayer provides an interface with the network layer protocols. The LLC sublayer is responsible for the ordered delivery of frames, including retransmission of missing or corrupt packets and for flow control (moderating flow so that one system does not overwhelm the other).[10]

IEEE 802.3u at the Data Link Layer

IEEE 802.3u (Ethernet) is used to provide connectivity between the Paclink server and WAP via the SOHO router. IEEE 802.3u specifies a standard capable of sending data at 100 Mbps (Newton, 2005, p 31).[11] At layer 2 Ethernet uses the CSMA/CD media access control.

The specific layer 2 functions of Ethernet include encapsulation and de-encapsulation of user data, media access management, collision detection and handling data encoding and decoding and finally, channel access to the LAN medium.[12]

Amateur Radio at the Data Link Layer

Amateur Radio protocols at layer 2 are AX.25 and Keep it Simple Stupid (KISS). The AX.25 protocol functions at both the physical and data link layers. KISS functions only at the data link layer. At layer 2, AX.25 encapsulates the e-mail messages for transmission over the air through radio frequencies. AX.25 ensures that compatibility exists between two Amateur Radio stations at layer 2.

The data rate between the TNC and radio is only 1200 bps. This provides a throughput of 1200 bps across the backbone link. The robustness and stability of this protocol are sufficient enough to make up for the low throughput. These qualities are suitable for text messages and small (30 kB) attachments.

KISS (Keep It Simple Stupid) is the layer 2 protocol used for connectivity between the Paclink server and the TNC. This connectivity is over an RS-232 serial port. The KISS protocol on the TNC gives the Paclink server complete control over and access to the contents of the HDLC (high level data link control) frames transmitted and received over the air.[13]

The TNC simply converts between synchronous HDLC, spoken on the half-duplex radio channel, and a special asynchronous, full duplex frame format spoken on the Paclink server/TNC link. Every frame received on the HDLC link is passed intact to the host once it has been translated to the asynchronous format; likewise, asynchronous frames from the host are transmitted on the radio channel once they have been converted to HDLC format.[14]

The KISS protocol uses p-persistence. P-persistence causes the TNC to wait for an exponentially distributed random interval after sensing that the channel has gone clear before attempting to transmit. With proper tuning of the parameters p and SLOTTIME, several stations with traffic to send are much less likely to collide with each other when they all see the channel go clear. One transmits first and the others see it in time to prevent a collision. This is similar to the CSMA/CA technology used by 802.11.[15]

Network Layer

Network Router at the Network Layer

The network layer of this integrative project employs the use of a router. The router is the gateway to the LAN and allows remote clients to access the e-mail server. The router forwards the packets throughout the LAN/WLAN based on their logical addresses.[16]

The network router used in this implementation is an SMC small office/home office (SOHO) router. This router uses logical addresses (IP addresses) to direct data between networks or segments.[17] The router used in this project has a WAN port that is connected to another network (separate broadcast domain). Nodes in the same broadcast domain can communicate with one another without passing data through a router.

Internet Protocol (IP) at the Network Layer

IP version 4 (IPv4) at the network layer of the OSI model is used for this project. The Paclink server and the wireless clients communicate by IP. The Paclink server is assigned a static IP address and the wireless clients may be addressed by dynamic or static configuration. The Paclink server is the e-mail gateway and provides access to the AX.25 channels. The WAP communicates with the Paclink server via the IP. Each wireless client, the WAP and Paclink use a 32 bit IP address. The addresses are within the same broadcast domain (network). The WAP has a management IP address that is in a separate broadcast domain.[18]

The Paclink server is the gateway device that provides connectivity between the IP network and the AX.25 network. The network layer IP datagram is passed through the gateway to the data link layer AX.25 protocol that resides on the Paclink server (gateway) for encapsulation and transmission through the Amateur Radio portion of the network. This process works in reverse as the frames come in through Amateur Radio and reach the TNC, then the gateway (Paclink Server) for transmission to the wireless clients.

Transmission Control Protocol (TCP) at the Transport Layer

TCP is the transport layer end to end protocol. TCP provides reliable, sequenced, and unduplicated delivery of bytes to users on the wireless LAN (WLAN) and LAN.[19]

TCP is a connection-oriented protocol. TCP first establishes a connection between the two systems that intend to exchange data. TCP formats segments for the network layer by breaking the segments into packets that are the appropriate size for the network.[20] TCP assigns each packet a sequence number. The packets are reassembled at the distant station in accordance with their sequence numbers. TCP uses a checksum to verify the accuracy of the message. If the checksum is accurate the recipient sends an acknowledgment (ACK). If the checksums do not match, the recipient asks the sender to resend the message.[21]

Figure 6 — The components of the integrated network are pictured left to right: Astron power supply, MFJ power strip, Yaesu FT-8800 transceiver with KPC3+ TNC sitting on top, Winbook laptop with *Paclink AGW, Paclink Post Office* and *AGW Packet Engine* software installed. To the right of the server is the SMC router and behind the router is the DWL-2100AP modified by NETKROM.

TCP uses ports to establish communications between the various application layer protocols used in this network. Ports are a logical point of connection in the context of TCP. TCP uses port values in the range of 0 to 65,535. The application level protocols and ports used in this network are shown in Table 1.

HTTP (application level protocol) port 80 is used for management of the WAP and router. SMTP port 25 and POP3 port 110 are used by the e-mail clients for messaging. On the client computer, additional ports are used at random to establish a connection on the server with the ports listed above. This was revealed during an analysis using an Ethereal protocol analyzer. Port 8000 is used to connect *Paclink AGW* to the *AGW Packet Engine*.

TCP/IP Sockets at the Session Layer

TCP/IP sockets are used at the Session layer of the OSI model. At this layer the logical links are bound and unbound between application layer protocols (users of service). The session layer maintains and controls the dialogue between the users of the service.[22]

In TCP/IP the socket number is the joining of the senders' (or receivers') IP address and port numbers for the service being used (Example: 192.168.25.38:80). The combined IP address and port number identifies the unique connection in the network.[23]

B2 Forwarding (B2F) Protocol at the Presentation Layer

B2F is used at the presentation layer for preparing messages for transmission over the single channel Amateur Radio.

B2F describes an alternate "automatic only" addressing and protocol scheme for delivering messages within the Winlink 2000 system. Poor, W5SMM, et al explained that "messages consist of three parts: header; body and attachments."[24] All parts of the message are combined into a single file that is compressed by *B2Compress.exe*, the B2F protocol compression program, as a unit before transmission.

Application Layer

SMTP at the Application Layer

The simple mail transfer protocol (SMTP) is used with the Paclink server. SMTP facilitates the outgoing message transfer function for e-mail clients. If an e-mail program such as *Outlook Express* is used on the Paclink server, the outgoing mail field is set to LOCALHOST. The WLAN and LAN client e-mail programs' outgoing mail field is set to the IP address of the Paclink server.

Post Office Protocol 3 (POP3) at the Application Layer

The POP3 service is provided by the Paclink server. The server facilitates the incoming message transfer function for e-mail clients. If an e-mail program is installed on the Paclink server this e-mail program's incoming mail field is set to LOCALHOST. The WLAN clients' e-mail program's (*Outlook*, *Netscape*, etc...) incoming mail field is set to the IP address of the Paclink server.

DHCP at the Application Layer

DHCP (Dynamic Host Configuration Protocol) is an application layer protocol (Dean, 2006).[25] DHCP is used in this network to provide automatic IP addressing for computers that connect to the integrated network through the WAP or directly to the switch. One of the many functions of the SMC small office/home office (SOHO) router is the DHCP server function. The Paclink server is not setup for DHCP. DHCP addresses could change automatically as leases expire therefore it is better to setup the Paclink server with a static IP address. Clients require seamless connectivity to the Paclink server. Changing the IP address on an inconsistent basis would disrupt the seamless connectivity. Dynamically assigning addresses to clients is a good idea because it lightens the administrative duties of the network administrator.

Software Packages Explained

The software packages used in this project provide connectivity and driver functions to facilitate the transfer, compression of data and transmission of data over the radio waves. The software used by the integrated Amateur Radio and 802.11 project include *AGW Packet Engine*, *Paclink AGW*, *Paclink Post Office* and the e-mail program, *Outlook Express*.

AGW Packet Engine

AGW Packet Engine is the TNC driver that resides on the Paclink server. The packet engine interfaces the TNC and *Paclink AGW* software. *AGW Packet Engine* is setup in KISS mode to communicate with the TNC. The packet engine controls the radio data rate and issues all commands required to facilitate communications between Paclink, the TNC, and radio. *AGW Packet Engine* creates channels with communications ports for *Paclink AGW*. These pre-defined channels allow Paclink to send data over the radio via the TNC.

Paclink AGW

Paclink AGW communicates with *Paclink Post Office* and *AGW Packet Engine*. *Paclink AGW* formats the messages for delivery by compressing the message with the B2F protocol. *Paclink AGW* has an open dialog box that allows the network administrator or radio operator to monitor the connection, compression and message dialog between the Paclink server and the PMBO. In addition to other functions provided by *Paclink AGW*, AX.25 functions and features are provided by this software.

Paclink Post Office

The integrated Amateur Radio and 802.11 network uses *Paclink Post Office* as a component of the Paclink server. *Paclink Post Office* is the program required to provide connectivity between *Paclink AGW* and the user's e-mail program. *Paclink Post Office* provides the POP3/SMTP mail server functions.

In this installation *Paclink Post Office* uses the Amateur Radio call sign KL1Y for the Paclink site. *Paclink Post Office* may be configured for use on the local machine and LAN. The SMTP port number used is 25 and the POP3 port number is 110. *Paclink Post Office* listens on these ports for connection requests from e-mail programs.[26] When each e-mail program requests to connect to the POP3 server for the purpose of sending and receiving e-mail, the Paclink POP3 server validates the username and password.

The use of tactical addresses and the ability to use a common e-mail application are two key aspects of this network that allow the Amateur Radio community to seamlessly integrate with supported agencies and provide quick and reliable support. Tactical addresses are non-Amateur Radio call signs. An example of a tactical address is: **fbksemcomm-1@winlink.org**.

E-mail Program

This project uses Microsoft *Outlook* and Microsoft *Outlook Express*. It is possible to install and use any e-mail program capable of POP3 configuration. Messages sent to targeted recipients are viewed by any e-mail program capable of viewing text messages.

The Support Team

John Champa, K8OCL, HSMM Chairman, was instrumental in providing advice and mentorship in developing this document. Many local Amateur Radio operators supported the development of this local implementation. The operators readily provided logistics support and technical expertise. Linda Mullen, AD4BL, obtained a grant to purchase the amateur gear used in the project, Kody Moore, KLØRN, hand made the interface cables that connected the radios to the TNC,

Larry Ledlow Jr, N1TX, provided guidance as my mentor during the entire project. Larry devoted countless hours to reading drafts and the discussion of technical details.

Jerry Curry, KL7EDK, was instrumental as the Participating Mailbox Office (PMBO) Operator and packet expert. Dan Wietchy, KL1JP, was helpful in providing feedback and advice for the original paper.

Conclusion

This integrated network provides connectivity to the Amateur Radio network through 802.11. The use of 802.11 in this scenario allows connectivity without wires. This extension of the radio network provides a convenient messaging system that can be quickly deployed.

In backbone architectures the VHF Amateur Radio network has proven much more reliable than 802.11 networks despite the low throughput of the Amateur Radio network. The use of 802.11 is not out of the question for the WAN links. An 802.11 WAN network is highly dependent upon line of sight connectivity with minimal obstruction.

Notes

[1]T. Dean, *Network+ Guide to Networks,* 4th Edition, Boston: Course Technology, 2006.

[2]See Note 1.

[3]T. Tuma and I. Fajfar, "Hands on approach to teaching the basic OSI reference model." *International Journal of Electrical Engineering Education, 37*(2), 157, 2000.

[4]W. Beech, D. Nielsen and J. Taylor, *AX.25 Link Access Protocol for Amateur Packet Radio,* Revised Edition, Tucson Amateur Packet Radio Corporation, 1998.

[5]H. Newton, *Newton's Telecom Dictionary,* 21st Edition. San Francisco: CMP, 2005.

[6]West Penn Wire. *RG-8/U Coaxial Cable Flexible Design*, 2005. **www.westpenncdt.com/pdfs/RF_Transmission_50-OHM_cables/808F.pdf**.

[7]See Note 1.

[8]M. Gast, *802.11 Wireless Networks,* 2nd Edition, Sebastopol, CA, O'Reilly Media, Inc, p 14.

[9]D. Spohn, *Data Network Design,* 2nd Edition, New York, McGraw-Hill, 1997, p 255.

[10]M. Myers. *Managing and Troubleshooting Networks*. Boston: McGraw-Hill, p 50.

[11]See Note 5, p 31.

[12]See Note 8, p 260.

[13]M. Chepponis, K3MC, and P. Karn, KA9Q, *KISS Protocol*, **www.ax25.net/kiss.htm**.

[14]See Note 13.

[15]See Note 13.

[16]See Note 1.

[17]See Note 1.

[18]See Note 5, p 444.

[19]See Note 5, p 828.

[20]See Note 5, p 829.

[21]See Note 5, p 829.

[22]See Note 5, p 755.

[23]See Note 5, p 778.

[24]V. Poor, W5SMM, H. Kessler, N8PGR, G. Muething, KN6KB, S. Waterman, K4CJX, **winlink.org/B2F.htm**.

[25]See Note 1.

[26]G. Muething, KN6KB, and V. Poor, W5SMM, "Paclink AGW a Modern AX.25 WL2K Packet Client Compatible with POP3/SMTP Clients," 2005.

Additional References

The ARRL Handbook for Radio Communication, 2007 Edition. Available from your ARRL dealer or the ARRL Bookstore, ARRL order no. 9760. Telephone 860-594-0355, or toll-free in the US 888-277-5289; **www.arrl.org/shop/**; **pubsales@arrl.org**.

R. Bass, J. Potter, K. McGinnid, and T. Miyahira, "Surveying Emerging Trends in Emergency-related Information Delivery for the EMS Profession," *Topics in Emergency Medicine, 26*(2), 93-102.

S. Bender, *Producing the Capstone Project*, Dubuque, IA: Kendall/Hunt**.**

H. Berghel, "Wireless Infidelity I: War Driving," *Communications of the ACM, 47*(9), 21-26.

F. Block and M. Pursley, "A Protocol for Adaptive Transmission in Direct-Sequence Spread-Spectrum Packet Radio Networks," *IEEE Transactions on Communications, 52*(8), 1388-1396.

M. David, "ARRL's Role in Rescue Offers Lessons for Future," *Electronic Design,*19.

Kantronics KPC-3+ Port Pinout Information, **www.kantronics.com/documents/kpc3ppinout.pdf**.

T. Lammle and A. Barkl, *Cisco Certified Design Associate second edition*. San Francisco: Sybex.

L. Luna, "Getting Back Backhaul Costs," *Telephony, 246*(24), 10-12.

D. Rickie, "A Three-dimensional Framework for Information Technology Solutions," *IBM Systems Journal, 39*(2), 336.

C. E. Strangio, *The RS-232 Standard*, **www.camiresearch.com/Data_Com_Basics/RS232_standard.html**.

B. Waldo, "Information Technology: Strategies for Success," *Nursing Economic$, 16*(1), 33-43.

K. Schwalbe, *Introduction to Project Management,* Course Technology, Boston.

Rod Mitchell, KL1Y, became a licensed Amateur Radio operator in September 2000. He is also a member of the Army MARS program and is licensed as ALM7AQ. He holds a Master of Science in Information Technology from Capella University. He also holds an FCC General Radiotelephone Operator License, is a Cisco Certified Network Associate, Cisco Wireless LAN Support Specialist, Foundry Networks Certified Network Engineer, CompTIA A+ and CompTIA Network+ certifications.

He currently is serving his 21st year in the US Army and holds the rank of Chief Warrant Officer Four (CW4). His present assignment is Officer-In-Charge of the Local Network Operations and Security Center at Fort Wainwright, Alaska. He has recently accepted an appointment as Director, US Army MARS — Alaska.

Rod's previous positions include Communications and Electronics Integration Officer for the 172nd Stryker Brigade, US Army Alaska, Avionics Maintenance Officer-In-Charge, Communications and Electronics Maintenance Officer with 82nd Signal Battalion, 82nd Airborne Division, 514th Signal Company, 35th Signal Brigade and 520th Maintenance Company, South Korea. Rod served as a Special Electronics Devices Technician and Instructor with the US Army. Rod's first opportunity to operate radios was while assigned as a radio telephone operator (RTO) with the 4th Infantry Division. Rod is an adjunct faculty member with the University of Alaska Fairbanks, Tanana Valley Campus, Information Technology Department. QEX

Network/Data Layer Messaging Protocol for Stand-Alone, Free-Field Communications Systems

The author proposes protocols and data formats for a self-organizing network of stations to pass messages.

Lindsay J. Robertson, ZL2LJR

Abstract

Protocols and data formats are proposed that will allow a completely self-organizing network of peer stations using free-field, physical-layer communications to pass message packets from an originating station to a designated destination station at arbitrary distance, needing no other equipment or systems. The proposed system is presented in enough detail to allow implementation, but most importantly, the paper establishes some general principles that can be extended and developed as required.

Briefly, a datagram header format that contains geographical location and a local identifier of the destination station is proposed: peer stations build up internal lists of ID's and locations of other peer stations that they can "hear" — and hence each station that progresses a datagram is able to automatically select an optimum station to which the transient datagram may be passed. Simple protocols are proposed for authenticating and verifying datagram transfer, for rerouting datagrams to ensure a high probability of delivery, and for purging of datagrams that are successfully passed towards their final destinations. An "open" approach that encourages user control and further optimization is proposed. This is different from present Mobile Ad-hoc Network (MANET) protocols, and it also differs in several aspects from current geographic routing proposals and current radio packet transfer systems.

lindsay@tech-vantage.com

Need for Robust, Free-Field Network Layer System

Life without instant, reliable communication is just about inconceivable — we simply assume reliable communication via the Internet, cellular and "landline" phone services.

Yet a review of existing systems shows that only the long-range point-to-point HF radio system is both independent of a "wired backbone" and capable of long-range messaging. Although workable, the point-to-point HF radio system has limited reliability. (It depends upon ionospheric conditions between two stations, and is a highly inefficient use of bandwidth.)

Reliance upon wired communication backbones represents a significant vulnerability. To appreciate the issue, one only has to consider how useless a cell-phone handset is, without the cell-phone nodes and inter-node routing systems. A news item "The Backhoe: A Real Cyberthreat" describes this issue eloquently.[1]

The existing systems therefore do not adequately address any of the following situations:

- Cases where a large number of users (each with limited power) want to exchange messages over long distances, without excessive use of bandwidth.
- Cases where the only open bands are not available to a particular station (stations of limited power, or only VHF.
- A user (particularly a VHF/UHF user) who lives in a geographically remote location, such as at the end of a long valley.
- The aftermath of a natural disaster, (or deliberate sabotage) when a user is affected by disruption of either "last mile" or backbone transmission lines, or the loss of third party communication facilities. See Note 1.
- The aftermath of software errors (or attacks) upon a system that relies on a hardwired backbone.[2, 3]
- A user who lives in a region in which backbone communication facilities are operated by authorities whose oversight is unwelcome.

Situations of these types, and the lack of adequate solutions, represent the "need" that is addressed in this paper.

[1]Notes appear on page 38.

Existing Systems

Classification of Existing Systems

Before considering any proposed "new" system, it is essential to review systems already in existence. Classifications of network systems have been published before, however these have generally been limited to relatively narrow fields. For the purposes of this paper, a very broad approach is taken, and the following categories are proposed:

"Wired" Systems. For these systems, all nodes are hard-wired, and for each route segment, a router selects the next destination node and switches the packet to that node.[4] (See the referenced text, starting on page 405.) Examples include the Internet, and landline telephones. These offer efficient, high-speed communication, but are totally dependent upon the "wired" connection, and vulnerable to either physical disruption of wired "backbone" (see Note 1), and electronic disruptions (see Notes 2 and 3).

Wireless Neighborhood Networks. These

are dense local collections of wireless (commonly short range) nodes. Examples include the Zigbee system, various "household control" nets, and "Motes" ("smart dust").[5, 6] The protocols used in these systems include (but are not limited to) Ad hoc on-demand distance vector (AODV), Multi-Radio Link-Quality Source Routing (MR-LQSR), and Destination-Sequenced Distance Vector Protocol (DSDV).[7] These systems offer good levels of network resilience, but they are generally designed for short-range meshes in which nodes are aware of each other. See also Notes 8, 9 and 10.

Wireless Access Systems. These systems are characterized by the use of a single wireless point-to-point hop, from a mobile station to a wired network. Examples include cellular telephone and WiFi (802.11) internet access systems.

Wireless End-to-End. These are the systems that allow true point-to-point communication between peer (radio) stations. These systems rely on a single-hop path, with every connected node having a unique identifier — (MAC or call sign). Examples include commercial or amateur HF transceivers. Although autonomous, these systems make very inefficient use of bandwidth, and are totally dependent upon long wireless transmission paths.

There are a great number of variations within these categories: Ethernet rings are perhaps closest to the semi-wired category, and VHF radio repeaters, the "digipeater" facilities, AX.25 protocols and ROSE switches offer a limited multi-hop capability.[11]

Although some systems (satellite phone) do not fit this taxonomy exactly, the above list is largely complete, and is sufficient to illustrate the points raised in this paper.

Control Data Flow in Existing Systems

As well as user data flows, data communication systems usually require control data communicated between nodes of the network, to configure and reconfigure the network. In wired systems, network data is communicated either automatically (routers sharing dynamic routing tables) or manually (the Network Operator edits static router tables).

In a typical neighborhood system, nodes undertake a complex request/response protocol, at the end of which each node has established a route to each destination node. See Note 11.

The semi-wired and "wireless access" systems introduce one further level of complexity; the wired nodes must exchange information about the unwired devices that are currently connected to each node. In other words, they must dynamically associate the user addressing information (my cell-phone number, and the cell-phone number of the person I am calling) with the node interconnection information.

Control data may also include user address translation, such as DNS lookup data to translate user addressing data into datagram information that can be used by routers to select a next destination.

Although less easy to define, all network systems also incorporate various levels of "assumed knowledge" — whether this is acknowledged or not.

Basis for Proposed System

Design objectives

The subject of this paper is the specification of a system able to address the deficiencies of existing systems. The proposed objectives are:

a) Reliability. The proposed system must have a provable high probability of packet delivery, from source to destination, over arbitrary distances.

b) Ad-hoc, on demand route determination. The protocols and data format must allow packets of data to be automatically forwarded via any number of intermediate stations to a defined destination station. The origin station must not need to know or pre-discover the full route of the packet.

c) Peer stations only required. No other hardware or software besides the ad-hoc network of peer stations shall be necessary. ("Peer station" is assumed to mean a transceiver with at least one channel, plus basic computing capability.)

d) No restriction on physical layer selection. Intermediate (peer) stations must be able to determine the physical layer protocol (frequency, mode) that will be used for each "hop" — it is assumed that not all "hops" will use the same physical layer protocol.

e) Open format. The data formats, and general design must be "open."

f) Extensible and hierarchical service options. The protocols must allow services/facilities in a hierarchy of sophistication: it must be possible for very simple devices to function using the most rudimentary subset of protocols, and for progressively more powerful devices to add greater levels of sophistication.

Principles

The proposed system assumes that each station/node comprises at least one free-field physical-layer communication channel (radio transceiver with antenna, or similar equipment), plus basic computing capabilities and some data memory. This is not an onerous requirement — a single-channel VHF transceiver, and a simple, single-board computer

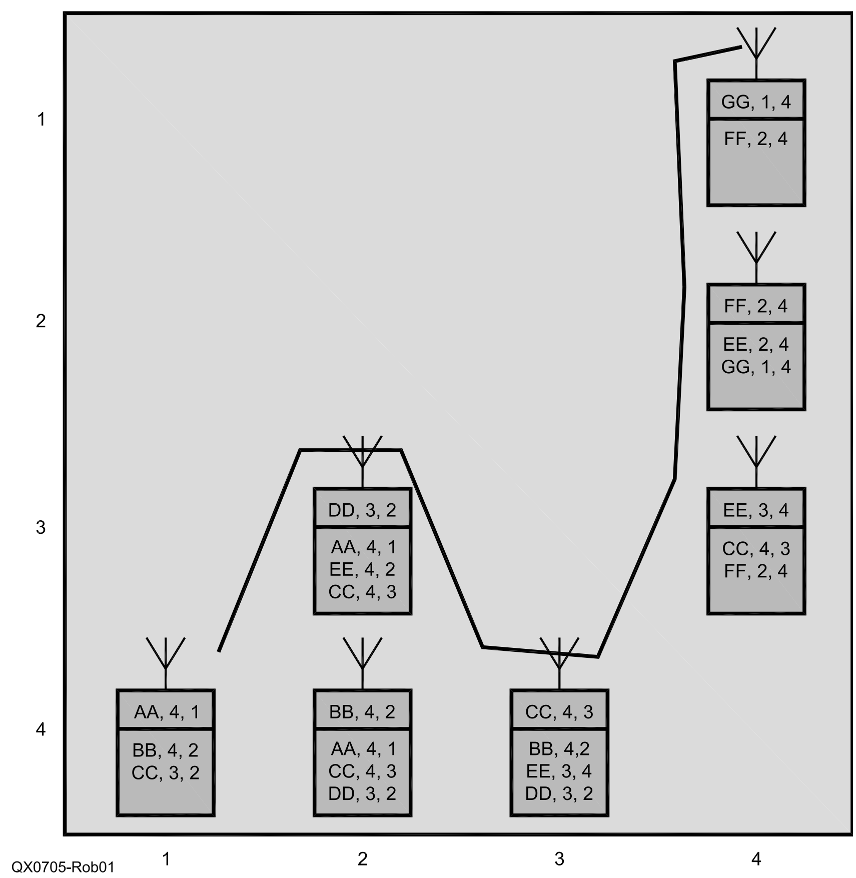

Figure 1 — Message route from AA to GG.

would be quite adequate. We can note that effective radio path distances of a few km are quite practical with the RF power levels readily available from handheld apparatus.

Three principles are essential:

a) Broadcast "Offer of service" and create local router table. Each station periodically broadcasts, on each physical-layer channel available to it, an "offer of service" (OOS) packet. These broadcasts advise other stations within reception range of its existence/identification, its location (geographical coordinates) and its available communication modes. Any "send" by a node/station is also treated by its listeners as an offer of service, on that channel. By scanning across its own receive channels, and storing data from the received "offer of service" packets, each station builds up its own file/record (analogous to a router table), of the identity, location and available physical-layer modes of stations that it can "hear".

b) Process, or pass-on datagram. When a station receives a packet (the packet has the receiving station's ID as either its final or immediate destination), it determines whether it is the final destination of the message, and if not it forwards the message. To forward a packet towards a distant destination station (whose exact ID, and approximate geographic location is contained in the message header), a users' station searches the list of stations that it has recently heard, and uses the listed station locations to calculate the one farthest in the desired direction (calculation of shortest route across the surface of a sphere). The users' station then places that (intermediate) station's ID into the packet header, and retransmits the message.

c) Acknowledge/purge datagram. Having received a packet, an intermediate or destination station confirms the integrity of the packet using the message digest, then sends an <ACK> that identifies itself, and identifies the packet by its message digest (CRC).[12] On receipt of this ACK, the (intermediate) source station deletes the packet from its memory.

Data packets carry the identity and the geographical coordinates of the packet's final destination, and progressively acquire a list of each station passed on its journey.

Some Theoretical Considerations

Node-to-Node Datagram Transfer

The proposed approach includes a "digest" in the datagram header (CRC or hash) of the data portion of the datagram. The essential property of a message digest is that it is highly unlikely that another set of data can have the same digest — hence the digest can, for practical purposes, be assumed to uniquely identify the data portion of the packet. This "digest" can therefore be used to prove the integrity of data transfer between two peer stations (nodes).

A true message-digest algorithm should be such that it is computationally impossible for two different datasets to generate the same "digest" — but such algorithms produce large outputs (the MD5 algorithm produces a 128-bit output).[13] This level of rigor is not required here; a shorter digest or hash function (possibly even such a simple functions as CCITT should be satisfactory.[14]

Origin-to-Destination Datagram Transfer

The proposed design allows the identity and location of each peer station that the datagram "passes," to be recorded in the datagram header. When a station receives a datagram, it identifies the "best" next hop destination — but if that station is listed in the datagram's header as having already been "passed," then clearly the route is a dead-end, and a "next-best" destination must be selected. Since the "worst" packet forwarding option (returning the packet to the previous station) is always available, this approach is effectively a depth-first search algorithm, which will ultimately find a path between source and destination if such exists.

Assumptions

A small number of assumptions/restrictions are inherent in the proposed design:

1) Assume that each user (station/node) has an ID (call sign) that is at least unique within its geographical area.

2) Assume that a destination user's approximate location is known or is predictable.

3) Assume that sufficient stations/nodes are implemented, so that at least one continuous corridor of transmission paths exists between source and destination.

Provided these assumptions/restrictions are accepted, then a long-distance, ad-hoc and extensible free-field messaging protocol is possible and practical.

Although one can postulate situations in which one or another of these criteria pose problems, it is respectfully suggested that for a very large proportion of practical situations, these are quite acceptable limitations, and furthermore that acceptable approaches are possible to mitigate these difficulties. I would argue that these are acceptable assumptions/restrictions.

The availability of higher ISO layers to handle the disassembly/reassembly of datagrams into files, can be assumed.[15]

The availability of encryption, to secure the contents of the message, can also be assumed. Although not covered in this paper, combinations of public/private key cryptography systems, and challenge/response identification systems could certainly be devised to prevent packet-spoofing problems. Since the datagram header is simply prepended to the message data, recovery and extraction of the message data is simple.

Proposed Implementation

Datagram Header Tags

In the field of data communications, data packet headers are commonly defined with fixed field lengths and without field delimiters. In a case where all fields must be used on all occasions, this approach has the advantage of incurring no bandwidth overheads for delimiting of fields. The approach does, however, have significant disadvantages. If all fields are not used all the time, there is wasted space, and conversely if insufficient (number or size) fields are defined, massive redesign is needed at a latter stage — this situation is the fundamental reason behind the move from IPv4 to IPv6.[16]

The system proposed in this paper places a high value on an "open" design approach, and for this and the above reasons, it is proposed to use an Extensible Markup Language (XML) format for the packet header.[17] The limited number of "tags" required allows single-letter tag names, reducing the size of the transmission overhead. The markup language approach offers an excellent combination of flexibility and extensibility.

The proposed data packet header is simply prepended to the data portion of the packet. See Table 1.

Datagram Formats

Three types of datagram (or packet) formats are required, as shown in Table 2.

It may appear that the use of a markup approach to defining header information imposes a significant transmission overhead. Closer inspection shows that because some information that would normally be supplied by higher ISO layers is already incorporated into the header of the SND datagram, the net overhead increase is small. For example, in the case of an e-mail message, the data portion of the IP packet will contain the "TO," "FROM" and other fields in ASCII text — information that is already contained within the "overhead" of an SND datagram. By restricting the size and number of tags in the proposed SND system, the real overhead is not excessive for moderate-sized messages.

A priority design principle is that of "openness" — in other words the accessibility of the system parameters and data by the user. This approach is somewhat at odds with the philosophy that requires equipment to be completely autonomous and able to cope with any eventuality. There is obviously a trade-off between user control and simplicity, but this issue can be easily managed by providing default settings.

Functions that should be accessible by the user include editing/updating of the router table, and editing/updating of station parameters.

Each station's router table is *local* and is prefiltered so only accessible modes are listed — when reduced to minimal level we have a station whose only purpose is to act as a single-mode relay station.

Since each peer station is functionally identical (acting as both an end-use station and a relay facility), the user located at the end of a long valley could provide a corridor of coverage by locating a series of minimal SND units strategically along the valley.

The proposed protocol requires that the approximate geographical location of the originating and destination stations must be known. The station ID tag links to each station ID, a datestamp (ccmmddhhmmss), and the station's latitude, longitude and height. With the assumption that individual sets have a range of a small number of km, this is not an onerous requirement for very many cases. The earth's circumference is about 40,000 km, so a 4-byte hex representation of longitude or latitude (for example, a3b4) allows a resolution of 600 meters — a practical option.

The station's "router" table should be a simple file containing repeating tuples with XML elements corresponding to Station_ID, latitude, longitude, height, time, frequency and mode. The use of the XML approach means that additional fields for permissions to access commercial stations, public keys, and so on, can be added in future.

Basic protocols

Broadcast Offer of Service, Update Router Table

The specification requires that each station periodically broadcast an "offer of service" packet, containing information that receiving stations can use to build up their internal router table.

These are proposed to be uniquely identified packet types, broadcast regularly on each physical-level channel available to the station. (See Note 15.) A station can also supply, in the body of each "offer of service" packet, more than one channel/mode data pair; hence provided that a station receives one "offer of service" packet from a peer, it can add all the possible channel/mode pairs available, without having to listen on multiple channels.

The data contained in the offer of service packet is the identity and location of the broadcasting station, and a set of data pairs identifying channel and mode combinations that are available

The data format is extensible (potentially to place limits on the duration of the offer of service), but provision for including authorization information, and the station's public key is anticipated.[18]

On receiving a broadcast "offer of service" message/packet, the receiving station uses the information in the broadcast packet to update its router table.

The ranking of stations within a router table, and further optimizations are easily envisaged, but not essential to the basic proposal of this paper.

Receive Datagram (Scan Channels), and ACK

In its default operational state, a station regularly scans each channel/frequency/mode available to it (that can be accessed by its physical-layer systems), listening for incoming data. Offer of service packets are not acknowledged.

Table 1
Packet Header Tag Formats and Descriptions

Tag, Name	*Description, Options, Example*
Header	Format <SND001 T=Type> Type options: "S" for Service, "A" for ACK, "D" for data. Example <SND001 T=A>.
Station ID (List)	Format <S Stn_type, Stn_ID, loc; Stn_type, Stn_ID, loc; etc > Stn_type = "FR" From, "TO" To, "PS" Passed, "NE" Next. Stn_ID = unique ID (eg call sign) Loc = ccmmddhhmmss,lo,la,ht — datestamp, latitude, longitude, height Example <S FR:ZL2LJR,123,123,123; PS: ZL1BOO,234,234,234; TO:ZL1ASD,123,123,123>
Channel (List)	Format: <C="Mode", "Frequency"> Example <C=FM,144.3; FM, 144.35; USB;3.600>
Validation	Format: <V Val_type,str LN=Length> Val_type options: CCITT32 Example <V CCITT32=a9f4R; LN=120>

Note: Although the route information increases the length of the header, because the "pass on datagram" protocol seeks the farthest station, the increase in length is the minimum possible.

Table 2
Datagram Formats

Datagram_type	*Format*
OOS	<SND001 T=O> <S FR=ZL2LJR,123,123,123 /> <C F=114.600,M=FM; F=115.00,M=FM /> </SND001>
MSG	<SND001 T=D> <S FR:ZL2LJR,123,123,123;; PS=ZL1AAA,123,123,123; TO=ZL1ABC,123,123,123 /> <V CRC=asdasd L=123 /> </SND001> .. Datagram content… (Note, the header is simply pre-pended to the message content)
ACK	<SND001 T=A> <S FR=ZL1AAA,123,123,123 /> <V CRC=asdasd /> </SND001>

If a broadcast offer of service packet or a data packet is received, then the "Update Router Table" function is invoked for that station on that channel. There is an important principle here; if a station can be "heard," its details are able to be added to other stations' router tables — for a user, the default option is that if the system is used, then the User's station is available to be used by the system also!

If a received packet is not complete, or its CRC is incorrect, it is ignored. If the receiving station does not (for whatever reason) have the capacity to process the message, the message is ignored!

If either the intermediate or final destination name of the incoming packet is the same as the receiving station, and if the receiving station decides not to ignore the packet, then the message is stored and processed.

Send and process ACK: When a station receives a datagram addressed to it (for example, the receiving station's ID is found against a Stn_type="TO" or Stn_type="NE" in the message header), the CRC is checked. If the CRC is valid, then an <ACK> datagram (containing the CRC of the received packet) is broadcast, and the receiving station's type is changed from "NE" to "PS" in the message header.

When a Station receives a broadcast <ACK> packet, the station scans its memory for a message with the same CRC. If a corresponding CRC is found, the Station concludes that this message has been successfully received by the (intermediate) destination station, and purges/archives the message from its memory.

User Control: If there is insufficient memory to store the incoming packet, then it is ignored. Each station's user-defined options control whether relay service is available — if not, then packets for which that station is not the final destination, are not <ACK>'d — in other words, are effectively ignored.

Process / Pass on Datagram

When a station receives a packet in which its ID is listed as the intermediate destination or as the final destination, the packet is processed. Then an <ACK> corresponding to that message is broadcast.

If the receiving station is designated as an intermediate station in the message, then the "Send-Onwards Datagram" function is invoked, and the attribute corresponding to the current station's ID is changed from "NE" to "PS" in the datagram header.

If the receiving station is the final destination of the data packet, then the "Accept Message" function is invoked.

Send-Onwards: The receiving station parses the coordinates of the final destination station (contained in the datagram). The receiving station then searches its "router" table. If the identification of the destination station is found in the router table (if the datagram's final destination is accessible), then the packet is broadcast.

If the destination station's ID is not in the router table, the station uses the coordinates of the packet's final destination, and computes from the coordinates of the stations in the router table, which of the stations is farthest along the path towards the final station's destination. If this proposed next station is already listed in the station ID tag, this indicates that the message has already passed that station, and found the route to be a dead-end; the station must therefore search the router table again for the next-best intermediate destination station. Having identified the next intermediate-hop station, that station's ID is inserted into the Station ID tag of the message's header, with the "NE" attribute.

The station then checks whether the frequency/mode for the next intermediate-hop station is free — if so the datagram is broadcast, otherwise the station waits and retries after a random delay — if channel is still in use, then the station reprocesses the router table, looks for another channel/mode that is equidistant or next-farthest towards the destination, loads that station's ID into the station ID field, then rebroadcasts.

The protocols automatically allow the use of any physical mode (medium, frequency, mode, speed and so on) for any particular hop, allowing good bandwidth utilization.

Packets that have been broadcast are retained in memory pending receipt of an <ACK> from the (final or intermediate) station to which they were addressed.

Following the broadcast of the packet, the sending station waits for an <ACK>: If an <ACK> is not received, the station retries (the number and frequency of retries is set by user-definable options), then reprocesses its router table, selects the next-farthest station from the router table, loads that station's ID into the packet's intermediate-station ID field, and rebroadcasts the datagram.

It is important to note that this procedure will eventually lead to the packet being sent back to the originating station, if no better destination is found: an important consideration in ensuring system robustness.

Note also that, by using the Stn_type="PS" attribute, the identify of each peer station that passes on a datagram, is recorded in the datagram header. While this approach potentially results in a large header, the absence of such a list would allow messages to be "trapped" in a dead-end coverage corridor — and by contrast, the presence of such a list allows a rigorous "depth-first" search for possible coverage routes to be conducted. The combination of the routing and <ACK> protocols, create a robust system; a node that does not <ACK> a message — for any reason — is automatically bypassed. A message that cannot be moved towards its destination is automatically returned to the previous node, allowing selection of an alternative route segment. This process is illustrated in Figure 1.

User Interface

Create Initial Datagram: To initiate the sending of a datagram, the user (application layer) needs to specify the location of the destination station. For practicality, a lookup table of locations/coordinates would be trivially easy to implement and would insulate the user from a possibly unacceptable level of detail.

Deal with Datagram Successfully Received at Final Destination:If a datagram whose final station ID is that of the current station is received, (so, the datagram has reached its final destination) then the datagram is passed on to the next highest protocol layer (possibly the user interface).

Conclusion

This paper has highlighted a serious vulnerability that is inherent in all "wired" communication systems. Having articulated the vulnerability, the paper described the functional necessities (specifications) of a highly decentralized, fully automated, peer-station network communication system.

Core protocols and data formats, that meet the specified need, have been defined: these core protocols and data formats are simple, robust and readily able to be both extended and optimized. The assumptions required to permit the proposed system to work have been examined, and it is suggested that these are acceptable and feasible for the vast majority of cases.

The technology elements required to implement the core protocols and data structures are readily available (basic transceiver, and basic computing capability — indeed, the core components are also present in cell-phone handsets)

Notes

[1]The Backhoe: A Real Cyberthreat, available online at **www.wired.com/news/technology/0,70040-0.html**.

[2]Anon, "The Day the Internet Died — Courtesy of the Florida Internet Exchange," 18 Aug 2003, available online at **flix.flirble.org/**.

[3]Cnet Staff Reporter "Router glitch cuts Net access," last modified 25 Apr 1997, 7:00 PM PDT. Available online at **news.com.com/2100-1033-279235.html?legacy=cnet**.

"'There are probably a hundred guys in back rooms keeping this stuff together, just barely,' Ricard said of the Internet."

[4]*Telecommunications: A Beginner's Guide*, Hill Associates, Inc, Pub 2002, McGraw-Hill/Osborne, Berkeley, CA, USA.

[5]ZigBee is a published specification set of high level communication protocols designed to use small, low-power digital radios based on the IEEE 802.15.4 standard for wireless per-

sonal area networks (WPANs). The specifications are available online at **en.wikipedia.org/wiki/ZigBee**. See also **www.merl.com/projects/zigbeestack/**.

[6]"Dust Networks," DustNetworks Ltd, available online at **www.dustnetworks.com/technology/overview.shtml**.

Also see A. M. Agogino, *MEMS "SMART DUST MOTES" FOR DESIGNING, MONITORING AND ENABLING EFFICIENT LIGHTING*(2003), Department of Mechanical Engineering, University of California, Berkeley, CA 94720. The Project Report 2002-03 for MICRO Project 02-001 is available online at **www.ucop.edu/research/micro/02_03/02_001.pdf**.

[7]C. E. Perkins, E. M. Royer, and S. R. Das, AODV (Ad-hoc On-demand Distance Vector), routing.draft-ietf-manet-aodv-06.txt, July 2000.

See also **www.usenix.org/events/osdi02/tech/full_papers/musuvathi/musuvathi_html/node12.html**.

[8]L. E. Miller, *Multihop Connectivity of Arbitrary Networks*, Wireless Communication Technologies Group NIST "Multihop connectivity," 29 March 2001, ConCalc.pdf.

[9]Richard Draves Jitendra Padhye Brian Zill, Microsoft Research, {**richdr**, **padhye**, **bzill**}**@microsoft.com**, *Routing in Multi-Radio, Multi-Hop Wireless Mesh Networks*, available online at **research.microsoft.com/mesh/papers/multiradio.pdf**.

[10]Ali N. Zadeh and Bijan Jabbari, George Mason University, Raymond Pickholtz and Branimir Vojcic, George Washington University, *Self-Organizing Packet Radio Ad Hoc Networks with Overlay (SOPRANO)*.

[11]Greg Jones, WD5IVD, *Introduction to Packet Radio*, available online at **www.tapr.org/pr_intro.html**.

See also L. Ehud, H. Eli, E. Amir, and D. Koren D, *X.25 Packets and Protocols*(2004). Available online at **www2.rad.com/networks/1996/x25/x25.htm**.

See also *Packet Radio: What? Why? How? / Articles and Information on General Packet Radio Topics*, TAPR, Publication #95-1. 1995. 130 pages. Particularly see the section about ROSE switches. Available online at **www.tapr.org/pr_intro.html** and **www.nzart.org.nz/nzart/digital/digital.html**. Particularly, see the "Digipeater" section.

[12]R. N. Williams, *A Painless Guide to CRC Error Detection Algorithms* (1996). Available online at **www.ross.net/crc/crcpaper.html**.

[13]Akadia AG, *MD5 — Message Digest* (fingerprint, checksum) (2000), available online at **www.akadia.com/services/md5.html**. See particularly the section on the MD5 algorithm.

[14]J. Geluso, *CRC16-CCITT* (2004), available online at **www.joegeluso.com/software/articles/ccitt.htm**.

[15]G. C. Kessler, *An Overview of TCP/IP Protocols and the Internet* (2003). Available online at **www.garykessler.net/library/tcpip.html**.

See also Anon, *OSI Layer Definitions* (2005). Available online at **www.webopedia.com/TERM/O/OSI.html**.

See also F. Halsall, *Data Communications, Computer Networks and OSI*, Second Ed, Addison-Wesley Publishing Co, Inc, 1988.

[16]Ipv6 Task Force, Mobile wireless working group report, available online at **www.ec.ipv6tf.org/PublicDocuments/IPv6TF-Mobilewireless.pdf**.

See also *RFC 3794*, available online: **rfc.net/rfc3794.html**.

[17]W3C, *Recommendation 10-February-1998 Extensible Markup Language (XML) 1.0*, available online at **www.xml.com/axml/testaxml.htm**.

[18]B. Schneier, *Applied Cryptography*, Second Edition. John Wiley & Sons, 1996, ISBN 0-471-11709-9.

See also Department of Commerce, National Institute of Standards and Technology, RIN 0693-AA86, A Proposed Federal Information Processing Standard for Digital Signature Standard (DSS), available online at **www.epic.org/crypto/dss/dss_fr_notice_1991.html**.

See also W. Stallings, *Cryptography and Network Security*, Third Edition(2005), available online at **williamstallings.com/Crypto3e/Crypto3e-student.html**

Lindsay Robertson, ZL2LJR, is a professional mechanical engineer working with a large engineering consultancy firm. He has held an Amateur Radio license since 1978. He is very interested in being contacted by anyone who might be interested and willing to work with him to further develop the material presented in this article.

An Automatic Noise-Figure Meter

Here is a project that will automatically measure the noise figure of your preamplifier projects. It has an operating range from 3 MHz to over 400 MHz.

Jim Koehler, VE5FP

Introduction

Anyone interested in building low-noise pre-amplifiers will want to measure the noise figure of the device. Commercial noise-figure meters, often called Precision Automatic Noise Figure Indicators (PANFI), exist, but they are expensive even on the surplus or used market because of the demand for them. There have been a few published construction articles in the ham literature, but they are either overly complex or don't compare to commercial test instruments.[1] This article describes the construction of a simple version, suitable for home construction, but which has many features of the best commercial instruments. See Photo A.

Theory

A good background to noise-figure measurement is given in a Hewlett-Packard (now Agilent Technologies) Application Note: AN 57-1. This note is available on the Agilent Web site, and is worth reading.[2] Noise figure, in an amplifier, is a measure of how much excess noise an amplifier adds to any incoming signal. The lower the noise figure, the less noise it adds. Noise figure can be expressed in a number of ways, but I prefer to think of it in terms of temperature. Every passive resistive electronic component generates some noise because of the random motion of charge carriers in it. The greater the temperature, the greater the motion of the charges, and therefore, the greater the random noise power generated by the component. The noise power generated by any component depends *only* on its temperature and the bandwidth that you are considering; it is given by the equation:

$$P = kTB \qquad \text{[Eq 1]}$$

where k is Boltzmann's constant, which is equal to 1.38×10^{-23} joules / kelvin, B is the bandwidth in Hz and T is the temperature in kelvins. A perfect amplifier would add no noise to incoming signals, but real ones do. We can specify this excess noise in terms of the temperature of a resistor at the temperature that would give that same amount of noise. This temperature, called the excess noise temperature, T_e, is a measure of how good the amplifier is; the lower the excess noise temperature, the better the amplifier. The amplifier may also be characterized by a *noise figure*, which is the ratio of the excess noise temperature (plus room temperature) to room temperature.

$$NF = \frac{(T_e + T_r)}{T_r} \qquad \text{[Eq 2]}$$

where T_r is the room temperature. This ratio is often expressed in dB. An ideal amplifier would have a T_e of zero and therefore a noise figure of 1.00, or 0.0 dB.

Modern noise-figure meters measure the noise figure of an amplifier by connecting a noise source, which can be turned off and on, to the amplifier input. A noise source is just that; a device with an output that is broadband noise of a known level, corresponding to a resistor at some temperature. Noise sources are characterized by their *effective noise ratio*, ENR, which is given by:

$$ENR = \frac{(T_h - T_r)}{T_r} \qquad \text{[Eq 3]}$$

VE5FP

Photo A — The front panel of the VE5FP automatic noise-figure meter.

[1]Notes appear on page 46.

2258 June Rd
Courtenay, BC V9J-1X9
Canada
jark@shaw.ca

where T_h is the hot temperature that a resistor would have to produce the same noise power as the noise source when it is switched on. When the noise source is switched off, it produces only the amount of noise that a resistor at room temperature, T_r, would produce.

Now, imagine an amplifier with a noise source at its input and a power meter at its output to measure the power coming out of the amplifier. When the noise source is turned off, the power going into the amplifier will consist of the power from the noise source at room temperature plus the amplifier's excess noise power. The output power will be this sum multiplied by the amplifier's amplification factor. When the noise source is turned on, the input power to the amplifier will be the noise power of the noise source when it is on, plus, again, the excess noise power due to the amplifier alone; the output will be this new sum again multiplied by the amplification factor of the amplifier. The ratio of the on-power to the off-power at the output of the amplifier is the *Y*-factor:

$$Y = \frac{(T_h + T_e)}{(T_r + T_e)} \qquad \text{[Eq 4]}$$

Noise-figure meters determine T_e by measuring the *Y*-factor and by knowing the value of T_h and T_r. T_r is normally assumed to be 290 K, so, rearranging Equation 4, we get;

$$T_e = \frac{(T_h - 290\ Y)}{(Y-1)} \qquad \text{[Eq 5]}$$

A PANFI is therefore just an instrument that has a power detector to accurately measure the output noise power of an amplifier and a means of turning the noise source on and off. It must then do the mathematics to display the excess noise temperature either as a temperature or as a noise figure. Noise sources are mostly solid state devices and most are designed to be turned on when they are supplied with +28.0 V dc. A more detailed discussion of how a PANFI works is given in the Appendix.

Before leaving this topic, let me make a few remarks about the precision of the measurement. What is being measured is the power due to wide-band noise. Noise is random and so there is some uncertainty in measuring its power level; the level will fluctuate over time. It is a well-known fact that the accuracy with which noise power may be measured depends on two things: the amount of time over which the power is averaged, τ, and the bandwidth of the noise, *B*, itself; the measurement error is proportional to

$$1/\sqrt{B\tau}\,.$$

The fact that the accuracy depends on the bandwidth may seem a bit strange but if you think of it statistically, the wider the bandwidth, the more "samples" of the noise you are taking, and hence the more accurate the average. So, to increase the accuracy, the noise power must be averaged over longer times and/or the bandwidth of the measuring instrument must be increased. Commercial PANFIs may average over periods of a few seconds and typically have measurement bandwidths of a few MHz.

Older PANFIs usually operated at a fixed frequency, often 30 MHz. To use them at any other frequency, it was necessary to convert the signal to this specific frequency. Many modern instruments have a much wider frequency range. The instrument described here operates over a frequency range from about 3 MHz to over 400 MHz.

Block Diagram

A block diagram of the instrument is shown in Figure 1. There is a wide-band amplifier with separate inputs and outputs that may be added to the outputs of the device being tested to increase the signal level. The detector is based on the Analog Devices AD8307 logarithmic detector.[3] This wonderful little device has a frequency response extending up to 500 MHz, and is linear (in logarithmic power) over 8 decades of power. The microprocessor board controls all aspects of the device operation. In the measurement mode, it turns on the external noise source by supplying +28 V dc to it and, using its internal A/D converter, measures the signal level detected by the AD8307. It stores this value and then turns off the noise source and again measures the level detected by the AD8307. This measurement is repeated 50 times over a period of about 1 second. Then the noise figure of the device is calculated and displayed on a 2-line, 16-character liquid

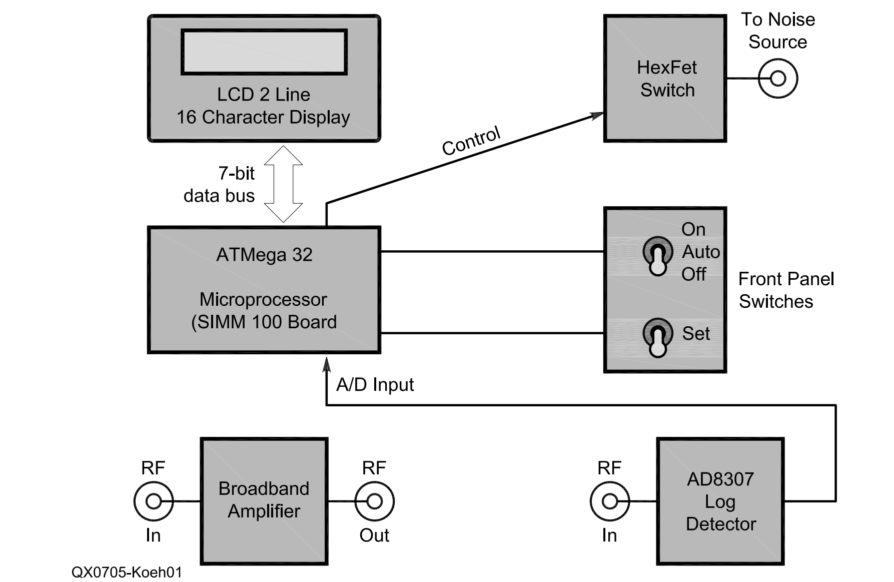

Figure 1 — This block diagram shows the sections of the automatic noise-figure meter.

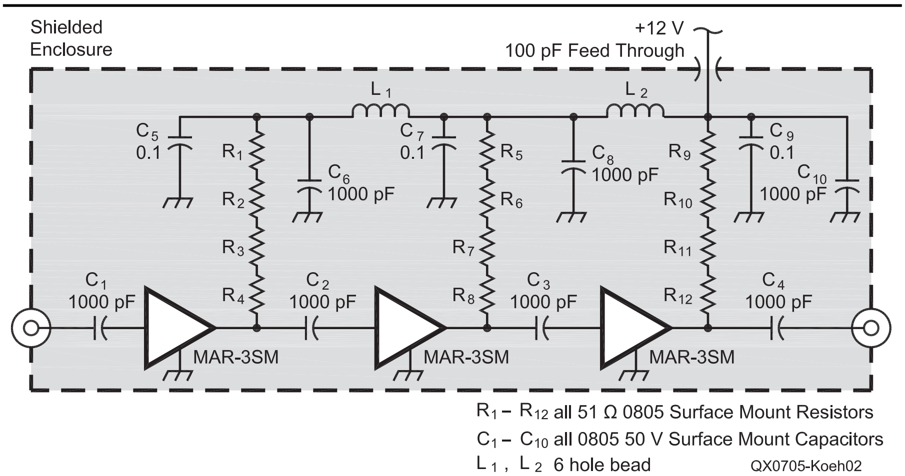

Figure 2 — The schematic diagram of the broadband amplifier shows that it uses three MiniCircuits MAR-3SM monolithic amplifiers.

crystal display (LCD). The A/D converter has a basic resolution of 1 part in 1024 (10 bits) but each of the 50 measurements is an average of 100 A/D conversions. Because of this, in the absence of noise, the expected overall resolution of each single power determination would be about 1 part in 70,000. Ultimately, the final calculated noise figure has an accuracy that depends mostly on the accuracy of the logarithmic response of the AD8307, and the fact that since the signal being measured is random noise, it has a limiting accuracy that depends on the bandwidth and the averaging time (in this case, about 1 second).

Detailed Circuit Description

The Broadband Amplifier

The circuit of the broadband amplifier is shown in Figure 2. It uses three MiniCircuits MAR-3SM monolithic amplifiers.[4] The overall gain is about 37 dB and the circuit, if laid out properly using strip lines of the correct width, has a bandwidth from about 3 MHz to close to 2 GHz. Using dead-bug type of construction, the bandwidth will probably be reduced, but since the AD8307's response starts to fall off at 500 MHz, this won't matter. The MAR-3 amplifier is specified to have a noise figure of about 6 dB in the range from a few MHz to 2 GHz. Each stage draws about 35 mA and the total power dissipated in each stage's bias resistance of 200 Ω is about ¼ W. I laid out my amplifier using strip lines and surface mount components. The 0805 size resistors I used were only rated at 0.1 W; therefore I used four 51-Ω resistors to make up this resistance. Using dead-bug construction, you would probably want to use a 200 Ω, ½ W resistor or two 100 Ω, ¼ W resistors.

The Detector Circuit

The circuit for the detector is shown in Figure 3. The AD8307 requires a supply voltage of 5 V but with a current drain of only a few mA, so a low power 78L05 regulator was used. The 51-Ω resistor at the input of the AD8307 should be connected between pins 1 and 8 with as close to zero length leads as you can manage. I used a surface mount version of the AD8307 and a surface mount 0805 size resistor located just 1 or 2 mm from these leads.

The detector is very sensitive and so the circuit should be well shielded. I put both the detector and the wide-band amplifier in a small box made of double-sided circuit-board material and soldered the lid on. See Photo B. The detector and amplifier are in separate compartments in this box. The coaxial inputs to and from the amplifier and to the detector have the shield braid soldered to the sides of the box. The dc supply voltage to the circuit and the detector output are fed into the box by feed-through capacitors.

VE5FP

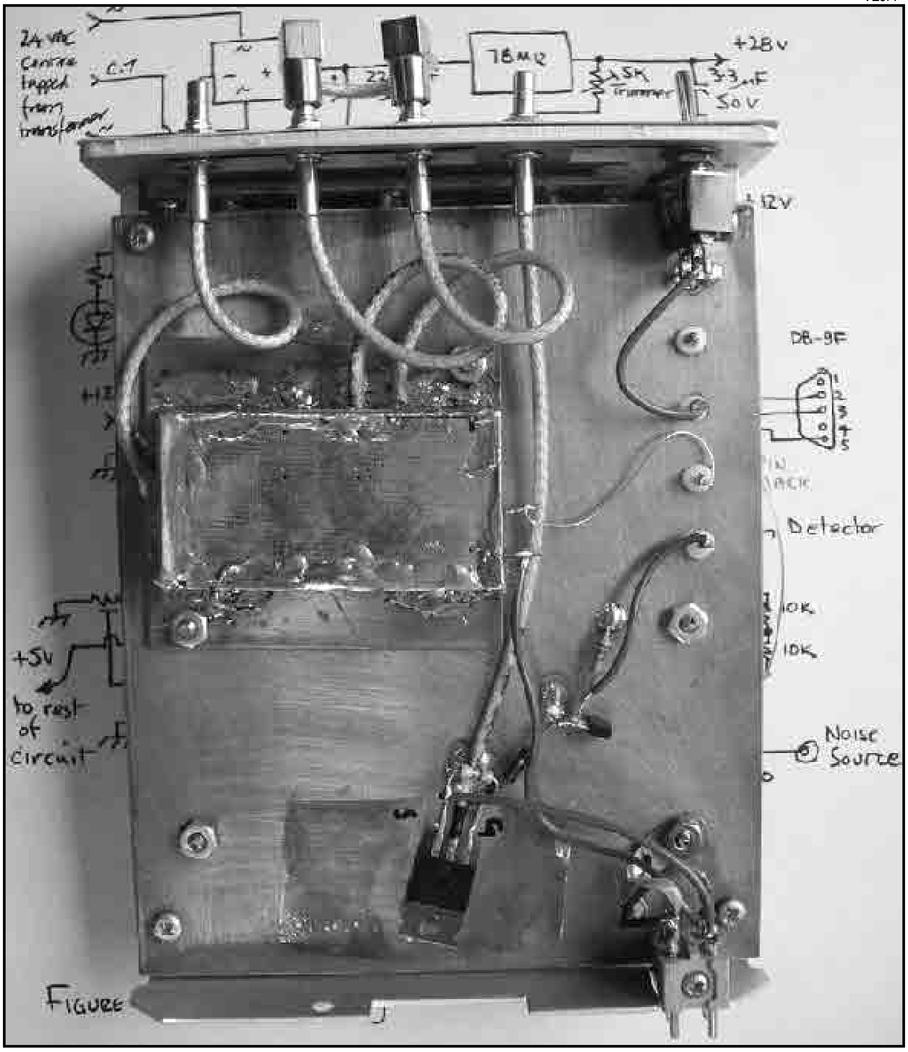

Photo B — The broadband amplifier is built into a circuit board box mounted inside the bottom of the project case.

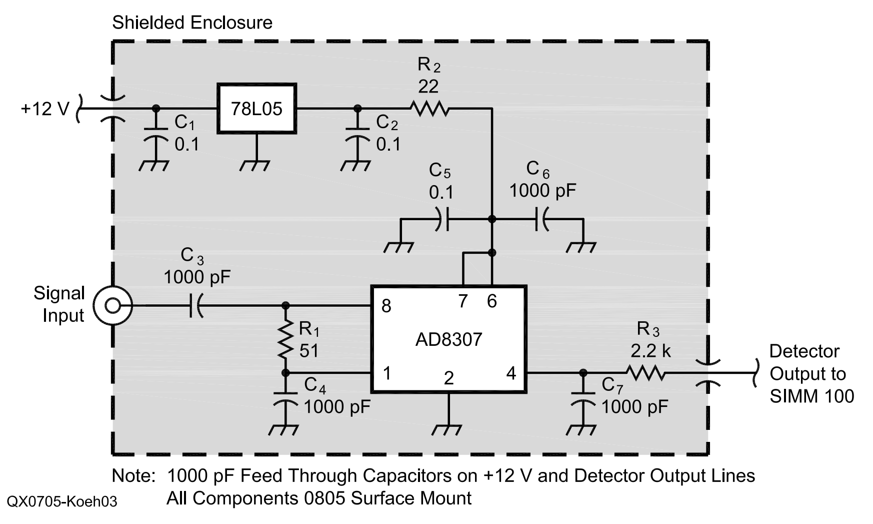

Figure 3 — An Analog Devices AD8307 logarithmic detector is the heart of the detector circuit.

The Microprocessor Module

The microprocessor used was an Atmel AVR-series ATMega32.[5] This microprocessor has eight channels of A/D and 24 other pins of I/O. I like the AVR-series of microprocessors because of their low price, their good performance and the fact that there are some very good development tools available for them. The source code for this project was all written for the Gnu C compiler, GCC. There is a version of this compiler that produces code for the AVR series of microprocessors. A complete package of the compiler and all the needed utilities is available as a package called WINAVR for installation on Windows computers. It is a first-class professional tool set and is completely free! I used a SIMM-100 circuit board, which is available from Dontronics for about $11 Australian and is a bargain.[6] Dontronics ships to the USA and the ordering and subsequent shipping is painless. The board should be assembled according to the accompanying directions. See Photo C. The board was originally designed for the AT90S8535 microprocessor but it is pin-compatible with the ATMega32. Use the 16PI version of the ATMega32, as it is rated for the industrial temperature range and for clock frequencies of up to 16 MHz. It costs just a few pennies more than the commercial grade. Use a good quality socket for the microprocessor.

The LCD requires seven I/O pins; there are two A/D channels used (of eight avail-

VE5FP

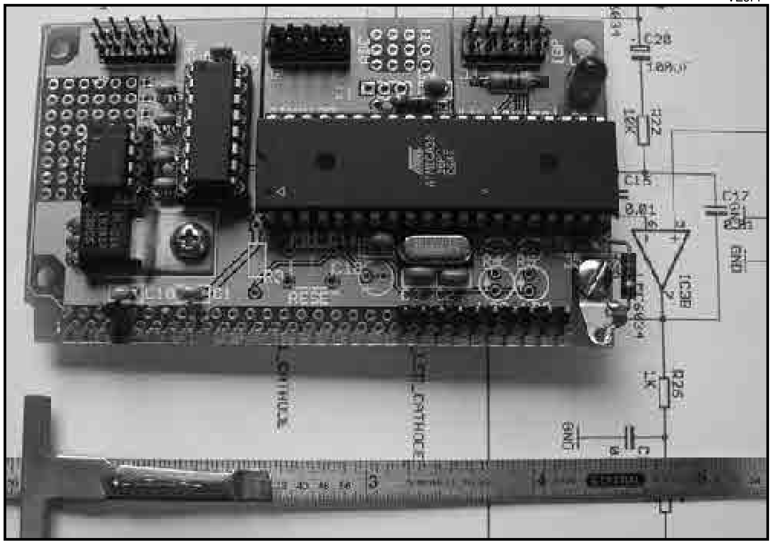

Photo C — This photo shows the assembled SIMM100 circuit board, with the ATMega32

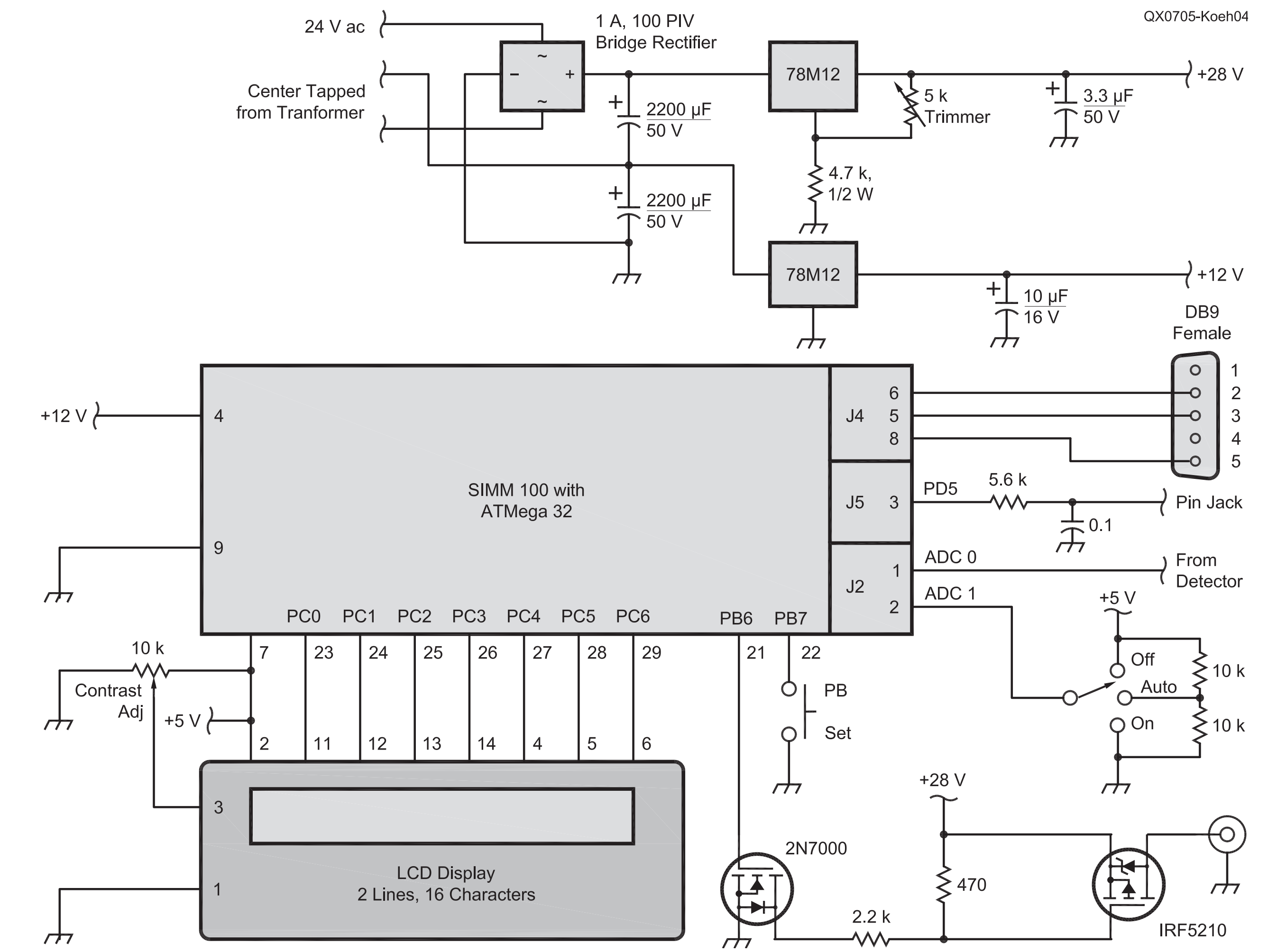

Figure 4 — An ATMega32 microprocessor on a SIMM100 circuit board provides the brains for the noise-figure meter. This schematic diagram also shows the power supply, display and control circuitry.

able) and there are two other digital I/O lines used. There is an RS-232 interface circuit built onto this board and it is used to provide communication to an external computer or terminal, which is needed for calibration of the finished unit. I used a 14.7456 MHz crystal in the oscillator and, with this clock, the serial RS-232 connection is at 19200 baud.

The Rest of the Circuit

The rest of the circuit is shown in Figure 4. There are two front panel switches. One of these is a spring-loaded toggle switch that is used to set levels prior to a measurement. A push-button switch could also have been used here. The other switch is a single-pole three position switch used to set the mode of operation. Again I used a toggle switch. Three-position toggle switches are not common and you could as easily use a rotary switch instead. There are a large number of LCDs available. Since they all use the same protocol, it doesn't much matter which one you choose. I built the instrument in a small case that had once housed a piece of Tektronix test gear. Photo D shows the circuit boards and wiring inside that case. If I were doing it over again, I'd put the instrument into a much larger box and use an LCD with larger digits because I'm getting old and my eyesight isn't what it used to be! The contrast trimmer potentiometer for the LCD should be adjusted to give the best contrast for the display. It will be set so that the voltage at the wiper is close to 0 V. The power supply provides +12 V and +28 V dc. I happened to have an old "wall wart" on hand, which provided 24 V ac, center-tapped. Any 24 V ac center-tapped transformer capable of supplying a total power of a watt or two is good enough. The trimmer potentiometer in the +28 V circuit is used to set the output voltage to exactly 28 V. Do this as accurately as you can.

Calibration and Operating

Calibration of the Power Detector

You need an external terminal or computer to do the calibration of the power detector. The RS-232 connector is designed to connect to a PC and you may use some terminal program to communicate with the instrument.

The internal instrumental calibration, which converts from AD8307 output levels to a dBm scale, is stored in the internal EPROM of the microprocessor. The programmed microprocessor has a default calibration based on the values specified in the AD8307 data sheet. These are fairly accurate for a broad range of input frequencies and most users will not want to bother trying to improve this accuracy. I have made provision for a more accurate calibration, however, for those who have good quality signal generators and coaxial attenuators and who wish to calibrate the instrument precisely at some specific frequency.

If you do have these, then the calibration procedure is as follows:

1. Connect a 50 Ω signal generator operating at the desired frequency to the SIGNAL INPUT connector on the instrument. Set the output level to a fairly high level — around 0 dBm.

2. Type the character "c" (upper or lower case) on the terminal and the microprocessor will respond with a line asking for the input level. Type the level being produced by your signal generator in dBm. Then, press the SET

VE5FP

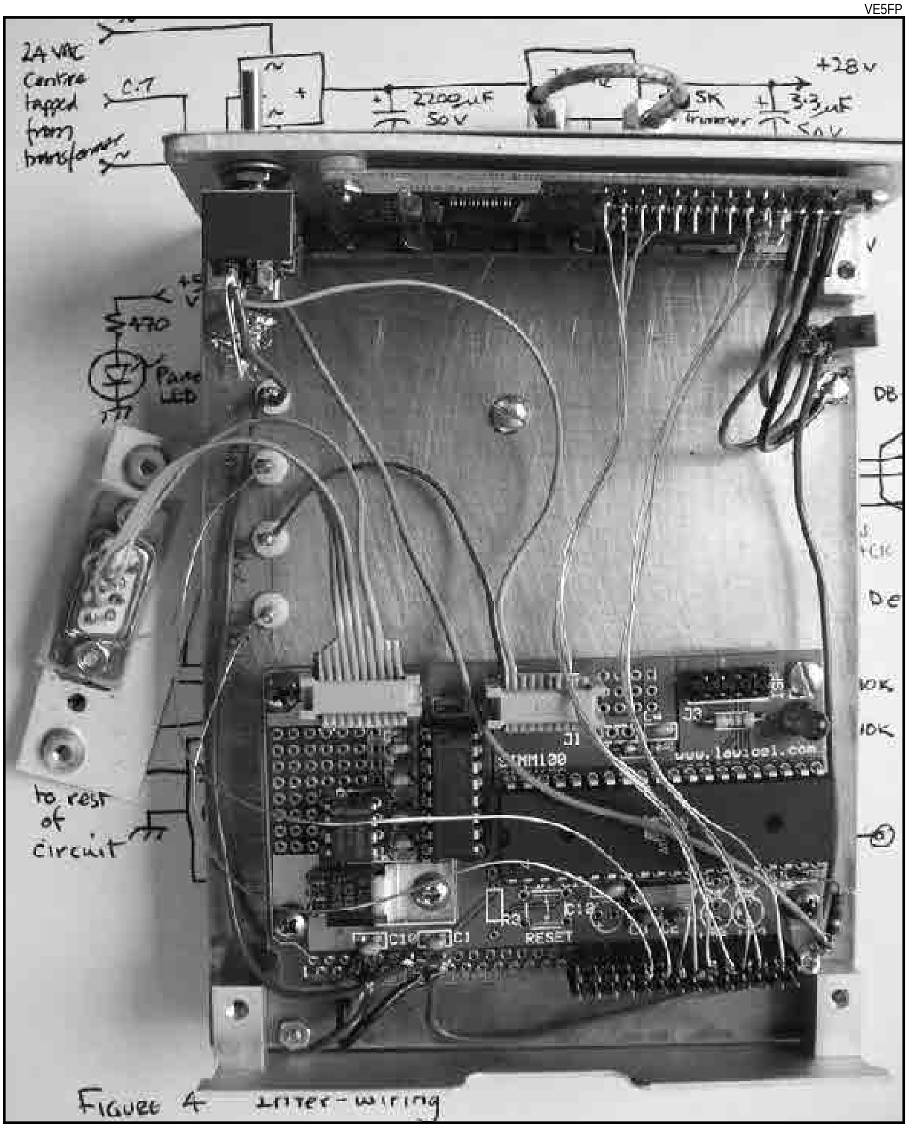

Photo D — This view shows the top of the project case, with the SIMM100 board, LCD and various wiring of the noise-figure meter.

VE5FP

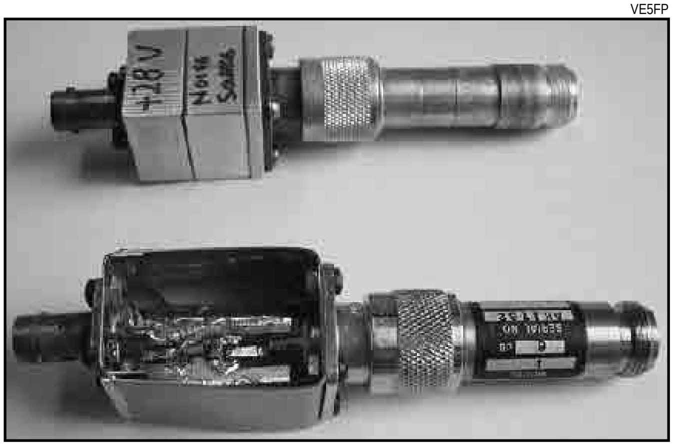

Photo E — This photo shows my homebrewed noise sources.

switch on the instrument.

3. The instrument will respond by asking for the next data point.

4. Set the generator to a new level about 10 or 20 dB lower. The preferred way to do this is just to leave the generator setting as it was before but to add a known attenuation into the line. Again, type the new signal level and press the SET switch.

5. Repeat the step above three more times for a total of five settings of the signal generator. Choose the five signal levels so that they are distributed fairly evenly (in dB) between –70 dBm and 0 dBm.

The order in which you set the levels doesn't matter. Internally, the five values are used to calculate the least-square best fit of a straight line to the data and the two parameters describing this line are stored in the instrument in EEPROM. These two parameters are subsequently used to translate from AD8307 output to dBm.

While connected to the terminal, you must also now tell the instrument the noise level of your noise source. Type a single character "e" (again, upper or lower case) and the instrument will respond by asking you to type the ENR, in dB, of your noise source. This value is also stored internally in EEPROM so it is there whenever the instrument is turned on again.

While connected to the terminal, you can also change whether the noise figures are displayed as temperatures or in dB. Type a "b" to select dB or a "t" to select temperature. The mode is also saved in EEPROM so it will remain in whatever state you left it the next time you turn it on. Finally, you may display all the internal settings of the instrument by typing the character "d".

I have not discussed noise sources here since they are a subject requiring a separate article. Paul Wade has written an excellent article about noise sources that tells you how you may make your own.[7] My own noise source is a homebrew design based on information from that article. See Photo E.

Operation

Before making any measurements, it is advisable to check to make sure that the detector and amplifier are shielded well enough. With the ON-AUTO-OFF switch in the ON position, make a note of the indicated signal level when you have a termination on the SIGNAL INPUT connector. Then switch it to the OFF position and again note the signal level. It should be the same to within 0.1 dB or so. If it isn't, you haven't shielded the detector or amplifier well enough and your measurements will not be accurate.

Assuming all is well, you are ready to make a measurement. First, connect the noise source to the instrument as shown in Figure 5A and press the SET switch. The band-pass filter shown should be appropriate to the device being measured. For example, if the device is a down-converter with an output at 144 MHz or a 144 MHz amplifier, the filter should be tuned to 144 MHz. After pressing the SET switch, the display will show the measured levels with the noise source on and off and also will show the excess noise temperature of the broadband amplifier in the instrument. This should be something in the neighborhood of 900 K. MiniCircuits specifies the MAR-3SM as having a noise figure of 6 dB, which corresponds to about that value. Then, connect the device-under-test (DUT) to the instrument as shown in Figure 5B. With the ON-AUTO-OFF switch in the OFF position, note the signal level measured by the instrument. It should be greater than –70 dBm and no more than about 0 dBm. If it is somewhere in this range, you are ready to go. Just put the ON-AUTO-OFF switch into the AUTO position and it will give you a measure of the excess noise temperature of the DUT. You may convert this to dB, if you wish, using Equation 2. The instrument will also show a value for the gain of the DUT. The noise temperature displayed has been corrected for the gain of the DUT and the noise contribution of the following stage.

If the signal level is lower than –70 dBm with the configuration shown in Figure 5B, you

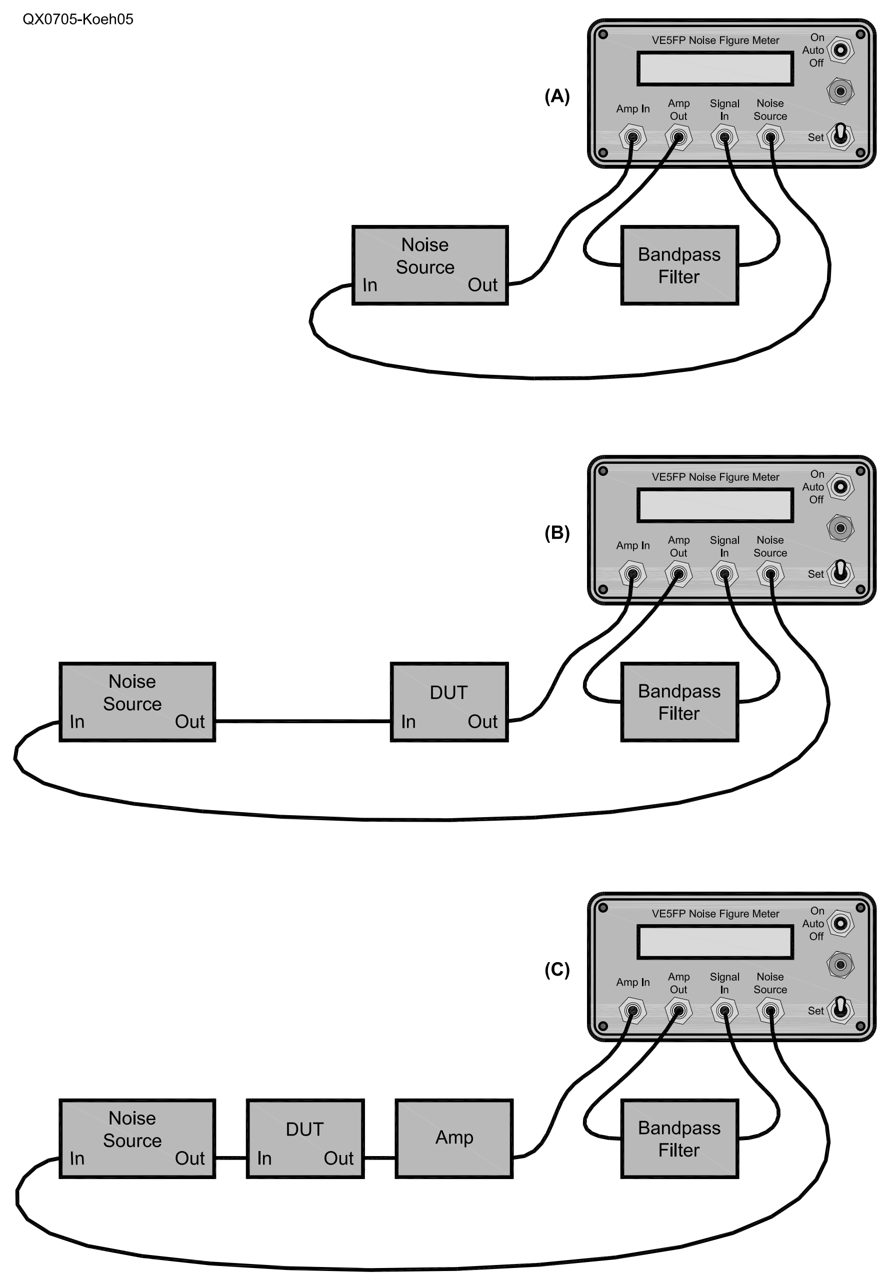

Figure 5 — This drawing shows the steps involved in making a noise-figure measurement. Part A shows the connections to measure the noise source. Part B shows the device under test connected between the noise source and the noise-figure meter. Part C shows that sometimes an additional amplifier will be needed if the device under test does not produce a signal with high enough power output.

will need to use an additional external amplifier to get the levels up to where the measurement can be made accurately. This amplifier should be inserted at the output of the DUT and before the input to the broadband amplifier. Connect the circuit as shown in Figure 5C and now look at the level when the ON-AUTO-OFF switch is in the OFF position. If it is still too low, you will need to add another external amplifier. If the signal level is too high, don't use the broadband amplifier and/or just add some attenuation before the SIGNAL INPUT connector.

If the DUT is a down-converter, the gain shown will be correct if the noise source ENR is the same for both the output frequency of the DUT and the input frequency. That is because in the SET measurement, the noise level was measured at the output frequency of the DUT whereas in the final noise measurement, the noise source is connected to the input of the DUT, which sees it at its input frequency.

If you want to measure the noise temperature of a LNA ahead of a down-converter, you must first SET the instrument with the down-converter in the circuit, as shown in Figure 6A. Then connect the LNA in front of the down-converter as shown in Figure 6B and set the switch to the AUTO position to read the noise temperature and gain of the LNA. If there is too much overall gain, you may want to by-pass the broadband amplifier and connect the output of the down-converter directly to the SIGNAL INPUT of the instrument.

Other Considerations

You will need to have a range of band-pass filters for the frequencies that you normally use. I made up some fixed double-tuned LC filters for 144 and 30 MHz and a small fixed cavity filter for 432 MHz. I also made a tunable cavity filter by modifying a surplus HP5253B frequency converter. Photo F shows the front panel of this filter. These units plugged into some older HP frequency counters and they have a very well-made tunable silver-plated cavity. They make very nice 50 MHz to 500 MHz tunable band-pass filters. One often sees these units for sale at hamfest flea markets for just a few dollars and they are worth picking up.

One disadvantage of the commercial PANFIs is that it is very difficult to tune something where the output is given by changing figures in a text display. Humans are better at evaluating an output if there is some analog value associated with it, such as a voltage that can be displayed by a meter. I added an analog output to the system with a very simple circuit addition. A low-pass filter consisting of a 5.6 kΩ resistor going to a 0.1 μF capacitor to ground is connected to pin 3, J5 on the SIMM100 board. This pin corresponds to PD5 of the microprocessor. I added software to pulse-width modulate this output to produce an analog voltage that is proportional to the measured value of Y. The voltage varies from 0 to 5 V as Y changes from N.00 to N.9999 volts, where N is an integer. For example, if Y is 2.4, the voltage will be $0.4 \times 5 = 2.0$ V. If Y were to vary from 2.95 to 3.05, the voltage would start at $0.95 \times 5 = 4.75$ V, increase up to 5 V, jump down to zero and then go up to $0.05 \times 5 = 0.25$ V. Just using the non-integer portion of Y is an easy way to make an expanded-scale voltmeter. To tune a system for lowest overall noise temperature, you just tune for maximum Y using a voltmeter on this output. I added a pin jack onto the front panel on my instrument for this output.

Conclusion

This instrument will make accurate noise-figure measurements if you take just a little care in the construction and operation. The circuit is very simple and easily reproduced. Analog Devices made it all possible with the AD8307 logarithmic detector. That, and the use of a microprocessor to massage the data, results in a first-class laboratory instrument.

Both the Agilent Application Note and the article by Paul Wade discuss some considerations to be observed when making noise-figure measurements and I recommend that you read them if you're serious about interpreting the results you get.

The source code and the HEX object code for the microprocessor are available on the ARRL *QEX* Web site.[8] The author will program ATMega32 microprocessors for the cost of return postage.[9]

Appendix: Measuring Noise Temperature

Consider the basic measuring system, which consists of an amplifier and a detector to measure output power as shown in Figure A1. The system is designed to measure the ratio of the two output powers when the external noise source is turned on, to the output power when the external noise source is turned off. This ratio is called the

VE5FP

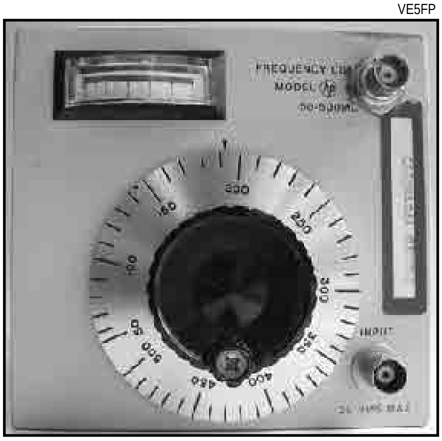

Photo F — I built a tunable cavity filter into an HP frequency counter box.

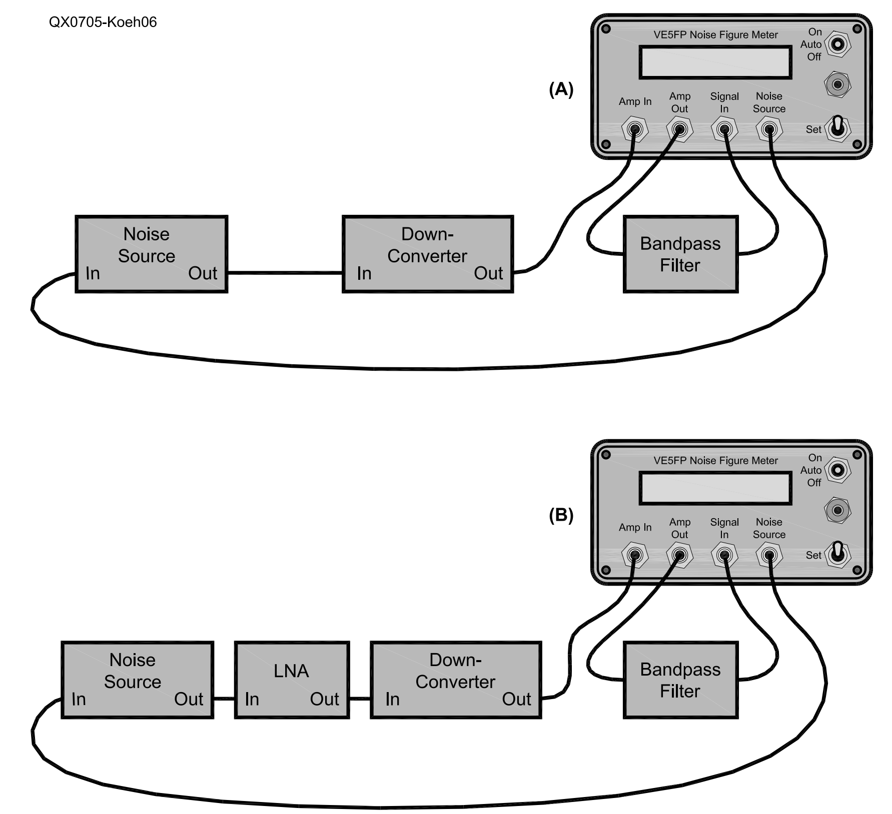

Figure 6 — This drawing shows the connections required if a down-converter is needed to bring the output frequency of the device under test into the range of the noise-figure meter. Part A shows that the noise source and down-converter are measured first, and then the device under test is added, as shown at Part B.

Y-factor. The gain of the system amplifier is G_s and the system noise temperature is T_s. The latter, the excess noise of the measuring system, can be represented by a resistance at temperature T_s at the input whose noise power is summed with the external input. When the external noise source is turned on, it acts as a resistance at temperature T_h and when it is turned off, it acts as a resistance at room temperature, T_c.

When the external noise source is turned on, the power output at the detector will be:

$$P_{oh} = (T_h + T_s)G_s \qquad \text{[Eq A1]}$$

When the noise source is turned off, the power output at the detector will be:

$$P_{oc} = (T_c + T_s)G_s \qquad \text{[Eq A2]}$$

T_c is commonly taken to be 290 K.

The ratio of these two powers, P_{oh} / P_{oc}, is the Y-factor for the system; Y_s.

This factor is thus:

$$Y_s = \frac{P_{oh}}{P_{oc}} = \frac{T_h + T_s}{T_c + T_s} \qquad \text{[Eq A3]}$$

We can rearrange the terms of Equation A3 to give the noise temperature of the system in terms of the Y-factor and the external noise temperature:

$$T_s = \frac{T_h - Y_s T_c}{Y_s - 1} \qquad \text{[Eq A4]}$$

Knowing T_s from Equation A4, we can also determine the measuring system gain by substituting it into Equation A1:

$$G_s = \frac{P_{oh}}{T_h + T_s} \qquad \text{[Eq A5]}$$

G_s will be in units of W / K.

To measure the noise temperature of an amplifier or a converter (or, the noise figure, which may be derived from the measured noise temperature), the noise temperature and gain of the measuring system are first measured by connecting the external noise source as shown in Figure A1. This provides the initial calibration of the measuring system. The amplifier or converter whose noise figure is to be measured is then inserted between the measuring system and the external noise source as shown in Figure A2. The Y-factor for the whole amplifier/converter measuring system combination is then measured. From this Y-factor, we can determine both the overall system noise temperature as well as the amplifier/converter noise temperature alone. Let the overall Y-factor be Y'. Then, the overall noise temperature of the combined system, T', is given by:

$$T' = \frac{T_h - Y' T_c}{Y' - 1} \qquad \text{[Eq A6]}$$

The true noise temperature of the amplifier/converter alone is given by:

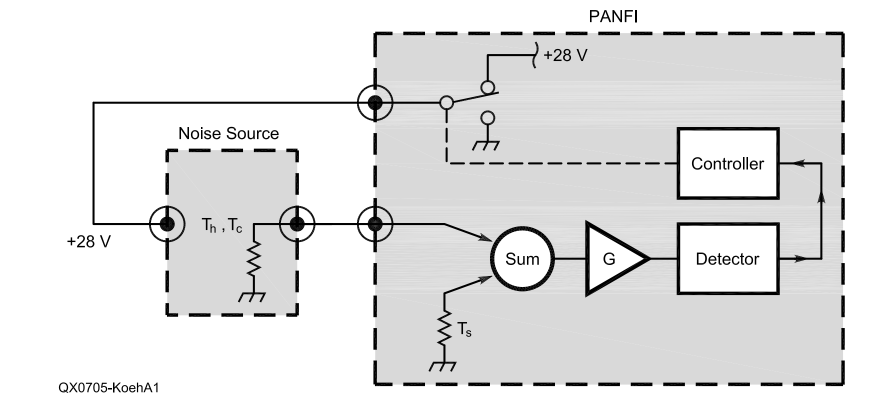

Figure A1 — A Precision Automatic Noise Figure Indicator (PANFI) switches the noise source on and off, and measures the noise power.

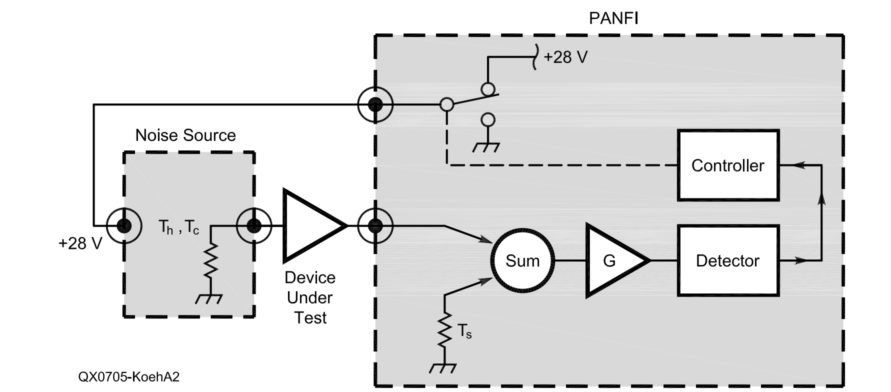

Figure A2 — With the device under test placed between the noise source and PANFI, the noise figure is measured.

$$T = T' - \frac{T_s}{G} \qquad \text{[Eq A7]}$$

Therefore, to determine the true noise temperature of the device, we must know the device gain. This can be found by an equation that uses the overall power output when the external noise source is turned on, P'_{oh}, and when it is turned off, P'_{oc}, as well as the system gain, G_s:

$$G = \frac{P'_{oh} - P'_{oc}}{G_s\left(T_h - T_c\right)} \qquad \text{[Eq A8]}$$

G_s has been measured previously.

In summary, in order to determine the true noise figure of an amplifier or a converter, you must first measure the measuring system noise temperature and gain using the set-up shown in Figure A1, where the external noise source is connected to the input of the measuring system. This is the calibration phase of the measurement. Then, you disconnect the external noise source from the input and connect the output of the amplifier or converter to the input of the measuring system and put the external noise source onto the input of the amplifier or converter. Then, the instrument will show the true noise temperature of the amplifier or converter as well as its gain.

Notes

[1]Harke Smits, PAØHRK, "A Noise/Gain Analyzer," *QEX*, Nov/Dec 1999, pp 5-10. See also references therein.

[2]The Agilent Technologies Web site is at **www.home.agilent.com**, and the direct link to the Application Note is **http://cp.literature.agilent.com/litweb/pdf/5952-8255E.pdf**

[3]**www.analog.com/en/prod/0,,759_847_AD8307,00.html**

[4]**www.minicircuits.com**

[5]**www.atmel.com/dyn/products/product_card.asp?part_id=2014**

[6]**www.dontronics.com/simm100.html**

[7]Paul Wade, N1BWT (now W1GHZ), "Noise Measurement and Generation", *QEX*, November, 1996, pp 3-12. Also, see references therein.

[8]The ATMega32 microprocessor source code and the HEX object code are available on the *QEX* Web site. Go to **www.arrl.org/qexfiles** and look for the file **5x07_Koehler.zip**.

[9]I can only handle the DIP version of the microprocessor. Send it in a padded envelope, along with an addressed return padded envelope, to J. Koehler, 2258 June Rd, Courtenay, BC, V9J-1X9, Canada. I cannot use US stamps so please enclose enough IRC's or $2 US to cover the postage.

Upcoming Conferences

2007 Society of Amateur Radio Astronomers Annual Meeting and Technical Conference

National Radio Astronomy Observatory, Green Bank WV

July 1-3, 2007

Call for Papers: 2007 Annual Meeting

The Society of Amateur Radio Astronomers (SARA) hereby solicits papers for presentation at its 2007 Annual Meeting and Technical Conference, to be held July 1-3, 2007, at the National Radio Astronomy Observatory (NRAO), Green Bank WV. Papers on radio astronomy hardware, software, education, research strategies, and philosophy are welcome.

SARA members or supporters wishing to present a paper should email a letter of intent, including a proposed title and informal abstract or outline (not to exceed 100 words) to the SARA vice president at **vicepres@radio-astronomy.org**, no later than 1 March 2007. Be sure to include your full name, affiliation, postal address, and email address, and indicate your willingness to attend the conference to present your paper. Submitters will receive an email response, typically within one week, along with a request to proceed to the next stage, if the proposal is consistent with the planned program. A formal proceedings book will be published in conjunction with this meeting. Papers will be peer-reviewed by a panel of SARA members with appropriate professional expertise and academic credentials. First-draft manuscripts must be received no later than 1 April 2007, with feedback, acceptance, or rejection e-mails to be sent within two weeks thereafter. Upon final editing of accepted papers, camera-ready copy will be due not later than 1 May 2007. Due to printer's deadlines, manuscripts received after that deadline will not make it into the proceedings book. Instructions for preparation and submission of final manuscripts appear in a **Guidelines for Submitting Papers** document on the SARA Web site (**radio-astronomy.org**).

41st Annual Central States VHF Society Conference

July 26-29, 2007, San Antonio, TX
Omni Hotel

Call for Papers

The Central States VHF Society is soliciting papers, presentations, and poster displays for the 41st Annual CSVHFS Conference on 26-28 July, 2007. Papers, presentations, and posters on all aspects of weak-signal VHF and above amateur radio are requested. You do not need to attend the conference, nor present your paper, to have it published in the proceedings. Posters will be displayed during the two days of the conference.

Topics of interest include (but are not limited to)**:**

Antennas including modeling/design, arrays and control

Test Equipment including homebrew, using and making measurements

Construction of equipment, such as transmitters, receivers and transverters

Operating including contesting, roving and DXpeditions

RF power amps including single band and multiband vacuum tube and solid-state

Propagation including ducting, sporadic E, tropospheric and meteor scatter, etc

Pre-amplifiers (low noise)

Digital Modes WSJT, JT65, etc

Regulatory topics

EME

Software-defined Radio (SDR)

Digital Signal Processing (DSP)

Generally, topics not related to weak signal VHF, such as FM repeaters and packet radio, are not accepted for presentation or publication. There are always exceptions, however. Please contact either Lloyd Crawford, N5GDB or Thomas Visel, NX1N at the email addresses below.

Deadline for Submissions

For the proceedings: Monday, 7 May 2007.

For presentations to be delivered at the conference: Monday, 2 July 2007.

For notifying us that you have posters to display at the conference: Monday, 2 July 2007. Bring your poster with you on July 26.

Further information is available at the CSVHFS web site (**www.csvhfs.org**), See "The 2007 Conference," "Guidance for Proceedings Authors," "Guidance for Presenters" and "Guidance for Table-top/Poster Displays."

Contacts:

Primary: Lloyd Crawford, N5GDB; **n5gdb@austin.rr.net**

Alternate: Thomas Visel, NX1N; **Thomas@neuric.com**

Mail: RMG, PO Box 91058, Austin, TX 78709-1058

The 26th Digital Communications Conference

September 28-30, 2007, Hartford, CT

The ARRL and TAPR Digital Communications Conference is an international forum for radio amateurs to meet, publish their work, and present new ideas and techniques. Presenters and attendees will have the opportunity to exchange ideas and learn about recent hardware and software advances, theories, experimental results, and practical applications. Full information can be found at **www.tapr.org/dcc.html**.

Call for Papers

Technical papers are solicited for presentation at the ARRL and TAPR Digital Communications Conference for publication in the conference proceedings.

Annual conference proceedings are published by the ARRL. Presentation at the conference is not required for publication. Papers must be received by August 6, 2007, and should be submitted to Maty Weinberg, ARRL, 225 Main St, Newington, CT 06111 or **maty@arrl.org**. Electronic files preferred.

Topics include, but are not limited to:

- Software defined radio (SDR)
- Digital voice
- Digital satellite communications
- Global position system
- Precise timing
- Automatic position reporting system (APRS)
- Short messaging (a mode of APRS)
- Digital signal processing (DSP)
- HF digital modes
- Internet interoperability with Amateur Radio networks
- Spread spectrum
- IEEE 802.11 and other Part 15 license-exempt systems adaptable for Amateur Radio
- Using TCP/IP networking over Amateur Radio
- Mesh and peer-to-peer wireless networking
- Emergency and Homeland Defense backup digital communications in Amateur Radio
- Updates on AX.25 and other wireless networking protocols
- Topics that advanced the Amateur Radio art.

Microwave Update 2007

October 18-20, 2007

Call For Papers

Any topics related to microwave theory, construction, communication, deployment, propagation, antennas, activity, transmitters, receivers, components, amplifiers, communication modes, LASER and practical experiences welcome. Abstracts should be submitted by June 1 and completed papers and articles by August 15, 2007.

Please submit your papers, articles and abstracts to W2PED, **pdrexler@hotmail.com** or to N2UO, **lu6dw@yahoo.com** in Microsoft *Word* or as an Adobe PDF file. Diagrams, photos and illustrations should be in black and white. Hard copies may be mailed to Paul E. Drexler, 28 West Squan Rd, Clarksburg, NJ 08510.

Microwave Update 2007 Details

Microwave Update 2007 will be held at historic Valley Forge, near Philadelphia, Pennsylvania. Thursday sightseeing or possible surplus tour. Conference Friday and Saturday; Flea Market Friday night, Vendors on site; Banquet Saturday night; Door prizes and raffles; Hospitality room. Hosted by the Pack Rats — Mt Airy VHF Radio Club. Spouses, friends and family invited. Alternative family/spouse programs available.

$79 early-bird registration until 9/1 includes Conference, proceedings and banquet; $89 from 9/1-10/1; $99 thereafter. Extra banquet Tickets $39. Special hotel rate $92 per night. Full info and registration at **www.microwaveupdate.org**.

Questions to chairpersons Philip Theis, Jr, K3TUF, e-mail **Phil@k3tuf.com** or David Fleming, KB3HCL, e-mail **kb3hcl@arrl.net**.

ARRL Seeks Comments on New HF Digital Protocol

The ARRL is seeking comments from amateurs concerning development of an open-source (non-proprietary) data communications protocol suitable for use by radio amateurs over high-frequency (HF) fading paths. This is *not* a Request for Proposals (RFP). An RFP may or not be forthcoming depending on evaluation of the information received.

Specifically, the League is asking for comments and information on the following issues:

- **Access Method:** Is Orthogonal Frequency-Division Multiplexing (OFDM) the best candidate technology, or should other competitive technologies be considered?
- **Data Rate and Bandwidth:** What data rates/throughputs are achievable at various bandwidths up to 3 kHz bandwidth?
- **Adaptivity:** What adaptive features should be considered, such as automatic adjustment of transmitter power, modulation waveform and coding, in order to maximize throughput and efficiency in two-way contacts?
- **Robustness:** What is achievable for reliable operation at power levels typical in the Amateur Radio Service and low signal/noise and interference ratios?
- **Error control:** What are the appropriate applications of error control suitable for HF channels? For example, how should Repeat reQuest (ARQ) and Forward Error Control (FEC) be applied to two-way contacts and one-to-many (roundtable and bulletin) transmissions?
- **Activity Detection:** What is an effective method of determining whether a frequency is busy prior to transmission?
- **Operating System:** What operating systems (such as *Windows* or *Linux*) are appropriate for Amateur Radio use with this protocol?
- **Hardware:** What practical and affordable hardware platforms are suitable for amateur stations? Consider the use of personal computers with or without sound cards. Provide any information about the need for an additional "box" if needed.

Please provide the following with your response: (1) name of respondent, (2) respondent's contact information, (3) related experience, and (4) type of respondent: (individual, partnership, corporation or group). Do not include proprietary information as part of your response.

Post, fax or e-mail your response by 1900 UTC, May 15, 2007 to:

Paul Rinaldo, W4RI
Chief Technology Officer, ARRL
3545 Chain Bridge Rd
Suite 209
Fairfax, VA 22030
Phone: 703-934-2077
Fax: 703-934-2079
E-mail: **w4ri@arrl.org**

QEX

Antenna Options

L. B. Cebik, W4RNL
1434 High Mesa Drive
Knoxville, TN 37938-4443
cebik@cebik.com

NVIS Antennas for Special Needs

The Jan/Feb 2007 Antenna Options column dealt with basic and advanced monoband NVIS antennas. Although we found a number of differences among the antennas, most of them showed reasonably circular azimuth patterns as determined by the ratio of the broadside to endwise half-power beamwidth. Virtually all of the antennas achieved their maximum upward gain at heights between 0.175 λ and 0.2 λ. We also saw clearly the relationship between gain and beamwidth, especially when we compared antennas like the dipole, the inverted-V, and the 1-λ loop with more complex arrays based on the lazy-H configuration.

In this follow-up set of notes, we shall look at two special needs within the overall NVIS scene: a desire for directional NVIS communications and the requirement — largely a function of newer Automatic Link Establishment (ALE) potentials — for very wideband communications antennas. To simplify our discussions, we shall place all antennas over bare average ground (conductivity = 0.005 S/m, relative permittivity = 13).

Directional NVIS Communications

Curiously, a few years back, I received — within a fairly short time — two notes via e-mail. One correspondent wished to know if there might be an effective NVIS antenna for his coastal location, since he wished to direct as much as possible of his signal inland. The second note, a few weeks later, asked if there might be an antenna for his coastal location that would allow NVIS communications out to sea with enough front-to-back ratio to quiet signals from land-based stations in the other direction. Not only do both inquiries have an affirmative response, they both might use the same antenna.

Figure 1 shows two candidates composed of no. 12 AWG copper wire and set at 45 feet apart (about 0.175 λ) for 3.9-MHz operation. The upper left sketch shows a conventional two-element driver-reflector Yagi. The element spacing provides a feed point impedance close to 50 Ω. As we lower the height of a directional antenna, the main forward lobe angles ever more upward. The Yagi shown has a takeoff (TO) angle of about 49°, with an elevation beamwidth that extends to nearly overhead. The maximum gain approaches 8.2 dBi at the TO angle, with a 7.5-dB front-to-back ratio. The radiation directly upward from the Yagi is only down about 3.5 dB or so from the maximum gain, so NIVS communications at the shortest ranges will be similar in strength to using a dipole or inverted-V. However, receiving sensitivity to the rear of the array will be well down from maximum gain. The result is directive NVIS operation, whether out to sea or inland from the sea.

The way to improve the NVIS directional pattern is not with more antenna gain, but with less. The more compact Moxon rectangle — consisting of no. 12 AWG copper wire — has a lower maximum gain value: about 7.9 dBi. However, the TO angle is about 55°, with a smoother pattern curve from front to rear. Hence, the zenith angle falls within the elevation pattern's beamwidth. As well, the rectangle's configuration provides an additional 2-dB of front-to-back ratio, resulting in further quieting in the unwanted direction. We might obtain similar results from the Yagi by lowering its height somewhat.

Because both antennas are horizontal directional beams, even at low heights, we have a limited horizontal beamwidth. *NEC-4* reports a value of 94° for the Yagi and 120° for the Moxon rectangle. These reports derive from the azimuth patterns that we took using the TO angle as the pattern elevation angle. Since both TO angles are quite high, we must use caution in accepting the reported values.

Every azimuth pattern over ground specifies an elevation angle for the pattern. Only if the elevation angle is 0° (illicit in *NEC-2*) will the pattern itself be circular. Azimuth-equivalent patterns in free-space may use 0° elevation and also yield a far-field tracing that is flat and circular. Every nonzero elevation angle entry in fact produces a pattern based on a conical surface, as suggested by the radically high elevation angle in Figure 2. Let's assume that the figure has sliced the cone from tip to base and therefore shows only the main forward lobe and not the rearward lobes. The actual half-power beamwidth on the surface of the cone is the angular distance between the points on the lobe that are 3 dB down from the peak gain value.

Unfortunately, limitations of software force us to project the pattern onto a flat circular plotting form. World maps suffer a similar problem when we project the features of a globe onto a flat page. The problem is distortion. With azimuth patterns, we do not

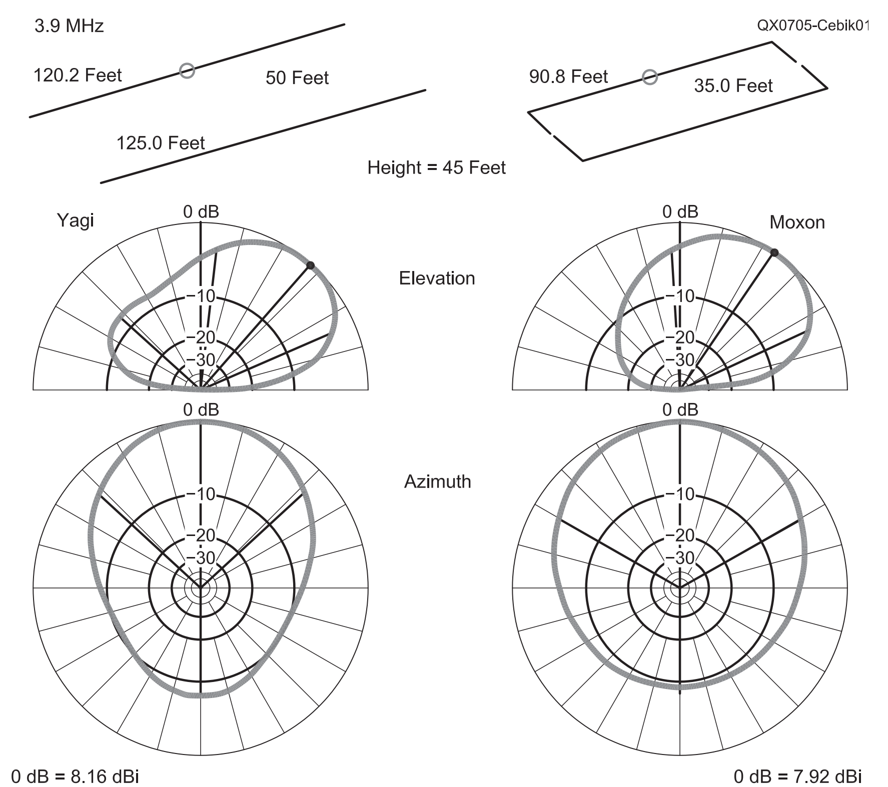

Figure 1 — Two directional NVIS antennas with elevation and azimuth patterns.

notice the problem with antennas that we use for long-distance communication, because we normally use fairly low elevation angles. Hence, the cone and the plotting form are very similar. However, for NVIS operations, we are interested in high to very high angles; that is, elevation angles from 45° to 90°. At these angles, the distortion can be high, and it increases as we increase the elevation angle. The right side of Figure 2 may seem to create only mild distortion, but the sketches show a 2:1 ratio between the angles on a flat surface and on the conical surface at the left.

We may quickly calculate an approximate corrected horizontal beamwidth value using a simple equation:

$$BW_a = BW_r \times \cos(\text{elevation angle}) \quad \text{(Eq 1)}$$

or

$$BW_a = BW_r \times \sin(\text{theta angle}) \quad \text{(Eq 2)}$$

BW_a is the actual horizontal beamwidth, BW_r is the *NEC* report of the beamwidth, and the indicated angles are the elevation or theta angles at which we take the phi/azimuth pattern. The use of an elevation angle or a theta angle will depend on the operative convention of your antenna modeling software. *NEC* operates using theta angles counting from the zenith downward. We convert theta angles to elevation angle by subtracting from 90°. The equation is only a handy approximation because it does not account for the fact that the pattern has side-to-side curvature on the surface of the cone, but it provides results that are as close as we need for virtually all applications.

One reason that we do not question beamwidth reports for lower angle azimuth patterns relative to the values that occur in free-space patterns is that the cosine of the elevation angle is 0.9 or higher for all such angles that are 25.8° or lower. However, the cosine of the elevation angle decreases ever more rapidly toward zero as we raise the elevation angle. The Yagi reported a beamwidth of 94° at a TO angle of 49°. The cosine of 49° is 0.646 and so the adjusted beamwidth is about 62°. The Moxon reported a beamwidth of 120° at an elevation angle of 55°. The corrected value is about 69°. Although the initial reports seemed to give the Moxon a large horizontal beamwidth advantage over the Yagi, the corrected values tell us that there is not much difference. Since wire NVIS directional antennas require aiming, correcting the high-angle azimuth beamwidth reports is essential if we are to know what coverage we can expect from it. Of course, coverage does not suddenly end beyond the beamwidth limit, but it may weaken rapidly.

Wide-Band Terminated NVIS-ALE Antennas

Automatic Link Establishment (ALE) equipment has become almost standard in military circles. By very rapid scanning and synchronization of codes and return codes, the central station can select the most promising frequency for successful communications. Other governmental agencies have seen a potential for adapting this system to emergency communications. Since the scanning central transceiver does its work so rapidly, it does not have time for the delays associated with changing matching networks to effect a match between the equipment and the antenna. As a result, antennas that exhibit a constant impedance over a very wide frequency range have once more become very popular government acquisition items.

Unfortunately, radio amateurs have also become enamored with these antennas. One of the most common misconceptions associated with these antennas is that they perform in all respects as smoothly across the frequency spectrum as the very low SWR value suggests. In general, we can rarely obtain such smooth performance over a 2:1 frequency range using an inverted-V configuration. Let's perform a small experiment. We can use the three antennas shown in Figure 3 as samples. Each

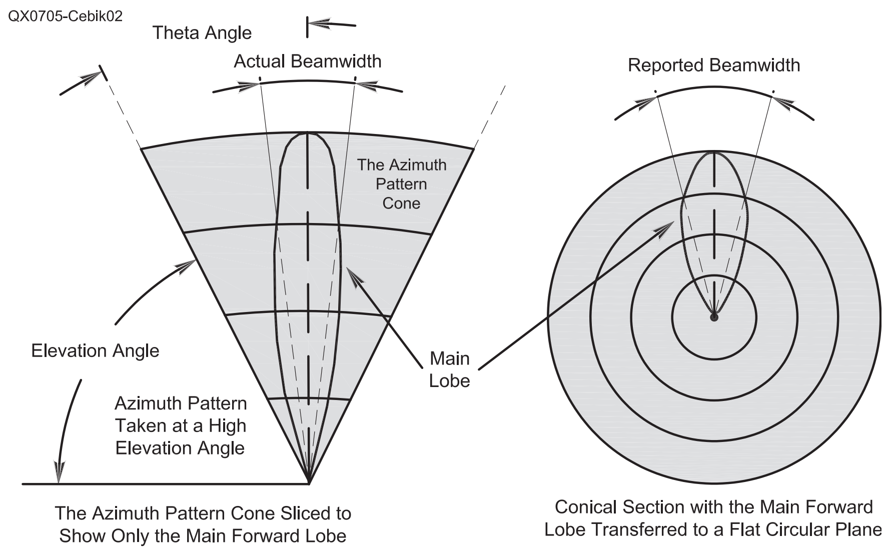

Figure 2 — Understanding azimuth patterns and the potential for distortion as we project them onto flat, circular plotting forms.

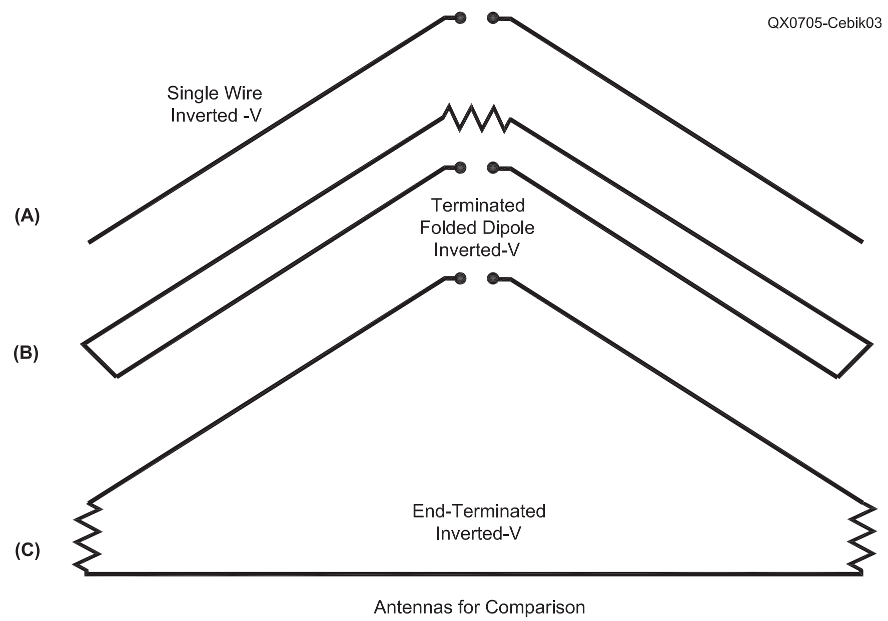

Figure 3 — Three inverted-V antennas for comparison: one unterminated (A), the other two, (B) and (C), terminated in different ways.

antenna is 42.5 feet high at the center and 2.5 feet above average ground at the ends. The distance between the center pole and the wire end is 50 feet. Each leg is therefore 64 feet long, for a total no. 12 AWG wire length of 128 feet. These dimensions apply to all three variations on the inverted-V installations. The operating range is 3.75 MHz to 7.5 MHz. Each antenna is initially a bit shorter than ½ λ electrically so that we may obtain adequate NVIS patterns throughout the passband.

The single-wire unterminated V forms a performance baseline for our comparisons. At the antenna feed point, we shall expect (and ignore in this context) a wide set of excursions for the resistive and reactive components. The resistance will begin quite low and reach a very high value at or near the upper frequency limit. The reactance begins as a moderate capacitive value and climbs to a very high inductive value. These progressions are normal for an antenna that begins at just under ½ λ and reaches about 1 λ at the upper frequency limit.

More significant for the present context are the data in Figure 4, which graphs the maximum gain and the broadside and endwise beamwidth values. The gain declines at the lower end of the spectrum as the antenna reaches ½ λ and then becomes even shorter. Otherwise, the gain level is relatively smooth and consistent with values that we saw for the inverted-V in the last episode. The broadside beamwidth shows a continuous climb with increasing frequency. In contrast, the endwise beamwidth remains relatively constant until we near the upper end of the passband.

The middle sketch in Figure 3 shows perhaps the most popular terminated wide-band antenna used by amateurs: the terminated folded dipole. There are many versions and a number of myths surrounding the antenna. The spacing between the no. 12 AWG conductors can vary from an inch to a foot or two with no difference in the basic performance that will show up in the model. Far more critical to any application is the length. An ideal terminated wide-band folded dipole antenna will be at least ½ λ long at the low-

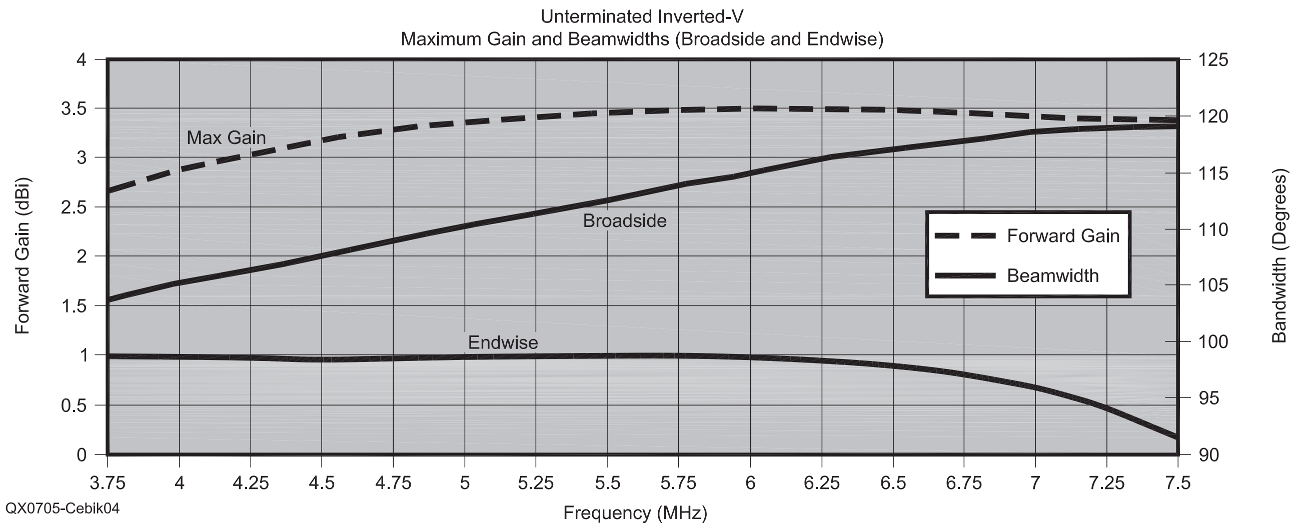

Figure 4 — The maximum gain and beamwidth (both broadside and endwise) curves for an unterminated inverted-V for use between 3.75 and 7.5 MHz.

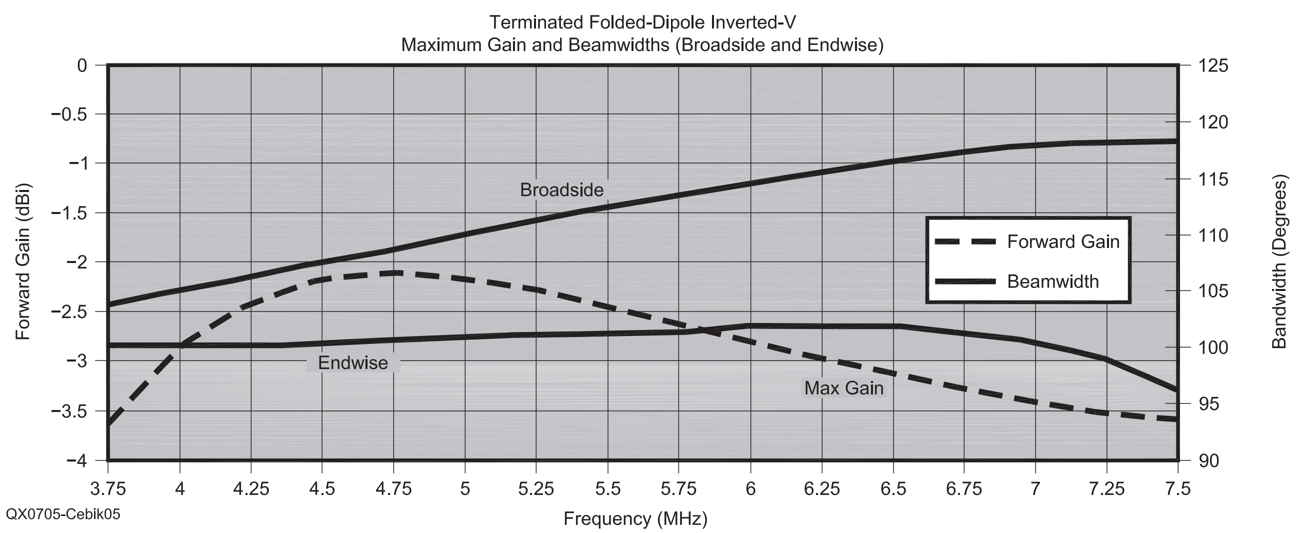

Figure 5 — The maximum gain and beamwidth (both broadside and endwise) curves for a terminated folded-dipole inverted-V for use between 3.75 and 7.5 MHz.

est operating frequency to remain above the performance "knee." The knee represents an electrical length below which performance falls off precipitously, as the antenna feed point resistance without the termination would decrease from about 70 Ω toward zero. The series termination would provide a stable feed point impedance, but also dissipate more and more of the energy. In the inverted-V configuration, the baseline nonterminated impedance would be closer to 50 Ω. Above the knee region, the impedances undulate around the value of the terminating resistor. A resistor in the vicinity of 800 to 900 Ω tends to yield the smoothest SWR curve. Of course, the antenna must include an effective method of converting the high terminal impedance down to a conventional coaxial-cable value.

Like the single-wire unterminated inverted-V, the terminated folded version is slightly short relative to the knee in order to produce acceptable patterns for NVIS operation within the 3.75 to 7.5 MHz passband. Because the amount of shortening below ½ λ is small, we should see only the start of the gain decline below about 4.5 MHz. The graph in Figure 5 confirms this suspicion. Below about 4.5 MHz, the curve takes a sharper downward direction than the corresponding gain curve for the unterminated inverted-V. Equally significant in Figure 5 are the beamwidth curves for broadside and endwise directions from the wire antenna. Compare these curves to the corresponding set in Figure 4. The fundamental similarity is inescapable.

An alternative method of developing a wide-band terminated antenna is to place the terminating resistors at the wire ends. These resistors require a ground-return line to provide them with a low impedance common point. The model for this basic configuration uses a wire that is 0.001 λ above ground so that the model will run on both *NEC-2* and *NEC-4*.[1] Commercial versions of the antenna

[1]Models for the antennas discussed in these notes are available at the ARRL Web site. All but the speculative log-spiral design are in *EZNEC* format. The log-spiral is in *NEC* format and uses at least one command unique to *NEC-4*. Go to **www.arrl.org/qexfiles** and look for **5x07_AO.zip**.

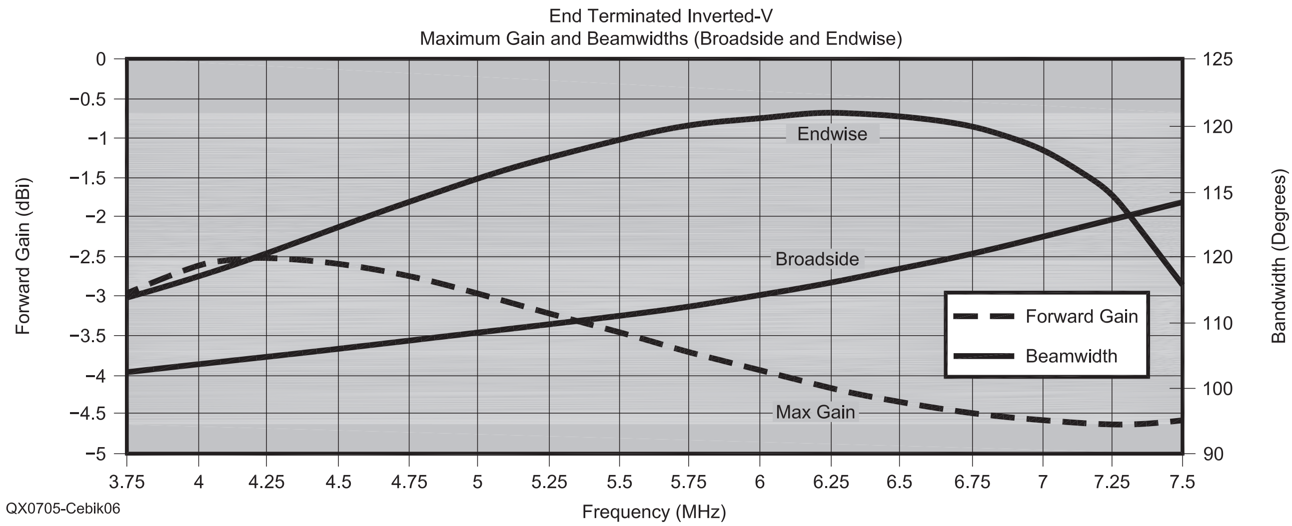

Figure 6 — The maximum gain and beamwidth (both broadside and endwise) curves for an end-terminated inverted-V for use between 3.75 and 7.5 MHz.

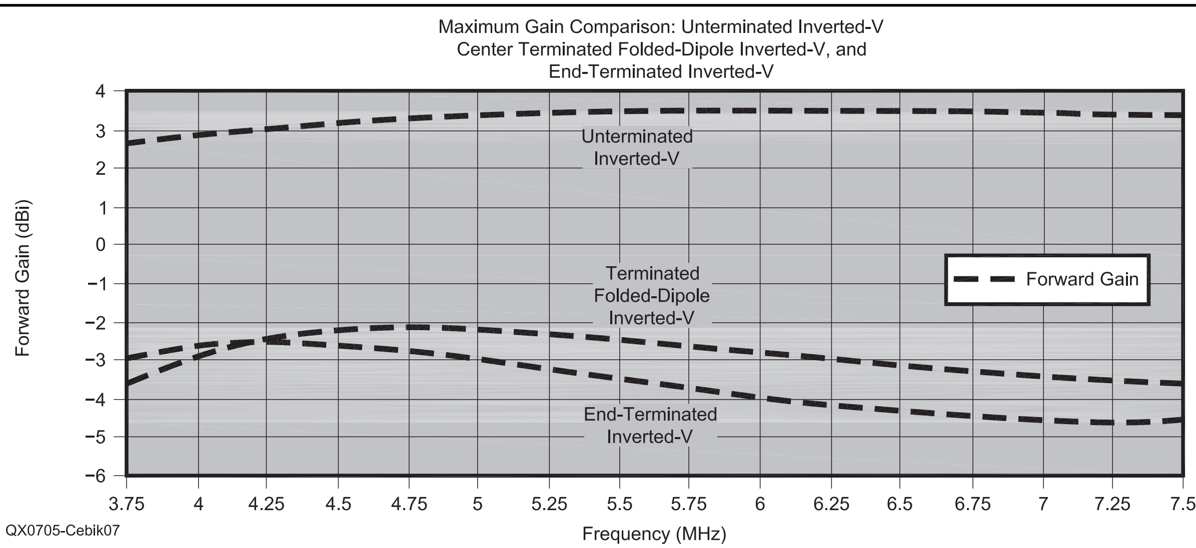

Figure 7 — A comparison of maximum gain curves for an unterminated inverted-V, a terminated wide-band folded dipole inverted-V, and an end-terminated inverted-V.

show variations on the basic theme. Some use fans of different-length elements joined at the terminated ends. Others bring the common line back up to the feed point. Most of the variations tend to yield somewhat smoother SWR curves. The modeled basic version uses a 500 Ω resistor at each end of the wire, with a 1000 Ω reference impedance. As with the folded dipole type of terminated antenna, the system needs an effective impedance transformation device to allow a coaxial feed line. One difference between the end-terminated system and the folded-dipole type occurs with the SWR performance below the knee region. Whereas the folded version shows a smoother SWR curve, the end-terminated version tends to show a rise in SWR. Hence, the SWR provides a warning apart from gain performance to tell the user when the antenna is too short.

Figure 6 graphs the maximum gain and the beamwidth values for the end-terminated antenna in its simplest form. The gain curve roughly parallels the folded-dipole curve, but with a slightly lower knee-frequency region — closer to 4 MHz than to 4.5 MHz. More interesting are the beamwidth curves. The broadside beamwidth is very close to what we found for the unterminated and the folded-dipole antenna types. However, the endwise beamwidth shows a greater variation across the passband than we found with the other two antennas. As well, the average endwise beamwidth is perhaps 25° greater and exceeds the broadside beamwidth throughout the passband. One consequence of this behavior difference is that commercial versions of the antenna tend to favor flatter installations than the 38° slope of the wires in these test models. The more level the wire, the lower the endwise beamwidth of the end-terminated wire, with a resulting equalization of beamwidths for NVIS operation.

We cannot escape an ultimate comparison of the gain curves for the three sample antennas. See Figure 7. The gain differential between the two terminated antennas is inconsequential compared to the deficit relative to the unterminated wire. The gain difference runs from a minimum of 5+ dB up to over 6.5 dB across the 2:1 frequency span. Since NVIS operations often call for working at the margins of acceptable transmitted and received signals, a central station using a terminated antenna loses ¾ of its transmitted power and over an S-unit of received signal strength compared to a simple unterminated wire. While terminated antennas might be used at field installations to simplify operation, they do not appear to offer the amateur operator any significant benefits for a durable installation.

The reason for limiting the three antennas to a 2:1 frequency span results from the fact that terminating a given length antenna does not change the far-field pattern shape. To illustrate this basic fact, Figure 8 presents some samples of overlaid endwise elevation patterns. Only the terminated folded-dipole antenna appears as the lower-gain entry for comparison with the unterminated antenna. Adding the end-terminated antenna would only create murky pattern outlines for the inner or weaker patterns. The essential feature of these patterns is the strict congruence between the stronger and the weaker patterns across the passband. Termination affects the radiated energy of an antenna, but not its patterns. I have included a pattern for 10 MHz to establish the reason for limiting the antenna passband. However smooth the SWR curve may be for a given terminated design, the bell-shaped pattern at 10 MHz indicates an endwise beamwidth that is usually too narrow for most NVIS operations.

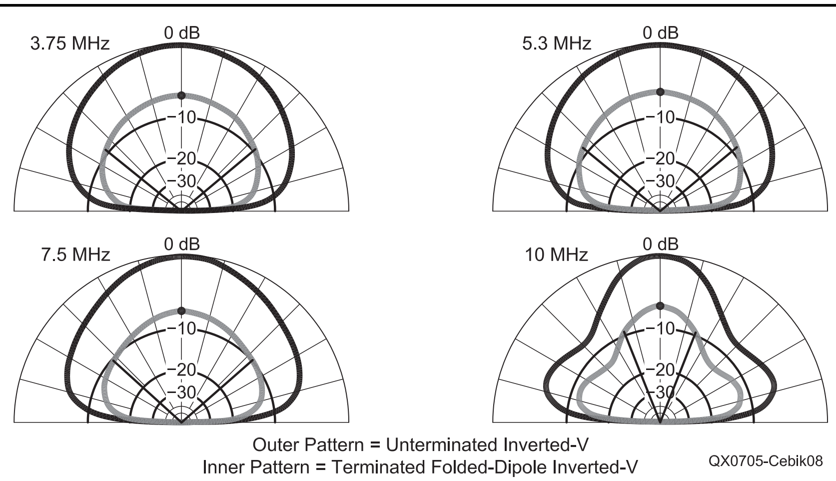

Figure 8 — Endwise elevation patterns for an unterminated inverted-V and a terminated folded-dipole inverted-V.

The Search for a Wide-Band Unterminated NVIS Antenna

ALE has added a fresh incentive to find an NVIS antenna that provides full unterminated wire antenna gain but with an exceptionally wide operating bandwidth. A more ideal antenna would exhibit relatively uniform gain directly upward with equal beamwidth values, that is, with a virtually circular azimuth pattern at any elevation angle. The half-power beamwidth values should fall within a range from 70° to perhaps 110° to assure adequate energy and receiving sensitivity at about a 45° elevation range to allow intermediate as well as short-range communications by this mode. The search for such an antenna has taken two basic directions — one relatively futile, the other more promising.

Both directions share a common feature: the use of frequency-independent design techniques. The most obvious technique is to apply LPDA design equations to a dipole array that points straight upward (or downward). In general, an LPDA design with linear elements fails to achieve the desired results due to a conflict between LPDA design criteria and the height range within which NVIS antennas perform best. For any number of elements covering any frequency range, the best height falls within the 0.125-λ and the 0.225-λ range. To obtain the best LPDA performance in terms of gain and feed point impedance we must increase the value of one of the calculation constants (σ) to a value higher than we find in most horizontally oriented arrays. For the 2.5 to 11 MHz range (a 4.4:1 frequency span), the result would be an exceptionally tall array. As well, the gain would yield beamwidths well below the desired 70° minimum value.

If we shorten the array by reducing the value of σ and reduce the number of elements, then LPDA performance over a wide frequency range tends to collapse. Numerous anomalous frequencies will appear. At these frequencies, the pattern will show multiple

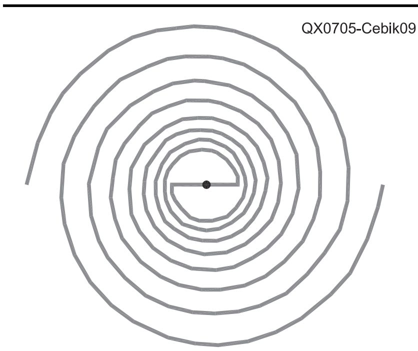

Figure 9 — A wide-band log-spiral "doublet" for wide-band (2.5-10 MHz) NVIS service.

lobes in unwanted directions and the main lobe will not be upward. As well, the impedance curve tends to vary widely. In general, the wider the frequency span for an LPDA, the closer that the design constants of τ and σ must come to the highest permissible values. As a result, if we try to place each element at a height that favors NVIS operation, we end up with an array that fails completely in its mission.

An alternative array that also uses basic LPDA principles in an expanded format has become popular among some commercial antenna makers for the corporate and government market: the log-spiral doublet array. Figure 9 shows the general outline for one such design. The spiral uses a factor of a^{Θ} to define the rate of radius increase with each wire segment. The design shown uses a pair of 4-turn spirals 180° apart to end up with the full structure.

Log-spiral antennas have their greatest use in the UHF region where the design can attend to the element diameter (or strip width on a substrate). A wire version in the HF range that uses a single wire diameter will thus be less ideal and subject to numerous finicky requirements. Most commercial designs do not use an inner limiting radius for the spiral. As well most use a conical or modified conical shape (with four or six sides). Some offerings use outer-end resistive terminations, although this practice seems to defeat the point of using such a complex structure, namely, to achieve full wire gain over a wide frequency span. Hence, the state of the art relative to log-spiral NVIS potentials remains uncertain. Nevertheless, Table 1 shows the modeled performance of the flat log-spiral design and thus suggests what may be possible some time in the future. Note that at only two frequencies does the beamwidth drop to less than 70° in one of the sampled planes. Patterns do not go completely askew until we pass 10.5 MHz. The sample array used here requires a 50-meter diameter just to contain the wire, with additional space needed for supports.

Table 1
Sample *NEC-4* data values for a model of a flat unterminated log-spiral antenna design. See Figure 9.

	0° Phi (Tip-to-Tip)		*90° Phi (Across Spiral)*	
Frequency MHz	*Gain dBi*	*Beamwidth Degrees*	*Gain dBi*	*Beamwidth Degrees*
2.5	5.86	70	5.86	76
3.5	6.83	70	6.83	76
4.5	7.49	70	7.49	76
5.5	6.47	72	6.47	98
6.5	6.59	84	6.59	94
7.5	7.01	114	6.99	58
8.5	6.78	86	6.78	102
9.5	6.68	102	6.48	70
10.5	5.93	68	6.23	110
11.5	6.51	108	4.83	52
12.5	3.66	142	5.24	126

Notes
[1]Antenna uses 0.002-mm wire throughout and is 10 meters above average ground
[2]A difference in the gain values in the 0° and 90° phi columns indicates that maximum gain does not occur at the zenith angle (0° theta or 90° elevation).
[3]Antenna model is set up for *NEC-4* and uses the *NEC-4* GH command to establish the log-spiral.

Conclusion

We began by identifying two special needs sometimes associated with NVIS operation. Obtaining a directional NVIS array proved to be the simpler project, since any number of relatively low-gain horizontal arrays might meet the operational criteria for an installation. Very-wide band NVIS operation across a large frequency spread presented the more difficult challenge. If we require relatively slow frequency changes, then we can easily press an inverted-V into service over a 2:1 frequency range for acceptable NVIS patterns. The higher rates of ALE frequency change, however, require an antenna that calls for no alteration of the impedance matching network in the course of operation. Some typical wide-band terminated antenna types can meet the need, with two restrictions. First, for many antennas that we might set up as inverted-Vs or as linear doublets, the operative frequency range for acceptable NVIS patterns remains about 2:1. Second, termination yields considerable loss of gain. Achieving a wide-band unterminated antenna design capable of covering 2.5 to 10 MHz with roughly similar gain levels and acceptable NVIS patterns without a need to switch networks remains a future goal for amateurs and an expensive project for commercial and government installations.

Tech Notes

Doug Smith, KF6DX
225 Main St
Newington, CT 06111
kf6dx@arrl.org

ELECTROMAGNETIC RADIATION: A BRIEF TUTORIAL

What is the physical basis of electromagnetic radiation?

Electromagnetic radiation is the propagation of energy through space by means of coupled electric and magnetic fields. Radio waves, light, X-rays, gamma rays and cosmic rays are all forms of electromagnetic waves. There is a quantum-mechanical explanation for radiation, too; but here, we shall concentrate on wave theory.

The history of our understanding of electromagnetic radiation began in the Renaissance with the study of light. Galileo tried to measure the speed of light using lanterns and shutters over a distance of several kilometers, but found that he could not — it was simply too fast. For many years, the assumption was that the speed of light was infinite.

Another of Galileo's experiments resulted in the discovery of four of the satellites of Jupiter when he turned his telescope on the planet early in the 17th Century. After watching the satellites for several months, he found that their orbital periods were quite regular and therefore made good clocks. The discovery solved the problem of longitude determination for land-based observers. Ironically, slight variations in the observed orbital periods of those satellites, as measured by Cassini and Rømer more than 60 years later, would reveal the speed of light. Those fellows succeeded where Galileo had failed because of the much larger scale of the system they were measuring.

By that time, other studies had shown the wave nature of light quite clearly. Properties of reflection, refraction, diffraction, interference and even polarization were well known. Scientists knew that light was wave-like and they knew its speed of propagation quite accurately; however, they knew neither how such waves could propagate without a physical medium, nor much about how light and other forms of electromagnetic radiation actually originate.

Four basic laws of electricity and magnetism were known by the mid-19th Century. They are:

1. Electric field strength, integrated over any closed surface containing a charge, is directly proportional to the enclosed charge.

2. All magnetic fields are caused by currents, which always produce both north and south magnetic poles.

3. The work done moving a charge in a complete circle is directly proportional to the negative of the rate of change of magnetic field strength.

4. The work done moving a (hypothetical) magnetic pole in a complete circle is directly proportional to the current passing through the circle.

Those laws explained almost every phenomenon in electricity and magnetism then known, but they could not account for the electromagnetic nature of light.

The third and fourth laws neatly state principles of electromagnetic induction, as discovered by Ampère and Faraday. They govern the behavior of electric motors and generators because they state that a current is generated in the presence of a changing magnetic field, and vice versa. A certain symmetry was missing, however. One British physicist, J. Maxwell, filled in the logical blanks. He recognized that if a changing magnetic field gave rise to a current, it must have generated an electric field to produce that current. He also recognized that the reverse was true: A changing electric field (or current) must give rise to a changing magnetic field that opposes the change in current — Lenz's Law. Finally, Maxwell realized that those laws explaining magnetism did so only in reference to real currents. In a traveling electromagnetic wave distant from its source, no actual movement of charge occurs to keep the wave going.

Because of those conclusions, and because conservation of charge demanded it, Maxwell introduced the concept of a *displacement current*, corresponding to the rate of change of the electric field. He therefore changed the fourth law to say:

4. The work done moving a (hypothetical) magnetic pole in a complete circle is directly proportional to the current passing through the circle *and to the rate of change of the electric field*.

Displacement current is not the actual movement of charge but it is equivalent in every way for changing fields.

At the time, Maxwell's theory was particularly remarkable because no one had any knowledge of electrons, or how to relate light to those discrete sources, or even whether the predicted waves existed in other forms. The theory showed that the speed of light could be calculated from relatively simple electrical measurements of the propagation medium. It also explained the refraction of light in terms of the electrical properties of materials, and a host of other phenomena.

Confirmation came with the experiments of H. Hertz in Germany. Hertz transmitted and received radio waves over short distances, measured their wavelengths, demonstrated their reflection and interference, verified the speed of their propagation and even built resonant circuits.

Frequency and Wavelength

All electromagnetic waves have one thing in common: they travel or *propagate* at the speed of light. That speed is approximately 3.00×10^8 meters per second in a vacuum. Electromagnetic waves have a length uniquely associated with each possible frequency. The frequency in hertz is simply the speed of propagation divided by the wavelength (λ) in meters:

$$f\ (\text{Hz}) = \frac{3.00\times10^8 \left(\frac{\text{m}}{\text{s}}\right)}{\lambda\ (\text{m})} \qquad \text{[Eq 1]}$$

and so wavelength is speed divided by frequency:

$$\lambda\ (\text{m}) = \frac{3.00\times10^8 \left(\frac{\text{m}}{\text{s}}\right)}{f\ (\text{Hz})} \qquad \text{[Eq 2]}$$

Example: What is the frequency of an 80.0-m RF wave?

$$f\ (\text{Hz}) = \frac{3.00\times10^8 \left(\frac{m}{s}\right)}{\lambda\ (\text{m})}$$

$$f\ (\text{Hz}) = \frac{3.00\times10^8 \left(\frac{\text{m}}{\text{s}}\right)}{80.0\ \text{m}}$$

$f\,(\text{Hz}) = 3.75 \times 10^6$ Hz

We could use a similar equation to calculate the wavelength of a sound wave in air, but we would have to use the speed of sound instead of the speed of light in the numerator of the equation.

To calculate the frequency of an electromagnetic wave directly in kilohertz, change the speed constant to 300,000 (3.00×10^5) km/s:

$$f\ (\text{kHz}) = \frac{3.00\times10^5 \left(\frac{\text{km}}{\text{s}}\right)}{\lambda\ (\text{m})} \qquad \text{[Eq 3]}$$

and

$$\lambda\ (\text{m}) = \frac{3.00\times10^5 \left(\frac{\text{km}}{\text{s}}\right)}{f\ (\text{kHz})} \qquad \text{[Eq 4]}$$

For frequencies in megahertz, use:

225 Main St
Newington, CT 06111-1494
kf6dx@arrl.org

$$f\ (\mathrm{MHz}) = \frac{300\left(\frac{\mathrm{Mm}}{\mathrm{s}}\right)}{\lambda\ (\mathrm{m})} \qquad \text{[Eq 5]}$$

and

$$\lambda\ (\mathrm{m}) = \frac{300\left(\frac{\mathrm{Mm}}{\mathrm{s}}\right)}{f\ (\mathrm{MHz})} \qquad \text{[Eq 6]}$$

You would normally just drop the units that go with the speed-of-light constant to make the equations look simpler.

Example: What is the wavelength of an RF wave whose frequency is 4.0 MHz?

$$\lambda\ (\mathrm{m}) = \frac{300}{f\ (\mathrm{MHz})} = \frac{300}{4.0} = 75\ \mathrm{m}$$

Within the part of the electromagnetic spectrum of most interest to radio applications, frequencies have been classified into groups and given names. Table 1 provides a reference list of those classifications. To a significant degree, the frequencies within each group exhibit similar properties. For example, HF or high frequencies, from 3 to 30 MHz, all exhibit *skip* or ionospheric refraction that permits regular long-range radio communications. This property also applies occasionally both to MF (medium frequencies) and to VHF (very high frequencies). More information on the terrestrial propagation differences among the frequency bands is found in the **Propagation of RF Signals** chapter of *The ARRL Handbook*.

Electromagnetic waves propagate even in the absence of a material medium. How does that happen and what gets them started?

Nonuniform Motion of Charge

A charged particle like an electron has an electric field around it in every direction. In the stationary frame, the orientation of that field is everywhere in the direction of the particle, as shown in Figure 1. The outward extent of the field is unbounded. Its inward extent is bounded by the surface of the particle itself, although all attempts to prove a nonzero physical size and shape for an electron fail in one way or another. For our purposes, an electron is a one-dimensional or *point charge*.

Table 1

Designation	*Frequency Limits*
VLF	3-30 kHz
LF	30-300 kHz
MF	300-3000 kHz
HF	3-30 MHz
VHF	30-300 MHz
UHF	300-3000 MHz
SHF	3-30 GHz
EHF	30-300 GHz

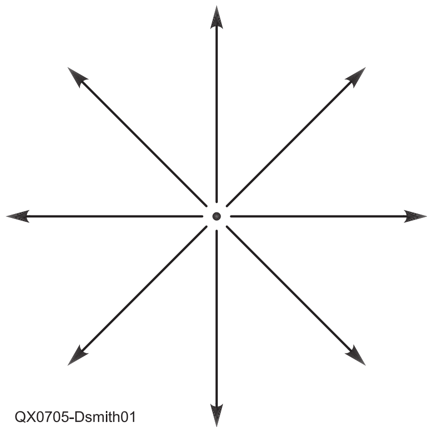

Figure 1 — The electric field around a stationary electron.

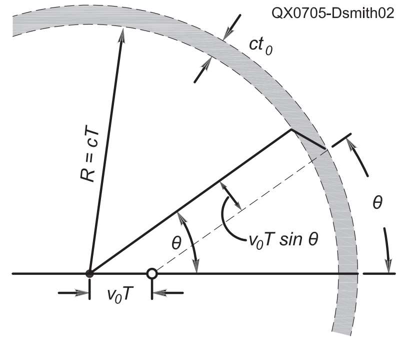

Figure 2 — A point charge experiencing a linear deceleration. (After E. Purcell, *Electricity and Magnetism*, 2nd ed., McGraw-Hill, 1984. Used with permission of The McGraw-Hill Companies.)

Now consider what happens when such a point charge experiences a force that decelerates it linearly from some initial velocity, v_0 to zero during time t_0. Refer to Figure 2. Before and during constant deceleration $a = v_0 / t_0$, the particle is moving from left to right in the diagram. Assume that the initial velocity is much less than the speed of light, c.

A long time, *T*, after all that occurs, the electric field has radiated at velocity c to a radius of $R = cT$ from the particle. The orientation of the section of field corresponding to the acceleration period is *not* in the direction of the particle but slightly transverse to it. For a field line at some angle θ to the direction of motion, the geometry of the pulse of radiation shows the ratio of the transverse component of the field to the radial component to be:

$$\frac{E_t}{E_r} = \frac{v_0 T \sin\theta}{\mathrm{c}t_0} \qquad \text{[Eq 7]}$$

$$\frac{E_t}{E_r} = \frac{aR\sin\theta}{\mathrm{c}^2} \qquad \text{[Eq 7A]}$$

The radial field E_r follows Coulomb's law, so the transverse field is:

$$E_t = \left(\frac{aR\sin\theta}{\mathrm{c}^2}\right)\left(\frac{q}{4\ \pi\ \varepsilon_0 R^2}\right) = \frac{qa\sin\theta}{4\ \pi\ \varepsilon_0 \mathrm{c}^2 R} \qquad \text{[Eq 8]}$$

where q is the charge of the particle. Note that this field decreases with distance as $1/R$, not $1/R^2$. Also note that the transverse field is zero along the line of motion and is maximum at right angles to that line. The energy per unit volume in the expanding spherical shell of thickness $\mathrm{c}t_0$ is proportional to the square of the field strength, or E^2, so the total energy contained in the shell remains unchanged even as it expands.

To calculate the energy in the transverse component of the field within the shell, we have to integrate E_t^2 over the entire shell and multply by $\varepsilon_0 / 2$. The result is:

$$U_{E_t} = \frac{q^2 a^2 t_0}{12\ \pi\ \varepsilon_0 \mathrm{c}^3} \qquad \text{[Eq 9]}$$

We know that changing electric fields give rise to magnetic fields and that magnetic fields also contain energy. In the same units as Equation 8, the magnetic field strength inside the shell is E_t / c, or:

$$B_t = \frac{qa\sin\theta}{4\ \pi\ \varepsilon_0 \mathrm{c}^3 R} \qquad \text{[Eq 10]}$$

To calculate its energy within the shell, we have to integrate over the entire shell and divide by $2\mu_0$. Since $\varepsilon_0\mu_0 = 1/\mathrm{c}^2$, the result is:

$$U_{B_t} = \frac{q^2 a^2 t_0}{12\ \pi\ \varepsilon_0 \mathrm{c}^3} \qquad \text{[Eq 11]}$$

or exactly the same energy as contained in the electric field. Therefore, the total radiated energy is:

$$U_{tot} = U_{E_t} + U_{B_t} = \frac{q^2 a^2 t_0}{6\ \pi\ \varepsilon_0 \mathrm{c}^3} \qquad \text{[Eq 12]}$$

Power is the rate of energy delivery, so dividing Equation 12 by t_0 yields power in watts:

$$P_{tot} = \frac{q^2 a^2}{6\ \pi\ \varepsilon_0 \mathrm{c}^3} \qquad \text{[Eq 13]}$$

Equation 13 is the famous *Larmor formula*, found by J. Larmor in 1897, which relates radiated power to its source — accelerated charge — without resort to the vector calculus of the so-called Maxwell equations. We have borrowed two of J. Maxwell's discoveries, however: $\varepsilon_0\mu_0 = 1/\mathrm{c}^2$ and $B_t = E_t$ / c. In fact, it was the former discovery that convinced Maxwell that light was electromagnetic in nature. Larmor was also working on the theory of light when he wrote Equation 13.

Radiation Resistance and Efficiency

With a neat equation in hand that relates radiated power to changing currents, we ought to be able to show how a resistance is associated with the conversion of energy from one form (acceleration of charge) to another (radiation). Indeed we can, and the proof, at least in part, confirms the theory that all energy conversion involves some kind of resistance.

Consider a linear dipole that is much shorter than the length of a resonant, half-wavelength dipole. In other words, its length $l << \lambda/2$. Apply a sinusoidal voltage E_t of angular frequency $\omega = 2\pi f$ to the dipole and from Ohm's law for impedance, a sinusoidal current of $\boldsymbol{I_t} = E_t$ / $\boldsymbol{Z}$ flows, where $\boldsymbol{Z} = R + jX$ is the impedance of the antenna at frequency f. Since the antenna is well below resonance, the current along its length is virtually constant. Reactance X is negative (capacitive) and much greater in magnitude than resistance R.

Nonetheless, we are mainly interested in R because it determines the real part of the current and contains the radiation resistance, R_{rad}. The other part of R is just the ohmic ac resistance of the antenna conductor, R_{ac}, which converts some of the applied energy to heat. Thus, $\boldsymbol{Z} = (R_{ac} + R_{rad}) + jX$.

Because current is the time variation of charge, we can make that substitution in the Larmor formula to find the total radiated power in terms of a sinusoidal current. We have to integrate over the length of the antenna, ℓ, to incorporate the contributions of all of its parts to the radiated power and average things over one complete ac cycle to get the RMS value. The substitution in the numerator of Equation 13 is:

$$q^2 a^2 = \frac{(2\ \pi\ f)^2\ \ell^2 I_{pk}^2}{2} \qquad \text{[Eq 14]}$$

where I_{pk} is the peak current in amperes, ℓ is in meters and f is in hertz.

The other useful substitution comes in the denominator of Equation 13. Wavelength λ = c / f, so $\mathrm{c}^2 = (f\lambda)^2$. Applying those substitutions to the Larmor formula, we get:

$$P = \frac{(2\pi\ f)^2\ \ell^2 I_{pk}^2}{12\pi\ \varepsilon_0 c (f\lambda)^2}$$

$$P = \frac{\pi\ I_t^2}{3\varepsilon_0 \mathrm{c}}\left(\frac{\ell}{\lambda}\right)^2 \qquad \text{[Eq 15]}$$

which compactly relates dipole length ℓ as a fraction of a wavelength to radiated power. Notice that the frequency terms cancel. Knowing that $P = I^2R$, we can write the equation for radiation resistance R:

$$R = \frac{P}{I^2}$$

$$R = \frac{\pi}{3\varepsilon_0 \mathrm{c}}\left(\frac{\ell}{\lambda}\right)^2 \qquad \text{[Eq 16]}$$

in ohms where the current is constant over length ℓ.

Example: What is the radiation resistance of a dipole two meters long at 2 MHz in a vacuum? Answer: λ is about 150 meters, so:

$$R = \frac{\pi}{3\varepsilon_0 \mathrm{c}}\left(\frac{\ell}{\lambda}\right)^2$$

$$\approx 0.0656\ \Omega$$

A ridiculously low number like that makes it difficult to achieve good efficiency in an antenna system because it is comparable with the ohmic resistances of the antenna conductor and of whatever system and transmission line are used to deliver the energy. Much of the energy would likely go to heat.

We define the efficiency, η, of an energy-conversion process as the ratio of the energy converted into a useful form to the total energy supplied. Total energy supplied is the sum of usefully converted energy and energy lost to "useless" forms like heat. Energy is directly proportional to resistance; thus, the efficiency of an antenna system is the ratio of the radiation resistance to the total resistance:

$$\eta = \frac{U_{useful}}{U_{useful} + U_{lost}}$$

$$\eta = \frac{R_{rad}}{R_{rad} + R_{ac}} \qquad \text{[Eq 17]}$$

Antenna system designers want R_{rad} to be high compared with R_{ac} to get high efficiencies.

Additionally, transmitter designers usually design their units for a specific resistive load impedance, often 50 + j0 Ω. The large capacitive reactance of the puny dipole in the example above would have to be transformed and cancelled using a resonant circuit of some kind, which in turn would introduce further inefficiencies. A better situation is obtained from an antenna that presents an inherently resistive impedance, as do both resonant and traveling-wave antennas. Such antennas are large with respect to a wavelength and current is *not* constant along their lengths. More information about them and their radiation patterns is in the

Antennas chapter of *The ARRL Handbook*.

What We Left Out

Despite the apparent complexity of the Larmor formula, our derivation of it above relies on several simplifications. Those simplifications are:

1. The velocity of the point charge is much less than the speed of light.
2. The point charge is massless.
3. The radial field of the point charge does not contribute to the radiated energy.
4. The radiated energy is unrelated to the force (and energy) that caused the point charge to accelerate in the first place.
5. The acceleration began and ended instantaneously.

Each of those numbered points can be accounted for, but only completely in the realm of sinusoidal currents, which is what Amateur Radio operators are interested in anyway.

Starting with point 1: It is a fact that the electrons we want to get moving to radiate a signal do not have to move at anything close to the speed of light, c. They can and do radiate electromagnetic fields when their velocities are many orders of magnitude less. When electron velocity does approach c, a relativistic modification of the Larmor formula exists and applies.

Point 2: Electrons do have significant mass and it takes significant energy to accelerate them. From Newton's law $F = ma$, where F is force, m is mass and a is acceleration, the kinetic energy of a mass moving at velocity v is known to be:

$$U = \frac{mv^2}{2} \qquad \text{[Eq 18]}$$

If the accelerated point charge in the derivation of the Larmor formula above were an electron, its kinetic energy (as computed by Equation 18) would dwarf its radiated energy (as computed by Equation 12) by a huge margin unless the acceleration were very large.

For example, accelerate the electron to 10^5 m/s (less than a thousandth the speed of light) in one nanosecond. Acceleration a is $10^5 / 10^{-9} = 10^{14}$ m/s^2 and radiated energy is:

$$U_{rad} = \frac{q^2 a^2 t_0}{6\,\pi\,\varepsilon_0 c^3}$$

$$\approx \frac{\left(1.6\times10^{-19}\right)^2 \left(10^{14}\right)^2 \left(10^{-6}\right)}{6\,\pi \left(8.9\times10^{-12}\right)\left(3.0\times10^{8}\right)^3}$$

$$\approx 1.7\times10^{-31}\ \text{J}$$

The particle's kinetic energy is:

$$U_{kin} = \frac{mv^2}{2}$$

$$\approx \frac{\left(9.1\times10^{-31}\right)\left(10^5\right)^2}{2}$$

$$\approx 4.6\times10^{-21}\ \text{J}$$

or more than 10 orders of magnitude greater than the radiated energy. Clearly, something strange is going on here.

The resolution to this apparent paradox lies in the nature of an electron's mass. An electron has both an electric field due to its charge and a magnetic field due to its spin. The energies stored in those fields have mass equivalents by the equation independently discovered by A. Einstein and H. Poincaré: $E = mc^2$ — perhaps the most famous equation ever — where variable E is energy, not to be confused with the variable used for voltage.

Scientists have measured the mass of an electron and the strengths of its electric and magnetic fields very accurately. Computations of the mass-equivalent energy in those fields, $m = E / c^2$, do in fact come very close to accounting for the entire mass of an electron. Interestingly, energy and mass are evidently almost equally divided between electric and magnetic fields.

That is an important result because when we move an electron, we do not have to drag its entire electromagnetic field with it — only the fields that exist near its position when we move it. The fields beyond the particle's immediate vacinity have propagated away at the speed of light and can no longer affect the particle itself. Fortunately, it is therefore much easier to get an electron moving than its mass as listed in reference books might indicate. Our conclusion is that a moving electron's mass is completely accounted for by the interaction of its own fields with itself.

This question in classical electrodynamics is still the subject of ongoing debate. For uniform harmonic motion in an antenna (sinusoidal currents), fortunately the situation is much clearer but it still leads to potential surprises, which come in the discussion of point 4.

Point 3: The static, radial electric field of an electron does contain energy, proportional to E^2, in the same way that a radiated field does; but only changing fields can transmit energy over a distance through electromagnetic induction. So we are safe in our simplification here.

Points 4 and 5: It is entirely reasonable that the force causing our radiating electron to move is the original source of the radiated energy: Energy is neither destroyed nor created, it is always conserved but may be transformed.

Energy is force times distance, so power is force times velocity, since velocity is distance per unit time. Those laws lead to the conclusion that radiated power must equal the opposite of the force that causes radiation resistance times charge velocity:

$$F_{rad}\, v = -P_{rad} \qquad \text{[Eq 19]}$$

One big trouble is that Equation 19 does not accurately describe actual physical behavior at small velocities. The nature of the trouble harkens back to Lenz's law, which states that the magnetic field created by a moving charge tends to oppose the creation of that magnetic field. What happens at low velocities is that electromagnetic energy cannot escape at velocity c before it nearly cancels the motion of charges that are trying to produce it. The effect is relativistic because of the finite speed of propagation, c, and it further restricts the ability of antennas to radiate at low frequencies.

We have asserted that radiated power is directly proportional to the square of charge acceleration. Now enter A. Einstein and his General Theory of Relativity. The theory is based in part on the so-called Equivalence Principle, which states that acceleration is locally indistinguishable from the presence of a gravitational field. We have a surprise there, because a charged particle sitting in one place on Earth's surface is clearly in a strong gravitational field but it does not radiate, at least not as measured by co-stationary observers.

In his *Lectures on Gravitation*, R. Feynman wrote, "...we have inherited a prejudice that an accelerating charge should radiate..." and he went on to show, as did H. Lorentz before him, that the force F_{rad} associated with radiation resistance is not proportional to acceleration, but to the *rate of change of acceleration*, or *jerk*, as it is commonly called. That discovery ably explains why a stationary charge in a gravitational field does not radiate, reconciling the issue with relativity theory. It also jibes with the Larmor formula for sinusoidal motions because position, velocity, acceleration and jerk are all sinusoids and the integrated values over a complete cycle still come out right.

It does *not* fully align with our derivation of the Larmor formula, which considers only nonharmonic, linear acceleration. The derivation assumed that uniform acceleration began the instant some unspecified force was applied and ceased instantly when the force was removed. Those assumptions imply that the rate of change of acceleration was infinite at the beginning and end of acceleration, which is clearly unrealistic. Solutions do exist, however, incorporating more reasonable acceleration profiles that seem to agree with the Lorentz-Feynman theory. As mentioned, this part of classical electrodynamics is the subject of ongoing study — we do not have all the answers yet! But we have presented and discussed some solid electromagnetic radiation theory.

Summary

All electromagnetic radiation is caused by the motion of charges. Specifically, it is the rate of change of charge acceleration, or jerk, that produces electromagnetic waves. Charges experience a resistance to their acceleration because they interact with their own electromagnetic fields as they go. That resistance is radiation resistance, which is directly proportional to the power radiated. Those precepts hold true on average for uniform harmonic motion (sinusoidal currents) of sufficiently high frequency.

At low frequencies, charges interact so strongly with their own fields that the fields tend to prevent radiation from escaping to infinity as traveling waves. Lenz's Law and relativistic effects severely degrade the efficiency of antenna systems at low frequencies.

The electric and magnetic fields of a traveling electromagnetic wave are perpendicular to each other and to the direction of propagation. Each field has energy exactly equal to the energy in the other field at every point along the line of travel. Electric and magnetic field strengths fall off as $1/R$ but energy per unit volume falls off as $1/R^2$.

Electromagnetic waves move at the velocity of light in whatever medium they are traveling. That velocity depends on the dielectric constant and the permeability of the medium according to $\varepsilon\mu = 1 / c^2$. For futher information, refer to the items in the Bibliography.

Bibliography

Goetz, P., Ed. in Chief, "Electricity and Magnetism" in *Encyclopedia Britannica*, 15th ed, Chicago, 1989, ISBN 085229493X.

Purcell, E., *Electricity and Magnetism*, 2nd ed, McGraw-Hill, 1984, ISBN 0070049084.

Terman, F., *Electronic and Radio Engineering*, 4th ed, McGraw-Hill, 1955, ISBN 0070857954.

Wilson, M., K1RO, Ed., 2007 edition *The ARRL Handbook for Radio Communications*, ARRL, ISBN 0872599760. *The ARRL Handbook* is available from your local ARRL dealer, or from the ARRL Bookstore, ARRL order no. 9760. Telephone toll-free in the US 888-277-5289, 860-594-0355, or fax 860-594-0303; **www.arrl.org/shop/**; **pubsales@arrl.org**.

QEX

In the next issue of QEX

Frederick H. "Fritz" Raab, W1FR, brings us up to date on the ARRL 500 kHz Experiment. Operating under a Part 5 experimental license as WD2XSH, domestic stations have copied signals over nearly the maximum terrestrial distance: half way around the world. Learn how it's done on the 600-m band, a largely neglected portion of spectrum that may find its way into the Amateur Radio stable in the future. This excellent article was solicited specifically for *QEX* and Fritz has come through vigorously. Don't miss it.

QEX

Letters to the Editor

Energy Conversion in Capacitors (Jul/Aug 2003)

Dear Mr. Smith,

I just discovered your *QEX* article on energy conversion in capacitors. You may be interested in a related article of mine published in the July 2005 English journal, *Physics Education*. Navigate to **www.iop.org/journals/physed** and search the database by my last name. The referenced article is "**Two Theorems on Dissipative Energy Losses in Capacitor Systems**." There is an abstract of the article on the Web site, along with information about subscribing to *Physics Education*, as well as information about purchasing individual articles. — *With best wishes, Ronald Newburgh;* **rgnew@verizon.net**

Antenna Options (Jan/Feb 2007)

Hello Mr. Cebik,

Your Antenna Options column is my favorite *QEX* reading. I look forward to it every two months. Also, I find your Web site (**www.cebik.com**) a fantastic resource.
— *73, John Green, W5AR*; **W5AR@hscaren.org**

Empirical Outlook (Jan/Feb 2007)

Doug,

I enjoyed your editorial about remote bases. I agree with you almost totally.

I have operated remote bases in one form or another since the early 1980s and have found that most hams are distressingly averse to them. As a matter of fact I must confess that I myself thought remote bases were supposed to be private systems. Milt Jensen, N5IA, pioneer of the now-defunct Zia Network linking New Mexico and Arizona wide-area repeaters, attended a repeater-enthusiast meeting in Silver City, New Mexico prior to his construction of that network. He promoted the idea of all of us combining our resources to put up a frequency-agile remote base instead of just another simple repeater.

Most of us thought it a dumb idea. My biggest objection to the concept was that I had always thought of a remote base as a private link, whether RF or landline, controlling a remote system. Milt's idea of a shared remote system allowing an entire club (or the ham public, for that matter) sounded very new and weird to me.

Within a couple of years, Milt's ideas took root with me and I have been fruitlessly promoting remote bases ever since. As you may well be aware, hams are *not* always enthusiasts of new things, whether hardware, software or even conceptual. I care not for the current "dumbing-down" debate about the state of ham radio: In my experience, most hams resist new technology or change of any kind. One of my closest friends still maintains his ham ticket, but he has not owned a radio since the mid-1960s because he was outraged at the multitudes of hams changing over to SSB from AM.

I have tried to *give* him semi-modern radios and antennas so I could stay in touch with him over the air. It's been too long — he has lost interest in radio entirely, and all he remembers is his bitterness about the SSB/AM change of so many years gone by. He surely must be one of the few left who are old enough to remember those days. But hams of all eras seem to get riled up about almost anything, especially change. I've heard old timers recall the spark versus CW change, the 1970s, when CB radio brought many (now mostly welcome) newcomers to the ham bands, and so on. Nowadays I know many highly technical hams who think the computerization of ham radio is terrible. They just don't get it: *Everything* now operates with a computer of some sort, whether it's your car or your HT.

Anyway, I have had an open-to-the-ham-public remote base on the air for almost 20 years. I have even published the control codes (except for the super secret shut-down and turn-on codes reserved for the *ultimate* control operator, me) in magazines and on the Internet, and how many users have ever gotten on and tried it? I think I can almost count them on one hand, especially the ones who actually got interested and tried it more than once.

One is the high school kid to whom I loaned a spare 220 MHz hand-held radio when he first got his license. He really stirred up the bands. This was just before the revolution of cell phones, and he would wander around school demonstrating his radio to anyone who would take a few minutes to listen. He'd call their families on the autopatch and let them talk on the radio to their folks and friends. Most of the time he would dial up the 10-m SSB remote (he was a Technician class licensee with Morse code credit in those days), call CQ and amaze his friends by talking across the country or the oceans with his hand-held radio, and then handing the radio to his friends so they could say, "Hi." A better ambassador for ham radio I've never met.

He had an uncle who was a ham, who came to town one hamfest weekend and convinced him and his mother that he should be on "HF, where the real hams are!"

His uncle attended the hamfest with him and convinced him to buy a used Kenwood TS-140, instead of his own 220 MHz hand-held radio, like I'd been coaching him to do. The kid hung a 10-m dipole from his apartment roof to a nearby tree. He was able to work *no one* because his RF got into all the phones in the building, including his Mom's, and thus a very active young ham went silent. I should have *given* him that loaner radio. It would have been the best investment in ham radio I'd ever made.

Another was an older guy, also a new ham, who used to get on the remote regularly to work 10-m SSB. He was a great guy and quite elderly and loved to work contest weekends through the remote (he was a Technician with no HF gear of his own), and I never had the heart to tell him his contest contacts through the remote base were not considered legitimate contest contacts.

Perhaps it would help to popularize remote bases if you (or someone) could convince ARRL to change the contest rules that disallow remote base/repeater contacts. At least they might be able to get discounted points for working through a remote, or maybe we should give them bonus points for using new technology.

In spite of the unpopularity of remotes, I find quite a few hams who are sort of closet remote-base operators. There are many more Internet-controlled remotes than most people are aware of. Their operators never discuss them on the air and certainly do not publish access codes or addresses for them.

I like Internet remotes when I am far from home; but so far, they leave a lot to be desired. The delays and intermittencies resulting from VOIP (voice over Internet protocol) are very frustrating, especially if you are trying to check into a net or round-table QSO involving quick-trigger-PTT operators — which includes most of us!

You might also put out a call for existing remote base "sysops" like myself, who are willing to list their publicly accessible systems. I'd *love* to be able to find UHF-to-HF remotes along my travel routes so I could stay in touch with the gang back home, or actually find someone to talk to (say, on 20 meters) when I'm within range of a system somewhere. Most of us who travel can key up literally dozens of repeaters at most points along our trips but we rarely find anyone with the time or inclination to answer our calls for information or a chat.

We have all these repeaters all over the USA, seemingly more than we have active hams to use them. What's the first thing most new hams talk about wanting to do? Put up another repeater? Wouldn't it be nice if some percentage of those could be convinced to set up remote-base access so their systems could actually be used to make contact with someone, no matter the time of day or night (such as on 80 through 10 meters)?

There are still far too many hams who:

1) are against anything new;

2) hate hearing touch tones or control codes in their speakers;

3) are fearful to try someone else's system, even if it is public, worrying they'll mess up;

4) hate the idea of a Technician licensee getting on 20 m (actual complaints I've heard), even though it's legal so long as a control operator is standing by; and

5) are exceedingly vocal about anyone doing something different than what they themselves are doing.

I think (as I think you do) that remotes are our hope for the future, especially for students, apartment dwellers, nursing home residents, and those thousands stuck in restrictive homeowner's-covenant situations. Perhaps ARRL and other organizations might be convinced to do more to promote the idea.

— *Jim Devenport, W5AOX*; **jim.devenport@transcore.com**

A Low-Budget Vector Network Analyzer for AF to UHF (Mar/Apr 2007)

Dear OM Baier,

I very much enjoyed your article about vector network analyzers, especially the elegant use of aliasing to obtain a wide frequency range.

You described two ways to generate the offset reference for the second DDS. One is to use a PLL to synthesize a 29.97 MHz reference. But you also mentioned that a DDS could be used for this instead. That made me think of a way to make this design even more flexible.

Suppose we used two more DDS sections, driven by a common clock. The two DDS outputs in turn would be the two clock inputs for the two DDS units you have in your design. Obviously, as you mentioned, we could then set one to 30 MHz and the other to 29.97 MHz, which would result in the same operation as you described. But it also would allow other settings.

For example, set one to 25 MHz and the other to 24.97 MHz. The spacing is the same but the aliases move. In particular, the crossovers shown in Figure 5 move. Similarly, the nulls in the spectral envelope shown in Figure 3 move. This should eliminate the two limitations you mentioned that prevent continuous frequency coverage in the original design (not enough power at integer multiples of the clock, and alias interference at odd half-multiples of the clock). Both of those could then be avoided by shifting the clock source DDS settings, whenever a particular measurement requires a frequency close to a crossover or null.

— *73, Paul Koning, NI1D*; **pkoning@equallogic.com**

In Search of New Receiver Performance Paradigms, Part 3 (Mar/Apr 2007)

Hi Doug,

Thank you for coming up with the cool combiner. I plan to build one for my test setup. I always check dynamic range at the MDS because my system runs out of steam above that level. My pair of HP8640Bs seem to have interaction at higher levels. My combiner barely has 30 dB of isolation.

Looking at your schematic on p 33, I see Z1 and Z2 could be mounted on their sides to accept Z3 and Z4 stacked, lying on their flat sides. This would allow for almost zero lead length. Now I need to study things to see if I can wind them without making any solder connections between cores.

I find the MDS with the generator going through the combiner to eliminate error in the combiner attenuation. The second input port is connected but the level is set very low. I measure phase noise dynamic range with a clean crystal oscillator and step attenuator. I tune the radio across the oscillator so it can be a fixed frequency.

Keep up the good work!

— *73, Frank Carcia, WA1GFZ*; **carcia@sbcglobal.net**

Hi Frank,

Yes, I think you can wind the hybrids without making any solder connections between them — I wish I'd thought of that!

By the way, there's a boo-boo in Part 3, Mar/Apr 2007, on page 30, in the third column, second paragraph: The peak displacement is almost two inches during 5 G shake testing at 5 Hz, not 50 Hz.

—*73, Doug Smith, KF6DX,* QEX *Editor,* **kf6dx@arrl.org**

In Search of New Receiver Performance Paradigms, Part 2 (Jan/Feb 2007)

Doug,

On page 24, in the left column, in the bottom paragraph, starting with the second sentence, the text says: "Not all manufacturers specify the acceptable range of input voltages, but ±15% is a reasonable range for testing. For 13.8 V dc equipment, that is 11.7 to 15.8 V dc; for 120 V ac gear, it's 102 to 138 V ac. In many areas of the world, the ac mains rarely remain within a few percent of its nominal value. AC-powered equipment needs to be checked at both 50 and 60 Hz. Most linear supplies lose significant capacity at 50 Hz and suffer from increased ripple."

When I worked doing CE mark testing, I

was taught by a guy who worked for TÜV in Bolder, CO to apply a ±10 % rule. For a rating of 230 V ac at 50 Hz this would be 207 V ac to 253 V ac. For testing for North America the nominal voltage was taken as 115 V ac at 60 Hz, for which the range would be from 103.5 V ac to 126.5 V ac.

On page 30, Note 2: "…see IEC1000-4…." You must have looked at an old copy: You have to add 60,000. The correct references are IEC 61000-4 and EN 61000-4. As an example, the old IEC 617 on graphic symbols is now IEC 60617.
— *73, Larry Joy, WN8P*; **lawrence_joy@yahoo.com**

Hi Larry,

Thanks for that information. I've been to TÜV Boulder for CE testing and I think I've worked with the gentleman you mention. What we're finding out is that in some countries of the world, the mains voltage is rarely within 8% of nominal and often fluctuates quite wildly. Europe might hold within 10% but hams really want to know at what voltage things quit working.

Out of the Box

Raymond Mack, W5IFS
17060 Conway Springs Ct
Austin, TX 78717-2989

SKYWORKS SOLUTIONS, INC

This is the first in a series of Out of the Box profiles of companies that supply products for the RF marketplace. Our focus will be on companies that are friendly to purchases in small quantities, either direct or through distribution. The first company is Skyworks Solutions, Inc of Woburn, Massachusetts. Skyworks was formed by a merger of Alpha Industries and the cell phone business of Conexant Systems in 2002. Skyworks has acquired additional product lines from other corporations, including the technical ceramics business.

Skyworks has a broad product line that focuses primarily on the microwave bands used by cellular telephones and wireless data. These lines have significant overlap with amateur bands, however. These include the following product lines:

Amplifiers
Attenuators
Diodes
Chip capacitors
Cellular infrastructure receivers and transmitters
Power dividers/combiners
Receivers
Switches
Synthesizers/PLLs
Technical ceramics
Transmitters

Several product categories are likely to be of interest to the amateur community. The dual fractional-N synthesizer line covers the frequency range of 100 MHz to 6100 MHz. Each of these products contain a synthesizer for the main RF as well as an IF synthesizer. The technical ceramic product lines include ceramic transmission lines and dielectric resonators for VCO and filter applications.

Some Skyworks products can be purchased in sample quantities directly from Skyworks, while others are available through distributors such as Avnet.

Skyworks Solutions, Inc, 20 Sylvan Road, Woburn, MA 01801; Phone (781) 376-3000; Fax (781) 376-3100; Web site: **www.skyworksinc.com**

Novel Direct Conversion Receiver from Skyworks

Skyworks has introduced the SKY73013 direct conversion receiver IC for the 5.7 GHz NII computer data band. The SKY73013 offers superior quadrature accuracy performance, noise figure and linearity specifications. The internal "no-pull" architecture offsets the local oscillator from the carrier frequency by a factor of 3 to 2. This novel arrangement greatly reduces LO pulling and DC offset issues, which are classic problems with direct conversion receivers.

The SKY73013 operates from 4.9 to 5.925 GHz, with a local oscillator range of 3.2 to 3.9 GHz. It has a 6-dB noise figure, and an input 1-dB compression point of –15 dBm. The SKY73013 is available in sample quantities directly from Skyworks.

Skyworks Solutions, Inc, 20 Sylvan Road, Woburn, MA 01801; Phone (781) 376-3000; Fax (781) 376-3100; Web site: **www.skyworksinc.com**